



DISCONTINUOUS PHASE TRANSITIONS IN DISCRETE OPINION DYNAMICS MODELS

by

Bartłomiej Nowak

Supervisors

Prof. dr hab. Katarzyna Sznajd-Weron
Prof. Michel Grabisch

A thesis presented for the degree of
Doctor of Philosophy

in the
Faculty of Fundamental Problems of Technology
Department of the Theoretical Physics



Wrocław University
of Science and Technology

Wrocław 2022

The work co-financed by the European Union under the European Social Fund

*“InterDok – Programy Interdyscyplinarnych Studiów Doktoranckich na Politechnice
Wrocławskiej”* Grant No. POWR.03.02.00-00-I003/16



**European
Funds**

Knowledge Education Development



Wrocław University
of Science and Technology

European Union
European Social Fund



“The world is your library to help you to become better at your craft”
Kobe Bryant

*“But people around you are biggest part of it...
Natalia, Antoni, Mateusz and all my supportive friends, thank you”*

ACKNOWLEDGEMENTS

First of all, I want to thank my mentors. Dear Kasia, you brilliantly guided me through the path of my PhD. I am grateful to have been able to soak up knowledge from you. Your work culture and passion for science are contagious. Dear Michel, although we have not worked together for that long, I thank you for the time and support I received from you. Interning with your group was an amazing experience. Not only did you open new scientific doors for me, but you also gave me a peaceful and friendly place that I want to return to someday. I am grateful to call you both not only my mentors, but also my friends.

The following thesis would also not have been possible without my beloved family. Dear Natalia, you were my rock and support when I needed it most. I would not have come this far if you had not been there for me. Dear Antoni, Bogusia, Mateusz, Marcin, Pulina and Rafał thank you for your support at every stage of my journey. You all are irreplaceable.

I also want to thank my friends. Filip, Siob, Sowa and Strachu you have been with me from the very beginning and have never been afraid to help me.

In the same way, I am grateful to several support groups. One from the scientific world, the spiciest group in the universe: Angelika, Basia, Arek duży, Arek mały, Kuba, Maciek, Mikołaj and Piotrek. It was a pleasure to work with you and discuss new scientific problems.

Others from my little doctoral universe: AMP, Andy, Ania, Bartek, Damian, Edzia, Karol, Karolina, Kasia, Maciek, Maks, Marta, Mateusz K., Mateusz Rz., Mateusz Ś., Michał, Norbix and Wojtek. To work surrounded by such great people and support in problems is something that cannot be valued.

The Paris Pan group: Andrian, Ewelina, Leczek, Maciek, Magda, Michał, Wojtek and Zosia. Every joke and sip of wine in your company was an incredible celebration and moment of joy that I will never forget. And I look forward to more.

Finally, all those I met on my way, and now we walk together: Bartek, Gosia, Hubert, Kasia, Kasia M., Marcin, mała Gosia, Ola, Patryk, Rejmanka and Xixian. United we stand, divided we fall.

お世話になりました
Bartek

ABSTRACT

The thesis examines the role of various factors in shaping the phase transition in discrete opinion dynamics models. To check how universal results are within these models, we investigate two types of them (1) the threshold and (2) the q -voter models. For the former, a homogeneous symmetrical version is proposed, and the role of the nonconformity and network are studied. In addition, we analyze how the transition type is affected by the distribution of thresholds in the classical asymmetric version of this model. For the second family of models, we generalize the q -voter model to s -state opinion, similarly as in equilibrium statistical physics the Ising model was generalized to the Potts model. This generalization is considered under two types of randomness, quenched and annealed.

The issues addressed in the dissertation have been published in international peer-reviewed journals. All articles are summarized in the body of the thesis and included after the summary. The analyzed models not only show interesting properties from the perspective of phase transitions. They are also rooted in social science. Thus, the work is interdisciplinary and should contribute to these scientific fields.

STRESZCZENIE

W rozprawie badana jest rola różnych czynników w kształtowaniu przejścia fazowego w dyskretnych modelach dynamiki opinii. Aby sprawdzić, na ile wyniki są uniwersalne w obrębie tych modeli, badamy dwa ich rodzaje (1) model progowy i (2) model q -wyborcy. Dla pierwszego z nich proponujemy jednorodną symetryczną wersję oraz badamy wpływ nonkonformizmu i sieci. Ponadto analizujemy, jak na typ przejścia wpływa rozkład progów w klasycznej asymetrycznej wersji tego modelu. W przypadku drugiej rodziny modeli uogólniamy model q -wyborcy na s -stanową opinię, podobnie jak w równowagowej fizyce statystycznej model Isinga został uogólniony na model Pottsa. Uogólnienie to jest rozpatrywane dla dwóch rodzajów losowości, quenched i annealed.

Zagadnienia poruszane w rozprawie zostały opublikowane w recenzowanych czasopismach międzynarodowych. Wszystkie artykuły są streszczone w treści rozprawy i zamieszczone po podsumowaniu. Analizowane modele wykazują nie tylko interesujące właściwości z punktu widzenia przemian fazowych. Są one również zakorzenione w naukach społecznych. Praca ma więc charakter interdyscyplinarny i powinna wnieść wkład do tych dziedzin nauki.

CONTENTS

Acknowledgements	1
Abstract	2
Streszczenie	3
1 Introduction	5
2 Objectives	7
3 Summary of the results	9
3.1 Homogeneous Symmetrical Threshold Model with Nonconformity: Independence versus Anticonformity	9
3.1.1 Related article	11
3.2 Symmetrical threshold model with independence on random graphs	11
3.2.1 Related article	12
3.3 The threshold model with anticonformity under random sequential updating	12
3.3.1 Related article	13
3.4 Discontinuous phase transitions in the multi-state noisy q -voter model: quenched vs. annealed disorder	13
3.4.1 Related article	14
3.5 Switching from a continuous to a discontinuous phase transition under quenched disorder	15
3.5.1 Related article	15
4 Conclusions	17
Bibliography	19
A Core articles	30
A.1 Article 1	31
A.2 Article 2	46
A.3 Article 3	57
A.4 Article 4	67
A.5 Article 5	81

 FIRST CHAPTER 

INTRODUCTION

The long-standing debate about the role of different factors in shaping the phase transition is, in fact, not finished. Of course, within equilibrium phase transitions, universality classes help us understand similarities between critical properties of different systems [1]. However, the further we are from equilibrium, the more difficult this issue becomes. Hence, understanding and determining what factors cause specific types of phase transitions is timely and of great interest to many researchers [2–10].

While searching for some universality, one can look at classic examples of equilibrium models. For example, within the Ising model [11], short-range interactions between nearest neighbors can emerge on a macroscale in the form of a continuous phase transition [12]. On the other hand, within the so-called q -states Potts model [13], the phase transition can switch from continuous to discontinuous. It is known that the critical behavior of this model is determined by the number of states q and the system's dimensionality d . For example, the order-disorder phase transition is discontinuous in high dimensions ($d>4$) if we have more than two possible states in the system ($q > 2$) [14]. Translating these concepts into nonequilibrium dynamics is possible [2, 15–18] and helps to understand how specific factors can shape the phase transition.

One such vital factor is the type of disorder (annealed and quenched). Within the former, some properties of the system change at each time step. Within the latter, these properties are fixed in time and usually set at the beginning of the process [19]. These two approaches are of great importance in the field of phase transitions. In particular, it has been shown that different types of disorders can produce different results. Some models exhibit only quantitative differences [20–24], while others qualitative, such as rounding the transition or even completely destroying the discontinuity [25–27]. The latter effect, known as rounding effect was observed recently within nonequilibrium systems [28–32].

The role of topology is also not overlooked. The nonequilibrium models are considered in various structures, but complex networks take the major step in the field [33–36]. These graphs are not only more realistic but also open possibilities for discovering new phenomena. Thus, it is not surprising that many studies around them were born in the field of statistical mechanics, including those that sought to provide analytical reasoning [32, 37–43]. Moreover, mentioned concepts from equilibrium physics can be easily introduced in such structures. This opens possibilities for comparative studies with classical results on regular lattices and, as already shown, can display interesting behavior on the topic of phase transitions

[32,37–51].

All of these concepts are also relevant to behavioral sciences. For example, mixing ferromagnetic and antiferromagnetic interplay has already been performed in terms of social interactions [52]. In fact, similar to ferromagnetic interactions, conformity was studied extensively at the beginning of the 20th century [53–55]. However, it has been argued that conformity alone is insufficient to capture the complex picture of human nature, prompting an examination of the idea of nonconformity [56–65]. Despite many factors that can cause conformity, the general consensus is that conformity is defined as following the group, and in result mimics ferromagnetic interactions. In contrast, nonconformity can define more than one type of behavior. Looking at previously mentioned studies, one can distinguish two types of nonconformity, independence and anticonformity (also called counterconformity or opposite conformity). The former is related to complete immunity from external norms and acting in relation to one's beliefs. Similarly to the temperature, which causes random flips regardless of neighborhood, independent entities act independently of the neighborhood. Anticonformity also tends to differentiate the system. However, anticonformists rebel against social norms rather than act independently, mimicking antiferromagnetic interactions. Even though, the general idea behind these concepts is clear, there is no general agreement on how to model them. Thus several variations have been established [39, 66–71]. Anticonformists, often called contrarians [20, 21, 72–77] or hipsters [78, 79], can also be found in majority-vote dynamics, represented by entities following the minority value [48, 80–88].

Different types of randomness also have their roots in the social sciences. The quenched and annealed approaches are connected with the long-standing person-situation debate. One can ask if people made their decisions based on their personality or situational circumstances [89–93]. Situationists claim that the actions of people vary in time and are different under a given state of the world. This behavior is similar to annealed randomness. The other side of this debate argues that people are more consistent with their actions within different situations or states of the environment. Their constant immutability in a decision-making process reflects the freezing of interactions in quenched disorder.

The similarities between physics and the social sciences do not end there. Phenomena such as hysteresis and discontinuous phase transitions are widely observed in the latter, and the phenomenon of social hysteresis has been studied in depth [9, 94–98]. Also, the debate about universality in social systems continues [97–101], as it does in nonequilibrium statistical physics.

The psychologically inspired models are attractive from the perspective of statistical mechanics. They not only provide the possibility of confirmation of some well-known rules and theories but also open the door for new, interesting phenomena. As mentioned above, the Ising model has inspired researchers for almost a century and has become the backbone of many ideas in the equilibrium phase transitions field. Simple mathematical models like voter model or threshold model, often inspired by social sciences, play a similar role. They are rich in behavior and can help develop theories of nonequilibrium phase transitions.

 SECOND CHAPTER 

OBJECTIVES

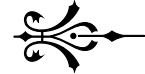
The main aim of this thesis is to determine how various factors that appear in discrete opinion dynamics models affect the type of phase transitions in the presence of different types of nonconformity (independence vs. anticonformity) and disorder (quenched vs. annealed). With respect to this objective, we consider two types of models (1) the threshold model and (2) the q -voter model. In their original formulations, both models belong to the broad class of binary opinion dynamics models, i.e., agents can be in one of two states (yes or no, active or inactive, -1 or 1, 0 or 1, etc.). Within the famous threshold model proposed by Schelling [102] and Granovetter [103], each agent i has a predetermined threshold value r_i , which is usually drawn from some probability distribution. For this model, the agent becomes active if the proportion of his active neighbors exceeds his threshold r_i . Otherwise, he becomes inactive. The q -voter model, on the other hand, does not take into account the whole neighborhood. Due to the conformity rule, the voter follows the value of the group created from q randomly chosen neighbors. Due to the anticonformity rule, the voter takes the opposite value to this randomly chosen group. In both cases, the influence is triggered if all agents among q chosen neighbors are unanimous. In the independence case, the voter changes his state randomly. The nonconformity rule, anticonformity or independence according to the version of the model, is applied to agents with probability p . With complementary probability $1 - p$, the conformity rule is followed [67].

These models have been investigated in many ways, and various versions have been proposed [49, 104–106]. This thesis introduces the new, homogeneous and symmetric version of the threshold model with nonconformity. We want to check if results known from binary models with nonconformity and up-down symmetry are universal. The model is investigated in the complete graph by analytical and numerical treatment. Moreover, this model in the version with independence is checked on complex networks to examine if results from the previously mentioned study are exclusive to the mean-field regime.

Furthermore, we analyze the threshold model in its classical nonsymmetrical version with anticonformity [107]. In contrast to original threshold models, our version is investigated under a random sequential updating scheme, i.e., one agent changes at a given period. Within this model, we check how the distribution of thresholds affects the type of phase transition.

For the binary q -voter model, it is already known how different types of nonconformity shape the phase transition [49]. However, this model has not yet been investigated with multi-state opinion. Therefore, we propose the generalization of the q -voter model with

nonconformity to s possible states, as it was done in equilibrium statistical mechanics for the Potts model [14]. In the Potts model, the introduction of additional states changes the type of phase transition from continuous to discontinuous. Thus, we want to check if this behavior will also be seen for the nonequilibrium model. Additionally, we examine the multi-state q -voter model from the perspective of different types of disorder (quenched and annealed). Within a model with quenched randomness, we are looking for the universal behavior in the form of a rounding effect [27].

 THIRD CHAPTER 

SUMMARY OF THE RESULTS

The thesis consists of five articles prepared during my Ph.D. studies. Four of them have already been published in international peer-reviewed journals: one in Complexity (IF 2.833), two in Physical Review E (IF 2.529), and one in Scientific Reports (IF 4.379). The last paper has been accepted for publication as a Regular Article in Physical Review E. In this chapter, the most important results of all articles are presented. They are divided into five sections, one for each publication. Three of them are devoted to different versions of the threshold model one of the most popular model of binary opinion dynamics. The first section discusses the symmetrical version of the Watts threshold model and how independence can cause a discontinuous phase transition in this model under the mean-field regime. In addition, we compare obtained results to those of the well-known majority vote and q -voter models [108]. The second section focused on the development of such a model in random graphs like Erdős-Rényi and Watts-Strogatz [109]. The third section summarizes the work on the threshold model in its classical, nonsymmetrical version, but with anticonformity [110]. The fourth and fifth paper concerns the study of the generalizations of the q -voter model, namely its multi-state version with both independence [111] and anticonformity [112]. Furthermore, the influence of independence and anticonformity is investigated under different approaches: quenched and annealed.

3.1 Homogeneous Symmetrical Threshold Model with Nonconformity: Independence versus Anticonformity

Within the binary q -voter model, it was shown that competition between conformity and nonconformity can lead to specific types of phase transition (continuous or discontinuous), which depend on the form of nonconformity (independence or anticonformity). The first type of nonconformity, in which individuals perform actions independently of the source of influence, leads to discontinuous order-disorder phase transitions for the size of the influence group $q > 5$. For $q \leq 5$, the transitions remain continuous. In the anticonformity case, where individuals rebel against society, the transitions are continuous despite the value of the parameter q [38, 67, 68, 113].

On the other hand, within the majority-vote model, only continuous phase transitions appear, regardless of the form of nonconformity [48, 88]. Looking at this result, a natural

question about the role of nonconformity in shaping the phase transition can arise. Is noise crucial to the existence of a discontinuous phase transition in the binary opinion dynamics models? Why do we not observe such a transition in the majority-vote model with noise?

To address these questions, we propose a new version of the Watts threshold model [104]. Both the q -voter and the majority-vote models are homogeneous, i.e., all agents are identical. Moreover, both models have up-down (positive-negative opinion) symmetry. Thus, we propose a symmetrical and homogeneous version of the threshold model to make it comparable with the two models recalled above and check if results obtained within different models with nonconformity and up-down symmetry are universal. Due to the symmetry of opinions, our model approves flips from the active (1) to the inactive state (-1). This remains in contrast to some models proposed for the diffusion of innovation, like the original Watts threshold model [104, 106, 114], where such flips were forbidden. Due to homogeneity, every individual in the system has the same threshold r , in contrast to classical versions of threshold models in which the threshold for each agent was chosen from a preset probability distribution [103, 104].

Our proposition consists of two twin models with two types of nonconformity, one with independence and the second with anticonformity. Agents are not set a priori to be conformist or nonconformist. Instead, they choose the behavior with a given probability, as was done for other models of opinion dynamics [67, 68, 88]. With probability $p \in [0, 1]$, which is the first parameter of the model, the agent behaves like a nonconformist while with probability $1 - p$ behaves like a conformist. In the conformity rule, the agent is convinced to change the opinion to 1 if the ratio of active neighbors is greater than the set threshold $r \in [0.5, 1]$, which is the second parameter of the model. Conversely, if the ratio of inactive neighbors is greater than r , the agent takes state -1. Thus the model can be treated as a super-majority model and for $r = 0.5$ reduces to the simple majority. In the anticonformity case, the agent chooses an opposite state to the majority. The independence mechanism is the same as in the q -voter, or in the majority-vote models, i.e., agents randomly pick one of the possible opinions (-1 or 1).

The analytical predictions were confronted with Monte Carlo simulations on the complete graph. We observed a good agreement between them. Both approaches show that the qualitative behavior of the model is determined by the threshold r . For the threshold $r = 0.5$, which corresponds to the majority rule, both model versions give continuous phase transitions. However, with rescaled transition point $p^* = 1/(2\lambda)$, where $\lambda = 1$ for the model with anticonformity and $\lambda = 1/2$ for the model with independence. In contrast, the supermajority $r > 0.5$ exhibits a more complex behavior and enhanced differences between anticonformity and independence. For the model with anticonformity, only order is reached, and no order-disorder transition is visible. On the contrary, the discontinuous phase transitions are visible in the model with independence, similarly to the noisy q -voter model. Moreover, there is an agreement with a generalization of the q -voter model, in which r among q randomly selected neighbors must share the same opinion to influence an agent. It was shown that there is a critical threshold r^* above which discontinuous phase transitions are possible [67, 115] as in our symmetrical threshold model. This critical r^* is visible even in the version where both forms of nonconformity were introduced simultaneously [116].

To heuristically explain the behavior of our threshold model, it is worth to mention that discontinuous phase transitions are possible within the majority-vote model with inertia. This inertia is defined as the importance of the voter's value and can be introduced by an external parameter θ [117, 118]. The higher the inertia, the more likely discontinuous phase transitions are visible. We obtained similar results within our symmetrical threshold model. In fact, the supermajority ($r > 0.5$) is a good representation of the inertia. For $r > 0.5$, it may

happen that voter will not collect a sufficient opposite majority and, as a result, will not change the state. However, it can flip due to independence, which is unaffected by the state of the system.

3.1.1 Related article

Bartłomiej Nowak and Katarzyna Sznajd-Weron, "Homogeneous Symmetrical Threshold Model with Nonconformity: Independence versus Anticonformity", Complexity, vol. 2019, 2019.

Contribution: analytical calculations, development of the software in Python and C++ for the numerical study of the model, analysis of the results, data visualizations, literature review, manuscript preparation, corrections and writing at all stages of the publicity process.

3.2 Symmetrical threshold model with independence on random graphs

This work is a natural continuation of the previous study on the symmetrical threshold model with nonconformity [108] described in the first section. We showed that the model with independence displays discontinuous phase transition on the complete graph if the threshold is large enough ($r > 0.5$). On the other hand, only continuous phase transitions were observed in the majority-vote case ($r = 0.5$). This result disagrees with an intuition that discontinuous phase transition will be possible for majority-vote in highly connected networks [88]. We showed this is not the case, even for the most connected network (complete graph).

The curiosity about the possibility of discontinuous phase transition within this model encourages more profound research on various topologies. The majority-vote model was introduced in square lattices [81, 88], directed graphs [83, 86], hypergraphs [119], modular networks [120] and random networks [48, 51, 84, 85, 121–123]. It seems that despite the topology and the presence of additional noise, only continuous phase transition is possible. However, it was shown that high inertia in the system can support the first-order transitions [118] even in random graphs [117]. We confirm this result within our symmetrical threshold model with independence on complete graph, where threshold $r > 0.5$ can be treated as high inertia in the system [108].

Considering this, one can ask if the symmetrical threshold model with independence gives discontinuous phase transitions only in a fully complete network, or is it a more general behavior? Looking at the results of the q -voter model with independence, it seems that first-order phase transitions are also possible in different topologies [38, 39, 113]. Moreover, it was shown that on random networks, the qualitative behavior of the model is similar to the mean-field one. In general, it depends on the size of the influence group q . For $q \leq 5$ continuous phase transitions were visible, whereas for $q > 5$ they are discontinuous. Also, the model's quantitative behavior depends on the value of the average node degree $\langle k \rangle$.

In this work, we show that discontinuous phase transitions are possible within the homogeneous symmetrical threshold model [108] on random graphs. We confront analytical calculations in the form of pair approximation [38] with Monte Carlo simulations on two types of networks (1) Erdős-Rényi [124, 125] and (2) Watts-Strogatz graphs [33]. The pair approximation predicts well the qualitative behavior of the model, which depends mainly

on the value of the threshold r and the average node degree $\langle k \rangle$. Similarly to results on complete graph, for $r = 0.5$, only continuous phase transitions are possible, regardless of the value of $\langle k \rangle$. For $r > 0.5$ the model undergoes tricritical behavior. For small values of $\langle k \rangle$ continuous phase transition is visible, whereas with increasing value of $\langle k \rangle$ hysteresis increases and results tend to those of mean-field model ($\langle k \rangle \rightarrow \infty$). The relation between the size of the hysteresis and the threshold r is far from trivial, i.e., it is nonmonotonic, having the maximum value for a given value of $r \in (0.6, 0.8)$, which depends on the average node degree.

The Watts-Strogatz model has three parameters (1) the size of the network N , (2) the mean degree K , and (3) rewiring probability $\beta \in [0, 1]$. Varying β allows to tune network structure between a regular lattice ($\beta = 0$) and a structure close to an Erdős-Rényi random graph ($\beta = 1$). The predictions from pair approximation are the closest to the Monte Carlo simulations for pure random structure ($\beta = 1$). Next to threshold r and average node degree $\langle k \rangle$, the rewiring probability impacts the model's behavior. The hysteresis increases with β , and the phase diagrams shift toward higher values of the control parameter p , similarly to the q -voter model [38, 50] or the threshold q -voter model [41].

3.2.1 Related article

Bartłomiej Nowak and Katarzyna Sznajd-Weron, "Symmetrical threshold model with independence on random graphs", Physical Review E, vol. 101, 2020.

Contribution: analytical calculations, development of the software in Python and C++ for the numerical study of the model, implementation of the algorithms for generating random networks in C++, analysis of the results, data visualizations, literature review, manuscript preparation, corrections and writing at all stages of the publicity process.

3.3 The threshold model with anticonformity under random sequential updating

Two previously described studies focused on a symmetrical and homogeneous version of the threshold model [108, 109]. We showed that the homogeneous threshold r controls the general behavior of the model. However, heterogeneous models, where each agent has its own threshold, seem to be more general from a theoretical and a sociological point of view [103, 107, 126, 127]. Moreover, they may undergo interesting behavior in terms of phase transitions. Therefore, we want to see what types of transitions such a model with anticonformity will exhibit. This kind of model has already been studied in [107]. In contrast to our previous study about threshold models, it was considered under a synchronous updating scheme, where all agents change their values simultaneously. Thus, we decided to investigate the nonsymmetrical threshold model under sequential updating. This research idea was born during my internship at the University of Paris 1 Panthéon-Sorbonne, where I worked with the first author of the original article [107].

We proposed the model in two versions, both with anticonformity. First, a homogeneous one, in which all agents have the same threshold r , exactly as it was done in the original work for the symmetrical threshold model [108]. Second version, heterogeneous, in which every agent has its own threshold, similarly to other threshold-like dynamics [103, 104, 107, 126, 127]. In both cases, the agent act like a conformist or anticonformist with probability $1 - p$ and p , respectively. In a heterogeneous case, we investigate the influence of beta distribution with

two shape parameters, α and β . This distribution support values in period $[0, 1]$, which is natural for threshold values. It has a well-defined cumulative distribution function, allowing analytical and numerical treatment. In addition, the beta distribution reflects the wide variety of shapes that have their inspiration and use in sociology [127, 128]. Moreover, parameters α and β allow us to tune the distribution from a uniform distribution ($\alpha = \beta = 1$) to one-point degenerate distribution ($\alpha, \beta \rightarrow \infty$), which reproduces homogeneous case.

The homogeneous model behaves linearly, similarly to the symmetrical model. For $r = 0.5$, it reproduces the result obtained for the homogeneous symmetrical threshold model with anticonformity. For $r \neq 0.5$, the discontinuity appears at $c = r = 1 - p$ for $r > 0.5$ and at $c = r = p$ for $r < 0.5$, contrary to the symmetric version.

Within the heterogeneous case, if the distribution of thresholds is a symmetric peak ($\alpha = \beta$), a continuous phase transition appears. This result converges to the solution from homogeneous symmetrical threshold model with $r = 0.5$, while $\alpha = \beta \rightarrow \infty$. Furthermore, if at least one of the shape parameters is greater than one, both are finite and different, the discontinuous jump appears. Moreover, hysteresis and critical mass are visible, as in some natural threshold systems [129–131].

In addition to the mean-field method, the Markov chain approach is confronted with Monte Carlo simulations. This method gives the stationary probability distribution of possible states for any system size n in the long run. It is found that some states have a much higher probability of being reached than others, like in the Monte Carlo simulations where fluctuations around attractive states are visible. The Markov approach correctly predicts results in both cases, homogeneous and heterogeneous. The former was proven analytically and numerically, while numerical study for the latter reveals excellent agreement.

3.3.1 Related article

Bartłomiej Nowak, Michel Grabisch, and Katarzyna Sznajd-Weron, “The threshold model with anticonformity under random sequential updating”, Physical Review E, 2022.

Contribution: formulation of the final version of the model, analytical calculations, development of the software in Python and C++ for numerical study of the model, analysis of the results, data visualizations, literature review, manuscript preparation, corrections and writing at all stages of the publicity process.

3.4 Discontinuous phase transitions in the multi-state noisy q -voter model: quenched vs. annealed disorder

In this work, we extend the study of the q -voter model. Within this model, the role of the nonconformity was investigated, but only for the binary opinion [38, 67, 68, 113]. Thus, we develop the model to a multi-state version in which agents can have one of s discrete opinions. Similarly, the multi-state version of the voter [132–137], majority-vote [47, 138–144] and other models of opinion dynamics [145] were introduced. It was shown that a more complex variable than a simple binary value can shape phase transition and change it from continuous to discontinuous. Such observation was done already in equilibrium statistical mechanics, for example, within the Potts model [14]. Moreover, the change to discontinuous transition was even possible in the three-state majority-vote model without inertia, for which such transitions were impossible in the binary regime.

Inspired by these results, we propose the multi-state generalization of the q -voter model with independence. As in the original version of the model [67], agents can conform to their q randomly chosen surroundings only if they are in unanimous agreement. Agents can also act like independent ones and choose one among all possible s states at random. Additionally, the model is considered with two types of disorder (1) annealed and (2) quenched. Within annealed version, as in the original binary q -voter model, conformity is introduced with probability $1 - p$ and independence with probability p . In the quenched version, the type of the agent is set a priori. As a result, the parameter p is a fraction of independent agents in the system. The rest are conformists, and agents remain with this behavior forever.

The mean-field analytical approach agrees with the Monte Carlo simulations performed on the complete graph. It correctly reproduces the original results for the binary q -voter model with independence [67, 68]. Both analytical reasoning and simulations indicate that the type of randomness is irrelevant to the existence of discontinuous phase transitions. They are already possible for $s = 3$ states in both formulations, quenched and annealed. This result agrees with those obtained within the multistate-majority vote model, where the introduction of one additional state changes all transitions to discontinuous [140]. In the original q -voter model with independence, the appropriate size of the influence group q is needed to obtain discontinuous phase transitions ($q > 5$) [67, 113]. Within multi-state version of the model they are obtained for every $q > 1$. Additionally, under the quenched approach all transitions are rounded, i.e., less sharp than under the annealed disorder.

The more opinions, the more possible stationary solutions. Some are saddle and have also been observed within the multi-state majority-vote [140] and three-state mean-field Potts [146] models. Such saddle solutions are those where more than two opinions dominate. These configurations also exhibit an order-disorder phase transition, as configurations with a single dominant value.

Although both kinds of disorder show the same type of phase transition for any q , there is a fundamental difference between them. Within the annealed approach, the upper and lower spinodals are non-monotonic functions of q for an arbitrary number of states. The general shape is also similar to the binary q -voter model. On the contrary, for the quenched version, they are strictly increasing functions of q . Moreover, the size of the group of influence q affects the lower spinodal under both approaches, but the number of states has an effect only under annealed randomness. In the quenched version, the lower spinodal for the arbitrary chosen q remains in the same place despite the number of states.

3.4.1 Related article

Bartłomiej Nowak and Bartosz Stoń and Katarzyna Sznajd-Weron, "Discontinuous phase transition in the multi-state noisy q -voter model: quenched vs. annealed disorder", Scientific Reports, vol. 11, 2021.

Contribution: formulation of the final version of the model, analytical calculations, development of the software in Python and C++ for numerical study of the model, analysis of the results, data visualizations, literature review, manuscript preparation, corrections and writing at all stages of the publicity process.

3.5 Switching from a continuous to a discontinuous phase transition under quenched disorder

This work is the second step in investigating the role of multi-state opinion in shaping the phase transition. Within the q -voter model with independence introduction of just one additional state makes all transitions discontinuous despite the value of parameter q [111]. This result is true for both kinds of disorder (1) annealed and (2) quenched, but with rounded transition under the latter. Thus, we ask if this behavior will be visible within a multi-state model with anticonformity. For the binary opinion, only continuous phase transition was observed. The model exhibits this result both on the complete graph [67, 68] and random networks [32, 50]. Moreover, the quenched disorder does not change the type of the transition and, in the mean-field regime, gives the same result as annealed randomness [30].

In our generalization of the q -voter model with anticonformity, conformity occurs in the same manner as in the previous work on the multi-state q -voter model with independence [111], that is the agent can follow the value of the randomly chosen q -panel if this panel is unanimous. On the other hand, within the anticonformity rule, the agent wants to act differently from the randomly chosen q -panel. In the binary regime ($s=2$), the voter can pick only one of two values, opposite to the value of the influence group. However, it is not clear how should we define it in a model with multi-state opinions. One way is to introduce the repelling function, defined on the distance between the agent's and q -panel's opinion [147]. This approach was proposed for the model with a bounded confidence behavior in which transitions between opinions are possible only in a particular range [148–151]. In our work, transitions between all states are possible within conformity. Thus, we want the same for the anticonformity. As a result, a value different from the opinion of the q -panel is taken randomly from $s - 1$ remaining possibilities. A similar approach was proposed for the multi-state majority-vote model: if there are more than two possible states in the majority or the minority, one state is chosen at random [140]. Additionally, we consider the model under both types of disorder, annealed and quenched, as in previous work [111].

Within the multi-state q -voter model with anticonformity, discontinuous phase transitions emerge under the quenched randomness as in our previous study. They appear already for one additional state ($s = 3$) despite the size of the group of influence q . However, under the annealed approach, only continuous transitions are possible. This is opposite to what is usually reported for such models, where annealed approach usually supports discontinuity, while quenched rounds it or even destroys it [25–28]. Furthermore, additional saddle solutions appear for our model similarly to the model with independence [111] and other models of multi-state dynamics [140, 146]. The saddle solutions are visible under both types of randomness, quenched and annealed.

In the multi-state q -voter model with independence, the upper and lower spinodals were qualitatively different for each type of disorder [111]. For the annealed randomness, they were non-monotonic functions of q , while for the quenched disorder, they were strictly increasing. On the other hand, for the model with anticonformity, spinodals are monotonically increasing functions of the parameter q despite the number of states.

3.5.1 Related article

Bartłomiej Nowak and Katarzyna Sznajd-Weron, “Switching from a continuous to a discontinuous phase transition under quenched disorder”, Preprint, 2022.

Contribution: formulation of the final version of the model, analytical calculations, development of the software in Python and C++ for numerical study of the model, analysis of the results, data visualizations, literature review, manuscript preparation, corrections and writing at all stages of the publicity process.

 FOURTH CHAPTER 

CONCLUSIONS

The main objective of this study was to understand how different ingredients known from discrete opinion dynamics shape the phase transition. The study was conducted for two types of models (1) the threshold model and (2) the q -voter model in several directions. We checked the role of nonconformity, topology structure, distribution of thresholds, or even multi-state opinion.

We proposed the symmetrical and homogeneous version of the threshold model. Our study confirmed that noise is crucial in the existence of discontinuous phase transitions under binary opinion dynamics. In this process, the high inertia in the form of a sufficiently high threshold $r > 0.5$ plays a vital part. Simultaneously, the majority-vote case ($r = 0.5$) displays only continuous phase transitions similarly as reported in various studies about this model [48, 88]. This behavior is also visible on random networks, where for $r = 0.5$ only continuous phase transitions were possible. On the other hand, the supermajority ($r > 0.5$) undergoes tricritical behavior. The size of hysteresis, in this case, is a nontrivial function of threshold r and average node degree $\langle k \rangle$.

Furthermore, we investigated the nonsymmetrical threshold model with anticonformity and homogeneous and heterogeneous thresholds. In the former, for $r = 0.5$ model reproduces the results of the symmetrical model. For other thresholds $r \neq 0.5$ additional jump or concentration is visible. For heterogeneous thresholds, the model can display continuous phase transition if the distribution of thresholds is symmetric peak. Moreover, the model for other distribution shapes exhibits the hysteresis and critical mass similarly to natural biological and sociological systems [129–131].

Finally, the role of multi-state opinion was checked within the q -voter model with nonconformity. Within the model with independence, introducing just one additional state changes all transitions to discontinuous. This behavior was observed for both types of randomness, but we observed a rounding effect under quenched disorder. Surprisingly for the model with anticonformity above behavior is not visible. In this case, discontinuous phase transitions are possible only under quenched disorder despite the size of the influence group q . Such a result was not already observed in the literature. The quenched disorder usually rounds or destroys the discontinuity, while annealed supports it.

The research conducted in this thesis confirms some well-known results from nonequilibrium statistical mechanics and brings fresh new insights to the field. For example, we showed that the rounding effect is not always visible. Moreover, we found a model for which

quenched disorder supports discontinuous phase transition, whereas annealed randomness is not. These results should provoke future studies on the topic of phase transitions.

BIBLIOGRAPHY

- [1] J. M. Yeomans, *Statistical mechanics of phase transitions*. Clarendon Press, 1992.
- [2] G. Ódor, “Universality classes in nonequilibrium lattice systems”, *Reviews of Modern Physics*, vol. 76, 2004. doi: 10.1103/RevModPhys.76.663
- [3] H. Hinrichsen, “Non-equilibrium phase transitions”, *Physica A: Statistical Mechanics and its Applications*, vol. 369, 2006. doi: 10.1016/j.physa.2006.04.007
- [4] M. Henkel, H. Hinrichsen, S. Lübeck, and M. Pleimling, *Non-Equilibrium Phase Transitions*. Springer, 2008, vol. 1.
- [5] R. Pastor-Satorras, C. Castellano, P. Van Mieghem, and A. Vespignani, “Epidemic processes in complex networks”, *Reviews of Modern Physics*, vol. 87, 2015. doi: 10.1103/RevModPhys.87.925
- [6] M. Fruchart, R. Hanai, P. B. Littlewood, and V. Vitelli, “Non-reciprocal phase transitions”, *Nature*, vol. 592, 2021. doi: 10.1038/s41586-021-03375-9
- [7] C. J. O. Reichhardt and C. Reichhardt, “An exceptional view of phase transitions in non-equilibrium systems”, *Nature*, vol. 592, 2021. doi: 10.1038/d41586-021-00886-3
- [8] K. Binder and P. Virnau, “Phase transitions and phase coexistence: equilibrium systems versus externally driven or active systems - Some perspectives”, *Soft Materials*, vol. 19, 2021. doi: 10.1080/1539445X.2021.1906703
- [9] E. F. W. Heffern, H. Huelskamp, S. Bahar, and R. F. Inglis, “Phase transitions in biology: from bird flocks to population dynamics”, *Proceedings of the Royal Society B: Biological Sciences*, vol. 288, 2021. doi: 10.1098/rspb.2021.1111
- [10] A. S. Mata, “An overview of epidemic models with phase transitions to absorbing states running on top of complex networks”, *Chaos: An Interdisciplinary Journal of Nonlinear Science*, vol. 31, 2021. doi: 10.1063/5.0033130
- [11] E. Ising, “Beitrag zur Theorie des Ferromagnetismus”, *Z. Physik*, vol. 31, 1925. doi: 10.1007/BF02980577
- [12] L. Onsager, “Crystal Statistics. I. A Two-Dimensional Model with an Order-Disorder Transition”, *Physical Review*, vol. 65, 1944. doi: 10.1103/PhysRev.65.117
- [13] R. B. Potts, “Some generalized order-disorder transformations”, *Mathematical Proceedings of the Cambridge Philosophical Society*, vol. 48, 1952. doi: 10.1017/S0305004100027419

- [14] F. Y. Wu, “The Potts model”, *Reviews of Modern Physics*, vol. 54, 1982. doi: 10.1103/RevModPhys.54.235
- [15] A. Lipowski and M. Droz, “Phase transitions in nonequilibrium d -dimensional models with q absorbing states”, *Physical Review E*, vol. 65, 2002. doi: 10.1103/PhysRevE.65.056114
- [16] A. Jędrzejewski, A. Chmiel, and K. Sznajd-Weron, “Oscillating hysteresis in the q -neighbor Ising model”, *Physical Review E*, vol. 92, 2015. doi: 10.1103/PhysRevE.92.052105
- [17] J.-M. Park and J. D. Noh, “Tricritical behavior of nonequilibrium Ising spins in fluctuating environments”, *Physical Review E*, vol. 95, 2017. doi: 10.1103/PhysRevE.95.042106
- [18] A. Azizi, J. Stidham, and M. Pleimling, “Dynamic critical properties of non-equilibrium Potts models with absorbing states”, *Journal of Statistical Mechanics: Theory and Experiment*, vol. 2018, 2018. doi: 10.1088/1742-5468/aae2dd
- [19] B. Derrida and D. Stauffer, “Phase Transitions in Two-Dimensional Kauffman Cellular Automata”, *Europhysics Letters (EPL)*, vol. 2, 1986. doi: 10.1209/0295-5075/2/10/001
- [20] J. J. Schneider, “The influence of contrarians and opportunists on the stability of a democracy in the Sznajd model”, *International Journal of Modern Physics C*, vol. 15, 2004. doi: 10.1142/S012918310400611X
- [21] D. Stauffer and J. S. Sá Martins, “Simulation of Galam’s contrarian opinions on percolative lattices”, *Physica A: Statistical Mechanics and its Applications*, vol. 334, 2004. doi: 10.1016/j.physa.2003.12.003
- [22] A. N. Malmi-Kakkada, O. T. Valls, and C. Dasgupta, “Ising model on a random network with annealed or quenched disorder”, *Physical Review B*, vol. 90, 2014. doi: 10.1103/PhysRevB.90.024202
- [23] M. A. Javarone, “Social influences in opinion dynamics: The role of conformity”, *Physica A: Statistical Mechanics and its Applications*, vol. 414, 2014. doi: 10.1016/j.physa.2014.07.018
- [24] A. Lipowski, K. Gontarek, and D. Lipowska, “Robust criticality of an Ising model on rewired directed networks”, *Physical Review E*, vol. 91, 2015. doi: 10.1103/PhysRevE.91.062801
- [25] Y. Imry and S.-k. Ma, “Random-Field Instability of the Ordered State of Continuous Symmetry”, *Physical Review Letters*, vol. 35, 1975. doi: 10.1103/PhysRevLett.35.1399
- [26] K. Binder, “Theory of first-order phase transitions”, *Reports on Progress in Physics*, vol. 50, 1987. doi: 10.1088/0034-4885/50/7/001
- [27] M. Aizenman and J. Wehr, “Rounding of first-order phase transitions in systems with quenched disorder”, *Physical Review Letters*, vol. 62, 1989. doi: 10.1103/PhysRevLett.62.2503
- [28] C. Borile, A. Maritan, and M. A. Muñoz, “The effect of quenched disorder in neutral theories”, *Journal of Statistical Mechanics: Theory and Experiment*, vol. 2013, 2013. doi: 10.1088/1742-5468/2013/04/p04032

- [29] P. Villa Martín, J. A. Bonachela, and M. A. Muñoz, “Quenched disorder forbids discontinuous transitions in nonequilibrium low-dimensional systems”, *Physical Review E*, vol. 89, 2014. doi: 10.1103/PhysRevE.89.012145
- [30] A. Jędrzejewski and K. Sznajd-Weron, “Person-Situation Debate Revisited: Phase Transitions with Quenched and Annealed Disorders”, *Entropy*, vol. 19, 2017. doi: 10.3390/e19080415
- [31] A. Jędrzejewski and K. Sznajd-Weron, “Nonlinear q-voter model from the quenched perspective”, *Chaos*, vol. 30, 2020. doi: 10.1063/1.5134684
- [32] A. Jędrzejewski and K. Sznajd-Weron, “Pair approximation for the q -voter models with quenched disorder on networks”, *Physical Review E*, vol. 105, 2022. doi: 10.1103/PhysRevE.105.064306
- [33] D. Watts and S. Strogatz, “Collective dynamics of ‘small-world’ networks”, *Nature*, vol. 393, 1998. doi: 10.1038/30918
- [34] A.-L. Barabási and R. Albert, “Emergence of Scaling in Random Networks”, *Science*, vol. 286, 1999. doi: 10.1126/science.286.5439.509
- [35] R. Albert and A.-L. Barabási, “Statistical mechanics of complex networks”, *Reviews of Modern Physics*, vol. 74, 2002. doi: 10.1103/RevModPhys.74.47
- [36] J. P. Gleeson, “Binary-State Dynamics on Complex Networks: Pair Approximation and Beyond”, *Physical Review X*, vol. 3, 2013. doi: 10.1103/PhysRevX.3.021004
- [37] A. Chmiel and K. Sznajd-Weron, “Phase transitions in the q -voter model with noise on a duplex clique”, *Physical Review E*, vol. 92, 2015. doi: 10.1103/PhysRevE.92.052812
- [38] A. Jędrzejewski, “Pair approximation for the q -voter model with independence on complex networks”, *Physical Review E*, vol. 19, 2017. doi: 10.1103/PhysRevE.95.012307
- [39] A. F. Peralta, A. Carro, M. San Miguel, and R. Toral, “Stochastic pair approximation treatment of the noisy voter model”, *New Journal of Physics*, vol. 20, 2018. doi: 10.1088/1367-2630/aae7f5
- [40] T. Gradowski and A. Krawiecki, “Pair approximation for the q -voter model with independence on multiplex networks”, *Physical Review E*, vol. 102, Aug 2020. doi: 10.1103/PhysRevE.102.022314
- [41] A. R. Vieira, A. F. Peralta, R. Toral, M. San Miguel, and C. Anteneodo, “Pair approximation for the noisy threshold q -voter model”, *Physical Review E*, vol. 101, 2020. doi: 10.1103/PhysRevE.101.052131
- [42] A. Chmiel, J. Sienkiewicz, A. Fronczak, and P. Fronczak, “A Veritable Zoology of Successive Phase Transitions in the Asymmetric q -Voter Model on Multiplex Networks”, *Entropy*, vol. 22, 2020. doi: 10.3390/e22091018
- [43] A. Abramiuk-Szurlej, A. Lipiecki, J. Pawłowski, and K. Sznajd-Weron, “Discontinuous phase transitions in the q -voter model with generalized anticonformity on random graphs”, *Scientific Report*, vol. 11, 2021. doi: 10.1038/s41598-021-97155-0

- [44] P. Holme and M. E. J. Newman, “Nonequilibrium phase transition in the coevolution of networks and opinions”, *Physical Review E*, vol. 74, 2006. doi: 10.1103/PhysRevE.74.056108
- [45] F. Vazquez, V. M. Eguíluz, and M. San Miguel, “Generic Absorbing Transition in Coevolution Dynamics”, *Physical Review Letters*, vol. 100, 2008. doi: 10.1103/PhysRevLett.100.108702
- [46] S. N. Dorogovtsev, A. V. Goltsev, and J. F. F. Mendes, “Critical phenomena in complex networks”, *Reviews of Modern Physics*, vol. 80, 2008. doi: 10.1103/RevModPhys.80.1275
- [47] H. Chen and G. Li, “Phase transitions in a multistate majority-vote model on complex networks”, *Physical Review E*, vol. 97, 2018.
- [48] J. M. Encinas, H. Chen, M. M. de Oliveira, and C. E. Fiore, “Majority vote model with ancillary noise in complex networks”, *Physica A: Statistical Mechanics and its Applications*, vol. 516, 2019. doi: 10.1016/j.physa.2018.10.055
- [49] A. Jędrzejewski and K. Sznajd-Weron, “Statistical Physics Of Opinion Formation: Is it a SPOOF?” *Comptes Rendus Physique*, vol. 20, 2019. doi: 10.1016/j.crhy.2019.05.002
- [50] A. Jędrzejewski, B. Nowak, A. Abramiuk, and K. Sznajd-Weron, “Competing local and global interactions in social dynamics: How important is the friendship network?” *Chaos*, vol. 30, 2020. doi: 10.1063/5.0004797
- [51] A. Krawiecki, “Ferromagnetic and spin-glass-like transition in the majority vote model on complete and random graphs”, *The European Physical Journal B*, vol. 93, 2020. doi: 10.1140/epjb/e2020-10288-9
- [52] S. Galam, “Fragmentation versus stability in bimodal coalitions”, *Physica A: Statistical Mechanics and its Applications*, vol. 230, 1999. doi: 10.1016/0378-4371(96)00034-9
- [53] F. H. Allport and R. S. Solomon, “Lengths of conversations: a conformity situation analyzed by the telic continuum and J-curve hypothesis”, *The Journal of Abnormal and Social Psychology*, vol. 34, 1939. doi: 10.1037/h0054465
- [54] S. E. Asch, “Opinions and social pressure”, *Scientific American*, vol. 193, 1955.
- [55] M. Deutsch and H. B. Gerard, “A study of normative and informational social influences upon individual judgment”, *The Journal of Abnormal and Social Psychology*, vol. 51, 1955. doi: 10.1037/h0046408
- [56] S. E. Asch, “Studies of Independence and Conformity: A Minority of One Against a Unanimous Majority”, *Psychological Monographs: General and Applied*, vol. 70, 1956. doi: 10.1037/h0093718
- [57] M. Jahoda, “Conformity and Independence: A Psychological Analysis”, *Human Relations*, vol. 12, 1959. doi: 10.1177/001872675901200201
- [58] S. E. Asch, “Issues in the Study of Social Influences on Judgment”, in *Conformity and Deviation*, A. Berg and B. M. Bass, Eds. Harper and Brothers Publishers, 1961. doi: 10.1037/11122-005 pp. 143 – 158.

- [59] B. Bass, "Conformity, Deviation and a General Theory of Interpersonal Behavior", in *Conformity and Deviation*, A. Berg and B. M. Bass, Eds. Harper and Brothers Publishers, 1961. doi: 10.1037/11122-003 pp. 38 – 100.
- [60] R. H. Willis, "Two Dimensions of Conformity-Nonconformity", *Sociometry*, vol. 26, 1963. doi: 10.2307/2786152
- [61] R. H. Willis, "Conformity, Independence, and Anticonformity", *Human Relations*, vol. 18, 1965. doi: 10.1177/001872676501800406
- [62] E. P. Hollander and R. H. Wilis, "Some current issues in the psychology of conformity and nonconformity", *Psychological Bulletin*, vol. 68, 1967. doi: 10.1037/H0024731
- [63] R. J. Smith, "Explorations in Nonconformity", *The Journal of Social Psychology*, vol. 71, 1967. doi: 10.1080/00224545.1967.9919774
- [64] L. N. Diab, "Conformity and Deviation: Two Processes or One?" *Psychological Reports*, vol. 22, 1968. doi: 10.2466/pr0.1968.22.3c.1134
- [65] P. R. Nail, G. MacDonald, and D. A. Levy, "Proposal of a four-dimensional model of social response", *Psychological Bulletin*, vol. 126, 2000. doi: 10.1037/0033-2909.126.3.454
- [66] S. Galam and F. Jacobs, "The role of inflexible minorities in the breaking of democratic opinion dynamics", *Physica A: Statistical Mechanics and its Applications*, vol. 381, 2007. doi: 10.1016/j.physa.2007.03.034
- [67] P. Nyczka, K. Sznajd-Weron, and J. Cisło, "Phase transitions in the q -voter model with two types of stochastic driving", *Physical Review E*, vol. 86, 2012. doi: 10.1103/PhysRevE.86.011105
- [68] P. Nyczka and K. Sznajd-Weron, "Anticonformity or Independence? - Insights from Statistical Physics", *Journal of Statistical Physics*, vol. 151, 2013. doi: 10.1007/s10955-013-0701-4
- [69] M. A. Javarone and T. Squartini, "Conformism-driven phases of opinion formation on heterogeneous networks: the q -voter model case", *Journal of Statistical Mechanics: Theory and Experiment*, vol. 2015, 2015. doi: 10.1088/1742-5468/2015/10/p10002
- [70] P. Siedlecki, J. Szwabiński, and T. Weron, "The Interplay Between Conformity and Anticonformity and its Polarizing Effect on Society", *Journal of Artificial Societies and Social Simulation*, vol. 19, 2016. doi: 10.18564/jasss.3203
- [71] A. Kononovicius, "Supportive interactions in the noisy voter model", *Chaos, Solitons & Fractals*, vol. 143, 2021. doi: 10.1016/j.chaos.2020.110627
- [72] S. Galam, "Contrarian deterministic effects on opinion dynamics: "the hung elections scenario""", *Physica A: Statistical Mechanics and its Applications*, vol. 333, 2004. doi: 10.1016/j.physa.2003.10.041
- [73] M. S. de la Lama, J. M. López, and H. S. Wio, "Spontaneous emergence of contrarian-like behaviour in an opinion spreading model", *Europhysics Letters (EPL)*, vol. 72, 2005. doi: 10.1209/epl/i2005-10299-3

- [74] C. Borghesi and S. Galam, “Chaotic, staggered, and polarized dynamics in opinion forming: The contrarian effect”, *Physical Review E*, vol. 73, 2006. doi: 10.1103/PhysRevE.73.066118
- [75] S. Tanabe and N. Masuda, “Complex dynamics of a nonlinear voter model with contrarian agents”, *Chaos*, vol. 23, 2013. doi: 10.1063/1.4851175
- [76] M. B. Gordon, M. F. Laguna, S. Gonçalves, and J. R. Iglesias, “Adoption of innovations with contrarian agents and repentance”, *Physica A: Statistical Mechanics and its Applications*, vol. 486, 2017. doi: 10.1016/j.physa.2017.05.066
- [77] N. Khalil and R. Toral, “The noisy voter model under the influence of contrarians”, *Physica A: Statistical Mechanics and its Applications*, vol. 515, pp. 81–92, 2019. doi: 10.1016/j.physa.2018.09.178
- [78] J. S. Juul and M. A. Porter, “Hipsters on networks: How a minority group of individuals can lead to an antiestablishment majority”, *Physical Review E*, vol. 99, 2019. doi: 10.1103/PhysRevE.99.022313
- [79] J. D. Touboul, “The hipster effect: When anti-conformists all look the same”, *Discrete and Continuous Dynamical Systems - B*, vol. 24, 2019. doi: 10.3934/dcdsb.2019124
- [80] S. Galam, “Social paradoxes of majority rule voting and renormalization group”, *Journal of Statistical Physics*, vol. 61, 1990. doi: 10.1007/BF01027314
- [81] M. J. de Oliveira, “Isotropic majority-vote model on a square lattice”, *Journal of Statistical Physics*, vol. 66, 1992. doi: 10.1007/BF01060069
- [82] P. L. Krapivsky and S. Redner, “Dynamics of Majority Rule in Two-State Interacting Spin Systems”, *Physical Review Letters*, vol. 90, 2003. doi: 10.1103/PhysRevLett.90.238701
- [83] F. W. S. Lima, “Majority-vote on Directed Barabási-Albert Networks”, *International Journal of Modern Physics C*, vol. 17, 2006. doi: 10.1142/S0129183106008972
- [84] F. W. S. Lima, “Majority-vote on Undirected Barabási-Albert Networks”, *Communications in Computational Physics*, vol. 2, 2007. doi: 10.4208/cicp.2007.v2.p358
- [85] E. M. S. Luz and F. W. S. Lima, “Majority-vote on Directed Small-World Networks”, *International Journal of Modern Physics C*, vol. 18, 2007. doi: 10.1142/S0129183107011297
- [86] F. W. S. Lima, A. O. Sousa, and M. A. Sumuor, “Majority-vote on directed Erdős-Rényi random graphs”, *Physica A: Statistical Mechanics and its Applications*, vol. 387, 2008. doi: 10.1016/j.physa.2008.01.120
- [87] A. L. M. Vilela and F. G. B. Moreira, “Majority-vote model with different agents”, *Physica A: Statistical Mechanics and its Applications*, vol. 388, 2009. doi: 10.1016/j.physa.2009.06.046
- [88] A. R. Vieira and N. Crokidakis, “Phase transitions in the majority-vote model with two types of noises”, *Physica A: Statistical Mechanics and its Applications*, vol. 450, 2016. doi: 10.1016/j.physa.2016.01.013
- [89] S. Epstein and E. J. O’Brien, “The person–situation debate in historical and current perspective”, *Psychological Bulletin*, vol. 98, 1985. doi: 10.1037/0033-2909.98.3.513

- [90] D. T. Kenrick and D. C. Funder, "Profiting from controversy: Lessons from the person-situation debate", *American Psychologist*, vol. 43, 1988. doi: 10.1037/0003-066X.43.1.23
- [91] W. Fleeson and E. Noftle, "The End of the Person-Situation Debate: An Emerging Synthesis in the Answer to the Consistency Question", *Social and Personality Psychology Compass*, vol. 2, 2008. doi: 10.1111/j.1751-9004.2008.00122.x
- [92] D. C. Funder, "Persons, situations, and person-situation interactions", in *Handbook of personality: Theory and research*, O. P. John, R. W. Robins, and L. A. Pervin, Eds. The Guilford Press, 2008, pp. 568 – 580.
- [93] R. A. Sherman, J. F. Rauthmann, N. A. Brown, D. G. Serfass, and A. B. Jones, "The independent effects of personality and situations on real-time expressions of behavior and emotion", *Journal of Personality and Social Psychology*, vol. 109, 2015. doi: 10.1037/pspp0000036
- [94] M. Scheffer, "Slow Response of Societies to New Problems: Causes and Costs", *Ecosystems*, vol. 6, 2003. doi: 10.2307/3658645
- [95] J. Bissell, C. Caiado, S. E. Curtis, M. Goldstein, and B. Straughan, Eds., *Tipping Points: Modelling Social Problems and Health*, ser. Wiley Series in Computational and Quantitative Social Science. Wiley, 2015.
- [96] M. Strand and O. Lizardo, "The Hysteresis Effect: Theorizing Mismatch in Action", *Journal for the Theory of Social Behaviour*, vol. 47, 2017. doi: 10.1111/jtsb.12117
- [97] J. N. Pruitt, A. Berdahl, C. Riehl, N. Pinter-Wollman, H. V. Moeller, E. G. Pringle, L. M. Aplin, E. J. H. Robinson, J. Grilli, P. Yeh, V. M. Savage, M. H. Price, J. Garland, I. C. Gilby, M. C. Crofoot, G. N. Doering, and E. A. Hobson, "Social tipping points in animal societies", *Proceedings of the Royal Society B: Biological Sciences*, vol. 285, 2018. doi: 10.1098/rspb.2018.1282
- [98] D. Centola, J. Becker, D. Brackbill, and A. Baronchelli, "Experimental evidence for tipping points in social convention", *Science*, vol. 360, 2018. doi: 10.1126/science.aas8827
- [99] C.-K. Hu, "Universality and scaling in human and social systems", *Journal of Physics: Conference Series*, vol. 1113, 2018. doi: 10.1088/1742-6596/1113/1/012002
- [100] V. Dakos, B. Matthews, A. P. Hendry, J. Levine, N. Loeuille, J. Norberg, P. Nosil, M. Scheffer, and L. De Meester, "Ecosystem tipping points in an evolving world", *Nature Ecology & Evolution*, vol. 3, 2019. doi: 10.1038/s41559-019-0797-2
- [101] A. Bejan, "Freedom and evolution in the dynamics of social systems", *Biosystems*, vol. 195, 2020. doi: 10.1016/j.biosystems.2020.104158
- [102] T. C. Schelling, *Micromotives and macrobehavior*. WW Norton & Company, 1978.
- [103] M. Granovetter, "Threshold Models of Collective Behavior", *American Journal of Sociology*, vol. 83, 1978.
- [104] D. J. Watts, "A simple model of global cascades on random networks", *Proceedings of the National Academy of Sciences*, vol. 99, 2002. doi: 10.1073/pnas.082090499

- [105] C. Castellano, M. A. Muñoz, and R. Pastor-Satorras, “Nonlinear q -voter model”, *Physical Review E*, vol. 80, 2009. doi: 10.1103/PhysRevE.80.041129
- [106] S. Oh and M. A. Porter, “Complex contagions with timers”, *Chaos*, vol. 28, 2018. doi: 10.1063/1.4990038
- [107] M. Grabisch and F. Li, “Anti-conformism in the Threshold Model of Collective Behavior”, *Dynamic Games and Applications*, vol. 10, 2020. doi: 10.1007/s13235-019-00332-0
- [108] B. Nowak and K. Sznajd-Weron, “Homogeneous Symmetrical Threshold Model with Nonconformity: Independence versus Anticonformity”, *Complexity*, vol. 2019, 2019. doi: 10.1155/2019/5150825
- [109] B. Nowak and K. Sznajd-Weron, “Symmetrical threshold model with independence on random graphs”, *Physical Review E*, vol. 101, 2020. doi: 10.1103/PhysRevE.101.052316
- [110] B. Nowak, M. Grabisch, and K. Sznajd-Weron, “The threshold model with anticonformity under random sequential updating”, *Physical Review E*, vol. 105, 2022. doi: 10.1103/PhysRevE.105.054314
- [111] B. Nowak, B. Stoń, and K. Sznajd-Weron, “Discontinuous phase transitions in the multi-state noisy q -voter model: quenched vs. annealed disorder”, *Scientific Reports*, vol. 11, 2021. doi: 10.1038/s41598-021-85361-9
- [112] B. Nowak and K. Sznajd-Weron, “Switching from a continuous to a discontinuous phase transition under quenched disorder”, *Preprint*, 2022. doi: 10.48550/arXiv.2106.11238
- [113] A. F. Peralta, A. Carro, M. San Miguel, and R. Toral, “Analytical and numerical study of the non-linear noisy voter model on complex networks”, *Chaos*, vol. 28, 2018. doi: 10.1063/1.5030112
- [114] D. J. Watts and P. S. Dodds, “Influentials, Networks, and Public Opinion Formation”, *Journal of Consumer Research*, vol. 34, 2007. doi: 10.1086/518527
- [115] A. R. Vieira and C. Anteneodo, “Threshold q -voter model”, *Physical Review E*, vol. 97, 2018. doi: 10.1103/PhysRevE.97.052106
- [116] P. Nyczka, K. Byrka, P. R. Nail, and K. Sznajd-Weron, “Conformity in numbers—Does criticality in social responses exist?” *PLOS ONE*, vol. 13, 2018. doi: 10.1371/journal.pone.0209620
- [117] H. Chen, C. Shen, H. Zhang, G. Li, Z. Hou, and J. Kurths, “First-order phase transition in a majority-vote model with inertia”, *Physical Review E*, vol. 95, 2017. doi: 10.1103/PhysRevE.95.042304
- [118] J. M. Encinas, P. E. Harunari, M. M. de Oliveira, and C. E. Fiore, “Fundamental ingredients for discontinuous phase transitions in the inertial majority vote model”, *Scientific Reports*, vol. 8, 2018. doi: 10.1038/s41598-018-27240-4
- [119] T. Gradowski and A. Krawiecki, “Majority-Vote Model on Scale-Free Hypergraphs”, *Acta Physica Polonica A*, vol. 127, 2015. doi: 10.12693/APHYSPOLA.127.A-55

- [120] F. Huang, H.-S. Chen, and C.-S. Shen, “Phase Transitions of Majority-Vote Model on Modular Networks”, *Chinese Physics Letters*, vol. 32, 2015. doi: 10.1088/0256-307x/32/11/118902
- [121] A. Krawiecki, “Stochastic resonance in the majority vote model on regular and small-world lattices”, *International Journal of Modern Physics B*, vol. 31, 2017. doi: 10.1142/S0217979217502149
- [122] A. Krawiecki, “Spin-glass-like transition in the majority-vote model with anticonformists”, *The European Physical Journal B*, vol. 91, 2018. doi: 10.1140/epjb/e2018-80551-9
- [123] T. E. Stone and S. R. Mckay, “Majority-vote model on a dynamic small-world network”, *Physica A: Statistical Mechanics and its Applications*, vol. 419, 2015. doi: 10.1016/J.PHYSA.2014.10.032
- [124] P. Erdős and A. Rényi, “On Random Graphs. I”, *Publicationes Mathematicae*, vol. 6, 1959.
- [125] E. N. Gilbert, “Random Graphs”, *The Annals of Mathematical Statistics*, vol. 30, 1959. doi: 10.1214/aoms/1177706098
- [126] E. Lee and P. Holme, “Social contagion with degree-dependent thresholds”, *Physical Review E*, vol. 96, 2017. doi: 10.1103/PhysRevE.96.012315
- [127] V. V. Breer, “Models of tolerant threshold behavior (from T. Schelling to M. Granovetter)”, *Automation and Remote Control*, vol. 78, 2017. doi: 10.1134/S0005117917070128
- [128] W. Fleeson and P. Gallagher, “The implications of Big Five standing for the distribution of trait manifestation in behavior: Fifteen experience-sampling studies and a meta-analysis”, *Journal of Personality and Social Psychology*, vol. 97, 2009. doi: 10.1037/a0016786
- [129] I. D. Couzin, C. C. Ioannou, G. Demirel, T. Gross, C. J. Torney, A. Hartnett, L. Conradt, S. A. Levin, and N. E. Leonard, “Uninformed Individuals Promote Democratic Consensus in Animal Groups”, *Science*, vol. 334, 2011. doi: 10.1126/science.1210280
- [130] V. Srivastava and N. E. Leonard, “Bio-inspired decision-making and control: From honeybees and neurons to network design”, in *2017 American Control Conference (ACC)*, 2017. doi: 10.23919/ACC.2017.7963250 pp. 2026–2039.
- [131] V. C. Yang, M. Galesic, H. McGuinness, and A. Harutyunyan, “Dynamical system model predicts when social learners impair collective performance”, *Proceedings of the National Academy of Sciences*, vol. 118, 2021. doi: 10.1073/pnas.2106292118
- [132] M. Starnini, A. Baronchelli, and R. Pastor-Satorras, “Ordering dynamics of the multi-state voter model”, *Journal of Statistical Mechanics: Theory and Experiment*, vol. 2012, 2012. doi: 10.1088/1742-5468/2012/10/p10027
- [133] G. A. Böhme and T. Gross, “Fragmentation transitions in multistate voter models”, *Physical Review E*, vol. 85, 2012. doi: 10.1103/PhysRevE.85.066117

- [134] S. Redner, “Reality-inspired voter models: A mini-review”, *Comptes Rendus Physique*, vol. 20, 2019. doi: 10.1016/j.crhy.2019.05.004
- [135] F. Vazquez, E. S. Loscar, and G. Bagietto, “Multistate voter model with imperfect copying”, *Physical Review E*, vol. 100, 2019. doi: 10.1103/PhysRevE.100.042301
- [136] F. Herrerías-Azcué and T. Galla, “Consensus and diversity in multistate noisy voter models”, *Physical Review E*, vol. 100, 2019. doi: 10.1103/PhysRevE.100.022304
- [137] N. Khalil and T. Galla, “Zealots in multistate noisy voter models”, *Physical Review E*, vol. 103, 2021. doi: 10.1103/PhysRevE.103.012311
- [138] P. Chen and S. Redner, “Consensus formation in multi-state majority and plurality models”, *Journal of Physics A: Mathematical and General*, vol. 38, 2005. doi: 10.1088/0305-4470/38/33/003
- [139] D. Melo, L. Pereira, and F. Moreira, “The phase diagram and critical behavior of the three-state majority-vote model”, *Journal of Statistical Mechanics: Theory and Experiment*, vol. 2010, 2010. doi: 10.1088/1742-5468/2010/11/P11032
- [140] G. Li, H. Chen, F. Huang, and S. Ch., “Discontinuous phase transition in an annealed multi-state majority-vote model”, *Journal of Statistical Mechanics: Theory and Experiment*, vol. 2016, 2016. doi: 10.1088/1742-5468/2016/07/073403
- [141] A. S. Balankin, M. A. Martínez-Cruz, F. G. Martínez, B. Mena, A. Tobon, J. Patiño-Ortiz, M. Patiño-Ortiz, and D. Samayoa, “Ising percolation in a three-state majority vote model”, *Physics Letters A*, vol. 381, 2017. doi: 10.1016/j.physleta.2016.12.001
- [142] A. L. Oestereich, M. A. Pires, and N. Crokidakis, “Three-state opinion dynamics in modular networks”, *Physical Review E*, vol. 100, 2019. doi: 10.1103/PhysRevE.100.032312
- [143] A. L. M. Vilela, B. J. Zubillaga, C. Wang, M. Wang, R. Du, and H. E. Stanley, “Three-State Majority-vote Model on Scale-Free Networks and the Unitary Relation for Critical Exponents”, *Scientific Reports*, vol. 10, 2020. doi: 10.1038/s41598-020-63929-1
- [144] B. J. Zubillaga, A. L. M. Bilela, M. Wang, R. Du, G. Dong, and H. E. Stanley, “Three-state majority-vote model on small-world networks”, *Scientific Reports*, vol. 12, 2022. doi: 10.1038/s41598-021-03467-6
- [145] P. Bańcerowski and K. Malarz, “Multi-choice opinion dynamics model based on Latané theory”, *The European Physical Journal B*, vol. 92, 2019. doi: 10.1140/epjb/e2019-90533-0
- [146] M. Ostilli and F. Mukhamedov, “1D Three-state mean-field Potts model with first- and second-order phase transitions”, *Physica A: Statistical Mechanics and its Applications*, vol. 555, 2020. doi: 10.1016/j.physa.2020.124415
- [147] F. Li, “Continuous Opinion Dynamics with Anti-conformity Behavior”, Ph.D. dissertation, Université Paris I Panthéon-Sorbonne - Centre Maison des Sciences Economiques; Bielefeld University - Department of Business Administration and Economics, 2021.
- [148] G. Deffuant, D. Neau, F. Amblard, and G. Weisbuch, “Mixing beliefs among interacting agents”, *Advances in Complex Systems*, vol. 03, 2000. doi: 10.1142/S0219525900000078

- [149] R. Hegselmann and U. Krause, "Opinion Dynamics and Bounded Confidence Models, Analysis and Simulation", *Journal of Artificial Societies and Social Simulation*, vol. 5, 2002.
- [150] G. Weisbuch, "Bounded confidence and social networks", *The European Physical Journal B*, vol. 38, 2004. doi: 10.1140/epjb/e2004-00126-9
- [151] W. Radosz and M. Doniec, "Three-State Opinion Q-Voter Model with Bounded Confidence", in *Computational Science – ICCS 2021*, M. Paszyński, D. Kranzlmüller, V. V. Krzhizhanovskaya, J. J. Dongarra, and P. M. Sloot, Eds., vol. 12744. Springer International Publishing, 2021. doi: 10.1007/978-3-030-77967-2_24 pp. 295 – 301.

 APPENDIX A 

CORE ARTICLES

A.1 Article 1

**Homogeneous Symmetrical Threshold Model with
Nonconformity: Independence versus Anticonformity**

Research Article

Homogeneous Symmetrical Threshold Model with Nonconformity: Independence versus Anticonformity

Bartłomiej Nowak and Katarzyna Sznajd-Weron 

Department of Theoretical Physics, Faculty of Fundamental Problems of Technology, Wrocław University of Science and Technology, Wrocław, Poland

Correspondence should be addressed to Katarzyna Sznajd-Weron; katarzyna.weron@pwr.edu.pl

Received 30 December 2018; Accepted 31 March 2019; Published 18 April 2019

Academic Editor: Yong Xu

Copyright © 2019 Bartłomiej Nowak and Katarzyna Sznajd-Weron. This is an open access article distributed under the Creative Commons Attribution License, which permits unrestricted use, distribution, and reproduction in any medium, provided the original work is properly cited.

We study two variants of the modified Watts threshold model with a noise (with nonconformity, in the terminology of social psychology) on a complete graph. Within the first version, a noise is introduced via so-called independence, whereas in the second version anticonformity plays the role of a noise, which destroys the order. The modified Watts threshold model, studied here, is homogeneous and possesses an up-down symmetry, which makes it similar to other binary opinion models with a single-flip dynamics, such as the majority-vote and the q -voter models. Because within the majority-vote model with independence only continuous phase transitions are observed, whereas within the q -voter model with independence also discontinuous phase transitions are possible, we ask the question about the factor, which could be responsible for discontinuity of the order parameter. We investigate the model via the mean-field approach, which gives the exact result in the case of a complete graph, as well as via Monte Carlo simulations. Additionally, we provide a heuristic reasoning, which explains observed phenomena. We show that indeed if the threshold $r = 0.5$, which corresponds to the majority-vote model, an order-disorder transition is continuous. Moreover, results obtained for both versions of the model (one with independence and the second one with anticonformity) give the same results, only rescaled by the factor of 2. However, for $r > 0.5$ the jump of the order parameter and the hysteresis is observed for the model with independence, and both versions of the model give qualitatively different results.

1. Introduction

Models of opinion dynamics are among the most studied models of complex systems [1–4]. This is not surprising, because they can be treated as a zero-level approach to various more complex social processes, including polarization of opinion [5–7], diffusion of innovation [8–10], or political voting [11–13]. In most of these models, public opinion is formed as an outcome from individual opinions of mutually interacting agents. Particularly interesting is a subset of the binary opinion models, including the voter model [14], the majority-vote model [14–16], the Galam model [17], the Sznajd model [18], the Watts threshold model [19], the q -voter model [20], or the threshold q -voter model [21, 22]. All these models belong to the broader class of binary-state dynamics, likewise the kinetic Ising models [23]. The binary decision/opinion framework is not only attractive

from physicist's point of view but also natural in the social sciences [19, 24].

In this paper, we will focus on a particular subclass of the binary opinion models with a single-flip dynamics, which means that one agent at most can change her/his state in a single update [25]. Such an updating scheme is used within the voter model, the majority-vote model, the Watts threshold model, and the q -voter model. There are several common features possessed by all these models, at least in their original formulations. Within these models, we have the following:

- (1) We consider N individuals that are tied to the nodes of some graph. Each node of a graph is occupied by exactly one agent.
- (2) Each individual is described by the dynamical binary variable $S_i(t) = \pm 1$, $i = 1, \dots, N$, that represents an opinion on a given subject (yes/no, agree/disagree,

etc.) at given time t . Such a variable reminds an Ising spin and therefore wording, “individual”, “agent”, “voter” and “spin”, is used interchangeably; $S_i = +1$ is often represented by \uparrow , whereas $S_i = -1$ is by \downarrow .

- (3) Interactions between agents are local; i.e., they take place only if two agents are directly linked.
- (4) At each elementary update a single spin is randomly chosen and it can flip to the opposite direction with a probability that depends on the model’s details.
- (5) Conformity, i.e., an act of matching opinions, attitudes, beliefs, and/or behaviors to the certain group of influence, is the main type (often the only type) of the social response.
- (6) Agents are memoryless, which means that opinion $S_i(t)$ of a given agent at time t depends only on her/his own opinion at the previous time step $S_i(t - \Delta t)$ and opinions of her/his neighbors also at the previous time step $t - \Delta t$.

The differences between models depend mainly on the condition under which the conformity takes place. In some models all neighbors of a given target agent influence her/him (this applies to the majority-vote model [14, 16] or the Watts threshold model [19]), whereas in others only a certain group of influence is chosen from the neighborhood (e.g., in the q -voter model [20, 21, 26]). In the q -voter model unanimity of opinion is needed to influence a voter [20], whereas in the majority-vote model absolute majority is sufficient [16]. The last and particularly important difference consists of the presence or the absence of the up-down symmetry. The linear voter, the q -voter model, and majority-vote are symmetrical; i.e., they are invariant to the swap of state labels, as the Ising model without the external field. However, the Watts threshold model is not symmetrical in its original formulation, because it was introduced as a model of innovation diffusion and flips from \uparrow to \downarrow were forbidden [19, 27]. Moreover, the Watts threshold model is heterogeneous, even on homogeneous graphs; i.e., each agent is characterized by its individual threshold needed for conformity. However, modification of the model to make it symmetrical and homogeneous (in a sense that all agents are characterized by the same threshold) is straightforward and will be investigated in this work.

One may ask what is the motivation to modify the Watts threshold model into the symmetric case? First of all, opinion dynamics concerns not only asymmetrical problems, as the diffusion of innovations, but many symmetric or almost symmetric issues, such as voting to one of two political parties and choosing one of two products on the duopoly market. Although the Watts threshold model was originally introduced to model the diffusion of innovation, the main idea of the threshold is also very natural in the broader context. It has been shown in many social experiments that simple majority ($> 50\%$) may not be sufficient to convince people; for short review see [28]. The second reason for the modification of the Watts threshold model comes from the basic research. Most of the binary opinion models within sociophysics have the yes-no (up-down) symmetry, so to

Complexity

make a comparison with them it is necessary to deal with the symmetric version of the Watts threshold model. In fact, the second reason was our main motivation. We wanted to understand the nature of the phase transitions observed within models of binary opinions with a single-flip dynamics and up-down symmetry.

Because all binary models, mentioned above, have been extensively investigated for years, many modifications and extensions of their original formulations have been proposed; a short review on modifications of the majority-vote model can be found in [29], on the Watts threshold model in [30], on the q -voter model in [31], and on the Galam model comprehensive review written by the author of the model [32, 33]. Among many extensions, going into different directions, the introduction of an additional type of the social response was particularly interesting from the point of view of social/psychological sciences, as well as the theory of nonequilibrium phase transitions. This new type of social response is called nonconformity and can take one of two possible forms: (1) independence (resisting influence) or (2) anticonformity (rebeling against influence) [21, 34, 35]. In the first case, the situation is evaluated independently of the group norm, which means that a state of a given spin is not affected by its neighborhood. In the second case, a voter is influenced by the others but takes the position that is opposite to the group of influence. Therefore it is said that anticonformity and conformity are opposites at the operational level but at the same time similar at the conceptual level, because both indicate behavior that has been influenced by the source [35].

It is clear that conformity increases agreement (ferromagnetic order) in the system, whereas both types of nonconformity act against consensus. As a result of this competition, an order-disorder phase transition emerges. Interestingly, the type of the phase transition (continuous or discontinuous) may depend on the type of nonconformity. For example, it has been shown that within the q -voter model with anticonformity only continuous phase transitions are possible, whereas for the q -voter model with independence tricriticality (a switch between continuous and discontinuous phase transition) appears [21, 26, 36–38]. The majority-vote model contains conformity and anticonformity in its original formulation, but recently an additional noise, in the form of independence, has been introduced [29, 39]. It has been shown that the presence of an additional noise does not affect the type of the phase transition, which remains continuous independently of the network structure.

The question that naturally arises here is “which factor is responsible for the discontinuous phase transition within the q -voter model, since we do not observe the analogous phenomenon within the majority-vote model?” We believe that investigating the modified version of the threshold model on the complete graph could help to understand this phenomenon. Due to our knowledge, the role of a noise has not been explored yet within the Watts threshold model [19, 30]. Therefore in this paper we will introduce two versions of the model, analogously as it was done for the q -voter model, one with independence and the second one with anticonformity.

Complexity

3

The paper is organized as follows. In the next section, we describe original versions of binary opinion models with single-flip dynamics. Then we present model's extensions, which consist of introducing the noise into the models and we describe briefly the results that show how this noise impacts phase transitions. In the following subsection, we modify the original Watts threshold model to make it symmetrical and homogeneous, which makes it comparable to other binary opinion models with single-flip dynamics. Subsequently, we propose two versions of the symmetrical, homogeneous Watts threshold model, one with independence and the second one with anticonformity. Then, we analyze the model on the complete graph, which corresponds to the mean-field approach. We compare results obtained within Monte Carlo simulations results with those obtained via analytical treatment. Moreover, we provide a heuristic explanation of the obtained results. Finally, we discuss results in the context of other binary opinion models with single-flip dynamics.

2. Methods

2.1. Binary Opinion Models with a Single-Flip Dynamics. The general framework of all binary opinion models with a single-flip dynamics has been described above so we will not repeat it here. Instead, we present updating rules that define the dynamics of models within this class. The most extensively studied among all is the linear voter model [14]. On the other hand, the linear voter model is a special case of the more general q -voter model [1] and thus we will not discuss it separately. The dynamics of the original q -voter model is the following:

- (1) At a given time t , choose one voter at random, located at site i .
- (2) Choose randomly q neighbors of site i from its k_i neighbors, where k_i is degree of a node i . In the original formulation and in some later versions repetitions were allowed to make the model universal (arbitrary value of q on the arbitrary graph is possible) [20, 40–42]. However, in many other papers repetitions were forbidden [21, 26, 28, 36].
- (3) If all q neighbors have the same opinion, the spin at site i takes the same state as q neighbors.
- (4) Otherwise, i.e., in lack of unanimity, spin at site i can flip to the opposite direction with probability ϵ . In most of later modifications $\epsilon = 0$ [21, 26, 28, 36, 40–42] and here we also refer to this case.
- (5) Time is updated $t = t + 1/N$.

In [43] two types of noise (interpreted as nonconformity) have been introduced to the model, but not simultaneously. Initially two versions of the model have been introduced: one with independence and the second one with anticonformity. In each of these models nonconformity (independence or anticonformity) takes place with probability p , whereas with complementary probability $1 - p$ agent conforms. Summarizing, the algorithm of a single step is as follows:

- (1) At a given time t , choose one voter at random, located at site i .

- (2) Update the opinion S_i :

- (i) Model I (with Independence)

- (a) With probability p , an agent changes opinion independently, i.e., she/he changes opinion to the opposite one $S_i \rightarrow -S_i$ with probability $1/2$.
- (b) With probability $1 - p$, an agent conforms, i.e., if all q agents, randomly chosen from all k_i neighbors of site i , are in the same state, then the voter at site i takes the same position as those q agents.

- (ii) Model A (with Anticonformity)

- (a) With probability p , an agent anticonforms, i.e., acts against a group of influence, i.e., if all q agents, randomly chosen from all k_i neighbors of site i , are in the same state, then the voter at site i takes the opposite position to those q agents.
- (b) With probability $1 - p$, an agent changes opinion as in Model I.

- (3) Time is updated $t = t + 1/N$.

The generalized versions of the model that consists of a threshold [21, 22] and two types of nonconformity simultaneously [28] have been also introduced. In the case of the threshold q -voter model, only r among q neighbors have to share the same opinion in order to influence a voter.

The q -voter model with independence was studied on the complete graph [21, 28, 43], as well as on various complex networks [36, 37], whereas the q -voter model with anticonformity only on the complete graph. It has been shown that within Model A only continuous phase transitions are possible for all $q \geq 2$, whereas within Model I both types of phase transitions appear; for $2 \leq q \leq 5$ there is continuous phase transition and for $q > 5$ transition is discontinuous. It has occurred that the tricritical point $q^* = 5$, even if q can take noninteger values [38].

It has been also shown that in the case of the threshold q -voter model there is a critical threshold $r^* = r^*(q)$ that decreases with q , above which discontinuous phase transitions are possible [21, 28]. In the most general case, when independence and anticonformity are introduced simultaneously, it occurs that $r^* = r^*(q)$ is monotonically decreasing function of q and r^* is always greater than 0.5, even for very large q [28]. Although the analytical form of $r^* = r^*(q)$ has not been found, it was predicted that for $q \rightarrow N$ the critical value $r^* \rightarrow 0.5$. It means that the absolute majority is not sufficient for the discontinuous phase transition, even if for very large q .

Another model with a single-flip dynamics, which has been analyzed in the presence of a noise, is the majority-vote model [14]. The dynamics of the original majority-vote model is as follows:

- (1) At a given time t , choose one voter at random, located at site i .
- (2) With probability f a spin at site i adopts the minority sign of k_i neighboring spins.
- (3) With complementary probability $1 - f$ a spin at site i adopts the majority sign of k_i neighboring spins.
- (4) Time is updated $t = t + 1/N$.

As seen from the above description, within the original majority-vote model anticonformity takes place with probability f and conformity with $1 - f$, similarly as within the q -voter model with anticonformity. Recently an additional noise has been introduced into the majority-vote model: with probability p a voter acts independently, i.e., analogously like within the q -voter model with independence, and flips randomly to the opposite direction with probability $1/2$. With complementary probability $1 - p$ the original rule is applied [29, 39]. The model has been investigated on the square lattice [29], as well as on several graphs, including homogeneous and heterogeneous structures, through the mean-field calculations and the Monte Carlo simulations [39]. It has been shown that only continuous phase transitions are possible within this model, similarly as for the model without additional noise. Discontinuous phase transitions do not appear even for highly connected networks. This result is consistent with the result obtained for the generalized threshold q -voter model [21, 28], as described above.

2.2. Symmetrical, Homogeneous Watts Threshold Model. In computational sociology, a particularly popular class of models describing the spread of innovation/idea/behavior are threshold models, based on the idea introduced by Granovetter [24]. Probably the simplest among them is the Watts threshold model [19]. The updating rule within its original formulation is as follows:

- (1) At a given time t , choose one voter at random, located at site i .
- (2) An agent at site i is influenced by its k_i neighbors. If at least a threshold fraction r_i of its k_i neighbors are in state 1, then an agent adopts this state; otherwise, nothing happens.
- (3) Time is updated $t = t + 1/N$.

There are two characteristic features that make the model different from other models described in the previous subsection. The first visible difference is heterogeneity. In other models it is introduced only by the heterogeneity of a graph; here, agents possess individual thresholds. Originally, each agent is assigned a threshold that is drawn at random from a given probability distribution function (PDF). Of course, as a special case, we can choose a one-point PDF, which takes the value equal to one at r , and zero otherwise. Within such a formulation r is an external (control) parameter of the model.

Another difference between Watts threshold model and other models, presented above, is the lack of the up-down symmetry. An agent who ones adopted cannot go back to an unadopted state. However, we can easily modify the model to make it symmetrical, in the following way:

Complexity

- (1) At a given time t , choose one voter at random, located at site i .
- (2) An agent at site i is influenced by all k_i neighbors:
 - (a) if at least a threshold fraction r of its k_i neighbors are in state 1, then an agent takes state 1, else
 - (b) if at least a threshold fraction r of its k_i neighbors are in state -1, then an agent takes state -1, else
 - (c) an agent remains in its old state.
- (3) Time is updated $t = t + 1/N$.

It should be noticed that within the above definition, the rules are defined unambiguously only for $r \in [0.5, 1]$. To clarify this, let us give here an example. Imagine that $r = 0.3$ and at a given time step $c(t) = 0.4$. It means that the ratio of the positive opinions is equal to 0.4 and the ratio of the negative opinions is equal to 0.6. Because $r = 0.3$ we have both conditions: (a) a threshold fraction r of neighbors are in state 1 and (b) a threshold fraction r of neighbors in the state -1 are fulfilled, which means that there is no unambiguous choice. Of course one could think about another model in which this ambiguity could be solved by introducing the probabilistic rule. However, in such a case interpretation of what is conformity and what is anticonformity would be far less clear. Therefore here we consider only $r \in [0.5, 1]$. This can be interpreted also as a supermajority (or a qualified majority), whereas $r = 0.5$ corresponds to the simple majority rule.

Now we are ready to introduce two versions of the model with nonconformity, one with Independence (Model I) and the second one with Anticonformity (Model A), analogously as it was done for q -voter model. Within Model A an agent conforms or anticonforms if the fraction of neighboring spins having the same state is larger than a fixed threshold r . In the conformity case (which takes place with probability $1 - p$), an agent follows the opinion of the group of influence, whereas in the case of anticonformity (which takes place with probability p) she/he takes the opposite opinion to the group, as in the majority-vote or in the q -voter model with anticonformity. Within Model I, instead of anticonformity, independence takes place with probability p : an agent flips to the opposite state with probability $1/2$.

The algorithm of a single update is as follows:

- (1) At a given time t , choose one voter at random, located at site i .
- (2) Update the opinion S_i :
 - (i) Model I (with Independence)
 - (a) With probability p , an agent acts independently; i.e., she/he changes an opinion to the opposite one $S_i \rightarrow -S_i$ with probability $1/2$.
 - (b) With probability $1 - p$, an agent conforms to its k_i neighbors:
 - (i) if at least a threshold fraction r of its k_i neighbors are in state 1, then an agent takes state 1, else

Complexity

5

- (ii) if at least a threshold fraction r of its k_i neighbors are in state -1 , then an agent takes state -1 , else
 - (iii) an agent remains in its old state.
- (ii) Model A (with Anticonformity)
- (a) With probability p , an agent anticonforms to its k_i neighbors:
 - (i) if at least a threshold fraction r of its k_i neighbors are in state 1 , then an agent takes state -1 , else
 - (ii) if at least a threshold fraction r of its k_i neighbors are in state -1 , then an agent takes state 1 , else
 - (iii) an agent remains in its old state.
 - (b) With probability $1 - p$, an agent conforms to its neighbors, analogously as in Model I.
- (3) Time is updated $t = t + 1/N$.

2.3. The Mean-Field Approach. In this work, analogously as in [26], we analyze the model on a complete graph, which means that, for each agent, all other agents in the system are neighbors. On the one hand, one can argue that in the case of the symmetric homogeneous threshold model such a structure will give trivial, easily predictable results. On the other hand, only for the complete graph the mean-field approach is exact. Moreover, most of the results for q -voter model with nonconformity were obtained on the complete graph, so this structure is adequate for comparison between models. Finally, we hope that such an approach will be helpful in understanding the nature of the phase transitions within the q -voter model and the majority-vote model, what will be discussed in the last section of this paper.

As an aggregated quantity, which fully describes the system in case of the complete graph, we choose an average concentration of agents with positive opinions:

$$c(t) = \frac{N_{\uparrow}(t)}{N}, \quad (1)$$

where $N_{\uparrow}(t)$ denotes the number of agents in the state \uparrow at time t . Alternatively, we could choose an average opinion (magnetization), which is a natural order parameter [44]:

$$m(t) = \frac{1}{N} \sum_{i=1}^N S_i(t) = \frac{N_{\uparrow}(t) - N_{\downarrow}(t)}{N} = 2c(t) - 1. \quad (2)$$

However, for the analytical treatment $c(t)$ is more convenient, because within the mean-field approach it gives the probability that a randomly chosen agent, at any site, is positive.

As for all other binary opinion models with a single-flip dynamics, in an elementary time step the number of up spins N_{\uparrow} can increase by one, decrease by one, or remain the same.

It means that the concentration of up spins c can change only by $\pm 1/N$. We follow the notation from [21, 26]:

$$\begin{aligned} \gamma^+ &= \text{Prob}\left(c(t + \Delta t) = c(t) + \frac{1}{N}\right), \\ \gamma^- &= \text{Prob}\left(c(t + \Delta t) = c(t) - \frac{1}{N}\right), \end{aligned} \quad (3)$$

where $\Delta t = 1/N$, as usual. Of course with the complementary probability $1 - \gamma^+ - \gamma^-$ the state of the system will not change.

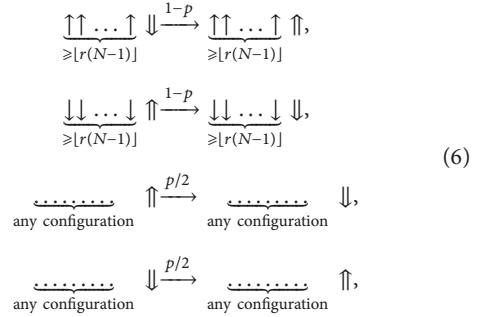
Using above probabilities, we obtain a recursive formula for the concentration of up spins:

$$c\left(t + \frac{1}{N}\right) = c(t) + \frac{1}{N}(\gamma^+ - \gamma^-), \quad (4)$$

which for $N \rightarrow \infty$ gives the rate equation [45, 46]:

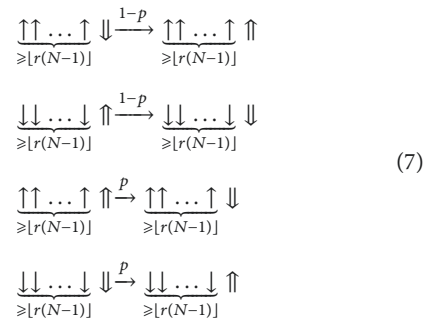
$$\frac{dc(t)}{dt} = \gamma^+ - \gamma^-. \quad (5)$$

Probabilities γ^+, γ^- depend of course on model's details and can be derived looking at all possible changes that may occur in a single update. Within the homogeneous symmetrical threshold model with independence (Model I), the following changes are possible:



where \Downarrow and \Uparrow denote states of a target agent, and $\lfloor r(N-1) \rfloor$ is the floor function of $r(N-1)$, which follows from the restriction that the number of agents can take only integer value, whereas r is a real number.

Within the homogeneous symmetrical threshold model with anticonformity (Model A):



In all other situations, the state of the system will not change. Therefore,

$$\begin{aligned}\gamma^+ &= (1-p)\alpha_{\uparrow} + p\beta_{\uparrow}, \\ \gamma^- &= (1-p)\alpha_{\downarrow} + p\beta_{\downarrow},\end{aligned}\quad (8)$$

where $\alpha_{\uparrow}, \alpha_{\downarrow}$ are probabilities related to conformity. They are the same for both versions of the model:

$$\begin{aligned}\alpha_{\uparrow} &= \sum_{i=\lfloor r(N-1) \rfloor}^{N-1} \left[\binom{N-1}{i} \right. \\ &\times \left. \frac{N_{\uparrow} \prod_{j=1}^i (N_{\uparrow} - j + 1) \prod_{j=1}^{N-1-i} (N_{\downarrow} - j + 1)}{\prod_{j=1}^N (N - j + 1)} \right] \\ \alpha_{\downarrow} &= \sum_{i=\lfloor r(N-1) \rfloor}^{N-1} \left[\binom{N-1}{i} \right. \\ &\times \left. \frac{N_{\downarrow} \prod_{j=1}^i (N_{\downarrow} - j + 1) \prod_{j=1}^{N-1-i} (N_{\uparrow} - j + 1)}{\prod_{j=1}^N (N - j + 1)} \right].\end{aligned}\quad (9)$$

Within conformity, an agent accepts the opinion of her/his neighbors; i.e., it takes the same state as the majority above the threshold r . Thus the probability α_{\uparrow} that an agent changes her/his opinion from -1 to 1 is equal to the probability that a randomly selected agent is at state -1 multiplied by the probability that at least $\lfloor r(N-1) \rfloor$ of her/his neighbors are in the state 1 . Analogously, the probability α_{\downarrow} that an agent changes her/his opinion from 1 to -1 is equal to the probability that a randomly selected agent is at state 1 multiplied by the probability that at least $\lfloor r(N-1) \rfloor$ of her/his neighbors are in the state -1 .

On the other hand, $\beta_{\uparrow}, \beta_{\downarrow}$ are related to nonconformity; i.e., they depend on the model's version. In the model with independence an agent changes her/his state to the opposite one with probability $1/2$. Thus β_{\uparrow} is equal to the probability that a randomly selected agent is at state -1 multiplied by $1/2$. Analogously, β_{\downarrow} is equal to the probability that a randomly selected agent is at state 1 multiplied by $1/2$ and thus

$$\begin{aligned}\beta_{\uparrow} &= \frac{N_{\downarrow}}{2N}, \\ \beta_{\downarrow} &= \frac{N_{\uparrow}}{2N}.\end{aligned}\quad (10)$$

Whereas for anticonformity,

$$\beta_{\uparrow} = \sum_{i=\lfloor r(N-1) \rfloor}^{N-1} \left[\binom{N-1}{i} \right.$$

$$\begin{aligned}&\times \left. \frac{N_{\downarrow} \prod_{j=1}^i (N_{\downarrow} - j + 1) \prod_{j=1}^{N-1-i} (N_{\uparrow} - j + 1)}{\prod_{j=1}^N (N - j + 1)} \right] \\ \beta_{\downarrow} &= \sum_{i=\lfloor r(N-1) \rfloor}^{N-1} \left[\binom{N-1}{i} \right. \\ &\times \left. \frac{N_{\uparrow} \prod_{j=1}^i (N_{\uparrow} - j + 1) \prod_{j=1}^{N-1-i} (N_{\downarrow} - j + 1)}{\prod_{j=1}^N (N - j + 1)} \right].\end{aligned}\quad (11)$$

Within anticonformity, an agent takes the opposite state to her/his neighbors, which are in the majority above the threshold r . Thus the probability β_{\uparrow} that an agent changes her/his opinion from -1 to 1 is equal to the probability that a randomly selected agent is at state -1 multiplied by the probability that at least $\lfloor r(N-1) \rfloor$ of her/his neighbors are in the state -1 . Analogously, the probability β_{\downarrow} that an agent changes her/his opinion from 1 to -1 is equal to the probability that a randomly selected agent is at state 1 multiplied by the probability that at least $\lfloor r(N-1) \rfloor$ of her/his neighbors are in the state 1 .

For the large systems $N \gg 1$ we use the following approximation, analogously as in [21]:

$$\begin{aligned}\frac{N_{\uparrow} + h}{N + g} &\approx c, \\ \frac{N_{\downarrow} + h}{N + g} &\approx 1 - c,\end{aligned}\quad (12)$$

where h, g are positive, finite constants. In such a case equations for γ^+ and γ^- take much simpler forms. For Model I,

$$\begin{aligned}\gamma^+ &= \frac{p(1-c)}{2} \\ &+ (1-p) \sum_{i=\lfloor r(N-1) \rfloor}^{N-1} \binom{N-1}{i} c^i (1-c)^{N-i}, \\ \gamma^- &= \frac{pc}{2} + (1-p) \sum_{i=\lfloor r(N-1) \rfloor}^{N-1} \binom{N-1}{i} (1-c)^i c^{N-i}.\end{aligned}\quad (13)$$

For Model A,

$$\begin{aligned}\gamma^+ &= p \sum_{i=\lfloor r(N-1) \rfloor}^{N-1} \binom{N-1}{i} (1-c)^{i+1} c^{N-1-i} \\ &+ (1-p) \sum_{i=\lfloor r(N-1) \rfloor}^{N-1} \binom{N-1}{i} c^i (1-c)^{N-i}, \\ \gamma^- &= p \sum_{i=\lfloor r(N-1) \rfloor}^{N-1} \binom{N-1}{i} c^{i+1} (1-c)^{N-1-i} \\ &+ (1-p) \sum_{i=\lfloor r(N-1) \rfloor}^{N-1} \binom{N-1}{i} (1-c)^i c^{N-i}.\end{aligned}\quad (14)$$

Complexity

7

Summations in above formulas can be calculated using the cumulative distribution function of the binomial distribution and thus we obtain for Model I

$$\begin{aligned}\gamma^+ &= (1 - c) \left[\frac{p}{2} + (1 - p) B_c \right], \\ \gamma^- &= c \left[\frac{p}{2} + (1 - p) B_{1-c} \right],\end{aligned}\quad (15)$$

and for Model A

$$\begin{aligned}\gamma^+ &= (1 - c) [p B_{1-c} + (1 - p) B_c], \\ \gamma^- &= c [p B_c + (1 - p) B_{1-c}].\end{aligned}\quad (16)$$

We use the following notation:

$$\begin{aligned}B_c &= P(X_1 \geq \lfloor r(N-1) \rfloor), \\ B_{1-c} &= P(X_2 \geq \lfloor r(N-1) \rfloor),\end{aligned}\quad (17)$$

where X_1 is a binomially distributed random variable with $N-1$ number of trials and success probability in each trial equal to c , and X_2 is a binomially distributed random variable with $N-1$ number of trials and success probability in each trial $1-c$:

$$\begin{aligned}X_1 &\sim B(N-1, c), \\ X_2 &\sim B(N-1, 1-c).\end{aligned}\quad (18)$$

For the system size N large enough, we can approximate binomial distribution by the normal one, which should simplify calculations. Unfortunately, even within such an approximation, we are not able to derive an analytical formula for $c(t)$, described by the rate equation (5). However, we can solve the equation numerically or, in a case of the finite system, calculate $c(t)$ by iterating (4).

However, usually, we are more interested in the stationary state than in the time evolution. Especially, the aim of this work is to understand the nature of phase transitions induced by the noise and thus we are interested in the dependence between the stationary value of the concentration of up spins c_{st} and the level of noise (probability of nonconformity) p .

From (4) we see that in the stationary state, the probability γ_+ and γ_- should be equal. Thus to calculate stationary values of concentration we should simply solve the equation

$$\gamma_+ - \gamma_- = 0. \quad (19)$$

Solving analytically (19), i.e., finding, c_{st} as a function of p is impossible, but we can easily derive the opposite relations satisfying (19), analogously as it was done for the q -voter model [26]. If we use formulas (15) and (16), then we obtain for Model I

$$p = \frac{c_{st} B_{1-c_{st}} - (1 - c_{st}) B_{c_{st}}}{1/2 - c_{st} - (1 - c_{st}) B_{c_{st}} + c_{st} B_{1-c_{st}}}, \quad (20)$$

whereas for Model A

$$p = \frac{B_{c_{st}} - c_{st} (B_{c_{st}} + B_{1-c_{st}})}{B_{c_{st}} - B_{1-c_{st}}}. \quad (21)$$

We have used above formulas to plot the dependency between c_{st} and probability p for several values of the threshold r on Figures 1 and 2. Although the relation $c_{st}(p)$ is unknown, only the relation $p(c_{st})$ was calculated; we can plot diagrams by rotating the figure, analogously as in [26].

3. Results

We have investigated the model within the mean-field approach, described in the previous section, as well as via the Monte Carlo simulations. We have conducted simulations for several system sizes varying from $N = 10^3$ to $N = 10^5$ and for $N = 5 \cdot 10^4$ we have obtained satisfying agreement with formulas obtained within MFA for the large system, what can be seen in Figures 1 and 2. Results were averaged only over 10 samples, but this was enough for this size of the system to get the good statistics—error bars in Figures 1 and 2 are of the same size or even smaller than the symbols. Solid lines indicate stable (attracting) steady values of concentration, whereas dashed lines indicate unstable (repelling) steady states.

It is seen that, generally, the dependence between c_{st} and p is quite trivial (linear) for both variants of the model. For $r = 0.5$, which corresponds to the simple majority, results for Model I and Model A are almost identical, only rescaled. For both models

$$c_{st} = \begin{cases} 1 - \lambda p & \text{for } p \leq \frac{1}{2\lambda} \text{ and } c(0) > \frac{1}{2} \\ 3\lambda p - 1 & \text{for } p \leq \frac{1}{2\lambda} \text{ and } c(0) < \frac{1}{2} \\ \frac{1}{2} & \text{for } p > \frac{1}{2\lambda} \end{cases} \quad (22)$$

where $\lambda = 1/2$ for Model I, whereas $\lambda = 1$ for model A. It means that for $p \leq p^* = 1/2\lambda$ there are two stable solutions: for any initial value $c(0) > 1/2$ the system eventually reaches $c_{st} = 1 - \lambda p$, whereas for any initial value $c(0) < 1/2$ the system eventually reaches $c_{st} = 3\lambda p - 1$. For $p > p^* = 1/2\lambda$ there is only one stable solution with up-down symmetry, i.e., $c_{st} = 1/2$. This behavior could be identified as the continuous phase transition, although the dependence $c_{st}(p)$ is trivial.

For any threshold $r > 0.5$, the situation is slightly more complicated. We can still identify a value $p = p^*$ below which c_{st} decays or increases monotonically with p , depending on the initial condition $c(0)$. However, this time it is not reached from arbitrary value of $c(0) \neq 1/2$. In order to reach one of the ordered state, denoted by the solid lines in Figures 1 and 2, the initial concentration of up spins $c(0)$ or alternatively initial concentration of down spins $1 - c(0)$ has to be larger than a threshold r ; i.e., $c(0) > r$ or $1 - c(0) > r \rightarrow c(0) < 1 - r$. Having this in mind, for $p < p^*(r)$ we can actually rewrite (22):

$$c_{st} = \begin{cases} 1 - \lambda p & \text{for } c(0) > r \\ 3\lambda p - 1 & \text{for } c(0) < 1 - r,\end{cases} \quad (23)$$

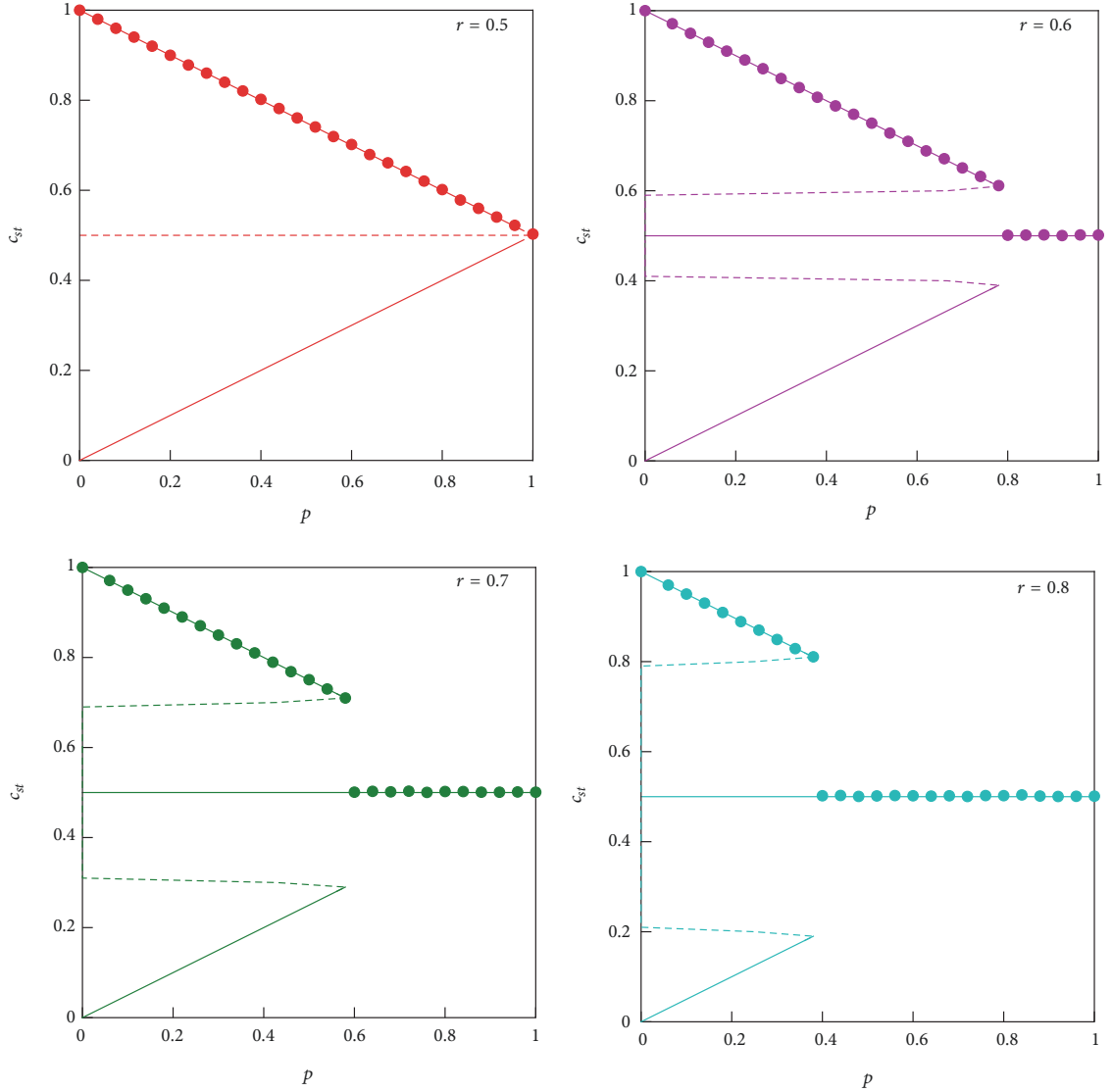


FIGURE 1: Phase diagrams for the model with independence for different values of the threshold r . Lines indicate the analytical prediction from MFA and dots represent results of the Monte Carlo simulations from the initial fully ordered state ($c(0) = 1$) for the system of size $N = 5 \cdot 10^4$.

and again $\lambda = 1/2$ for Model I, whereas $\lambda = 1$ for model A for arbitrary value of r . The threshold $p^*(r)$ can be easily derived from the condition:

$$1 - \lambda p^*(r) = r \longrightarrow p^*(r) = \frac{1-r}{\lambda}. \quad (24)$$

We see that for $r = 1/2$, we obtain $p^* = 1/2\lambda$, as expected, and (23) becomes almost identical as (22).

However, there is one crucial difference between the case $r = 1/2$ and $r > 1/2$. For $r = 1/2$, independently on the version of the model, disordered steady state $c_{st} =$

$1/2$ is unstable for $p < p^*$ and stable for $p > p^*$. For $r > 0.5$ each version of the model behaves differently. To better illustrate differences between Model I and Model A, we present trajectories for $p < p^*$ on Figure 3, as well as the flow diagrams on Figure 4 for a fixed value of $r = 0.7$.

Let us first discuss results for Model I, shown in Figure 1 and on the left panels of Figures 3 and 4. In this case, $c_{st} = 1/2$ is stable for any value of p and for $p < p^*$ two additional symmetrical unstable steady states appear: $c_{st} = r$ and $c_{st} = 1-r$. This means that from the initial state $c(0) \in (1-r, r)$ the system will be attracted to the disordered state for any value

Complexity

9

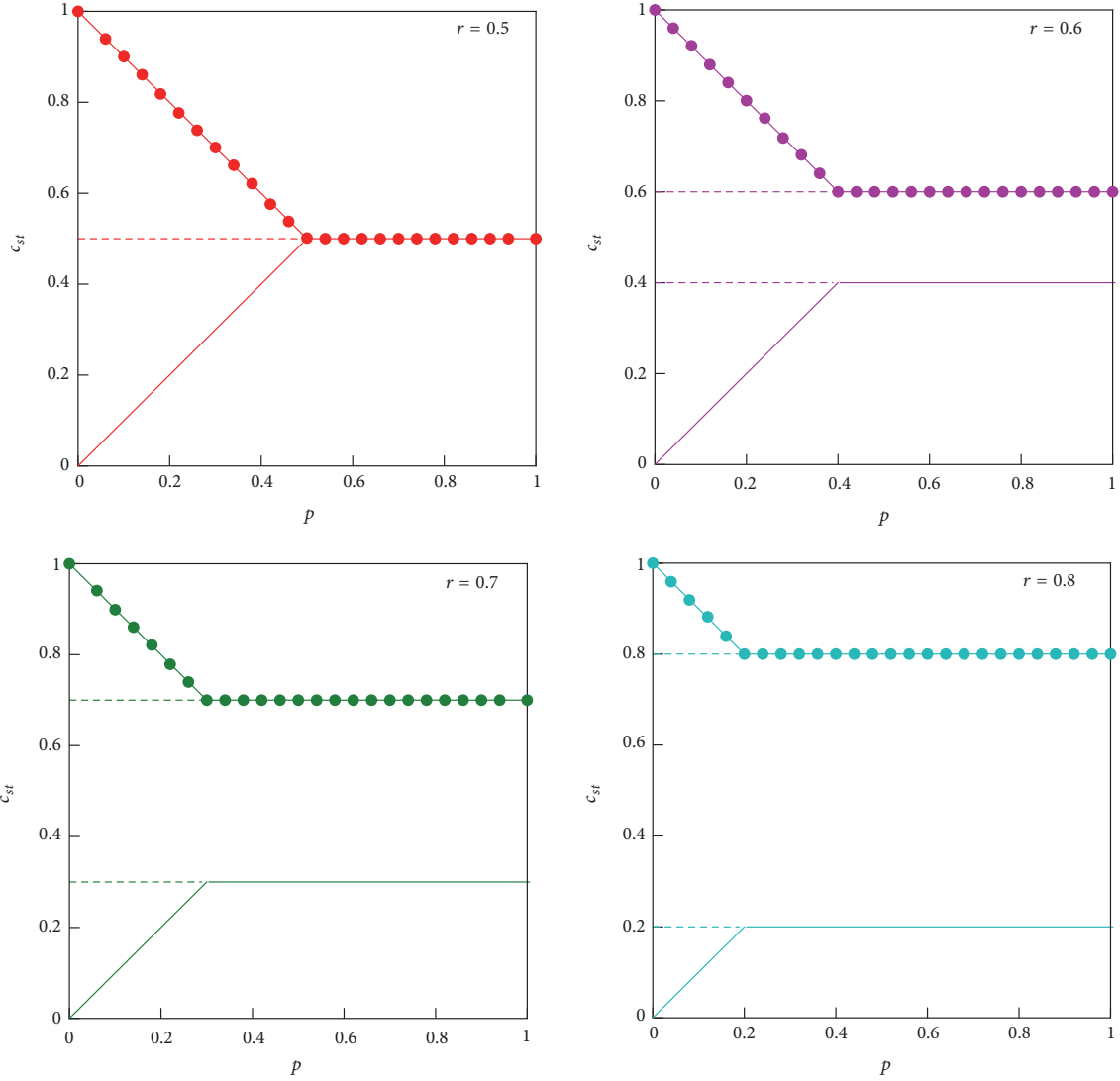


FIGURE 2: Phase diagrams for the model with anticonformity for different values of the threshold r . Lines indicate the analytical prediction from MFA and dots represent results of the Monte Carlo simulations from the initial fully ordered state ($c(0) = 1$) for the system of size $N = 5 \cdot 10^4$.

of p . In result there is jump of size $r - 1/2$ at $p = p^*(r)$, where from (24)

$$p^*(r) = 2(1 - r). \quad (25)$$

Moreover, one could also identify hysteresis, because for $p \in (0, 2(1 - r))$ the stationary concentration of up spins c_{st} depends on the initial state $c(0)$. So, looking naively at Figure 1 one could argue that for the model with independence for any value of $r > 1/2$ there is a discontinuous phase transition: the jump of the order parameter increases, whereas hysteresis decreases with growing r . Of course, again this result is trivial after a short moment of reflection, but we will discuss it later.

For the model A, as shown in Figure 2 and on the right panels of Figures 3 and 4, there is no jump and even for $p > p^* = 1 - r$ the system remains ordered; i.e., $c_{st} = r$ if we start from the initial condition $c(0) > r$ or $c_{st} = 1 - r$ if we start from the initial condition $c(0) < 1 - r$. For $c(0) \in [1 - r, r]$ system does not evolve and $c_{st} = c(0)$.

Probably, some of the readers wonder why we use such a formal approach, which eventually led to (20)-(21), as well as the time-consuming Monte Carlo simulations, if nearly all results could be easily deduced directly from the model's assumptions, without any calculations. Indeed, in the case of this model it would be possible and will be discussed in the next subsection. However, usually the standard approach

10

Complexity

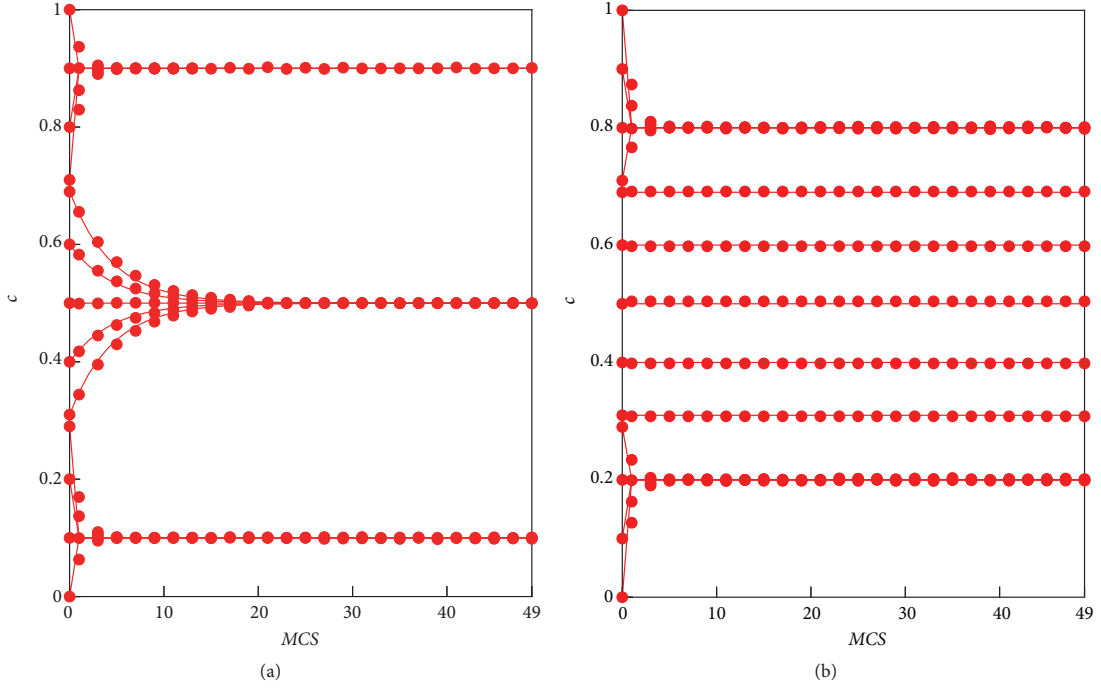


FIGURE 3: Average trajectories for the system of the size $N = 5 \cdot 10^4$ for the probability of nonconformity $p = 0.2$ and models with (a) independence and (b) anticonformity both with $r = 0.7$. Dots represent an outcome of the Monte Carlo simulations and solid lines refer to MFA results.

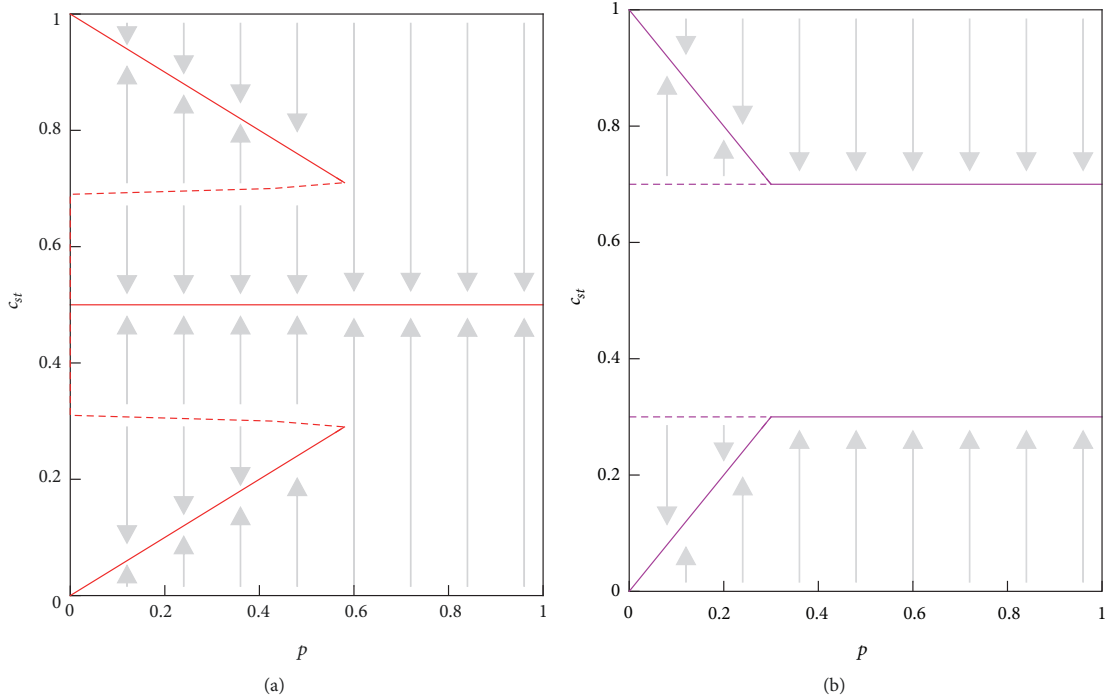


FIGURE 4: Flow diagrams for the threshold model with $r = 0.7$ with (a) independence and (b) anticonformity. Solid lines indicate stable steady states, whereas dashed lines represent unstable ones. Arrows indicate the direction of flow in the space of parameters $(c(0), p)$.

that we have presented above is the only possible way to obtain results. That was the case for q -voter model with independence for which the Monte Carlo simulations, as well as analytical results have been obtained on the complete graph [26] and on various random graphs [36]. Still, heuristically it was not explained why discontinuous phase transition appears in such a model.

Before we proceed to the heuristic explanation of the observed phenomena, let us summarize the most important results. Within the model with independence: (1) a discontinuous phase transition is observed, (2) from the completely ordered initial state the jump of the order takes place at $p^* = 2(1-r)$ and the jump size is equal $r-1/2$, and (3) consequently for $r = 0.5$ the transition is continuous. Within the model with anticonformity: (1) for $p < p^* = 1-r$ the stationary concentration of the positive opinion decays with p and for $p > p^* = 1-r$ it has a constant value $c_{st} = r$ or $c_{st} = 1-r$ depending on the initial value of $c(0)$ and (2) consequently for $r = 0.5$ a continuous phase transition is observed at $p^* = 0.5$.

3.1. Heuristic Explanation of the Obtained Results. We start with the heuristic explanation for independence. If the fraction of up spins is smaller than threshold r , i.e., $c(t) < r$ at any time t and simultaneously the fraction of down spins is smaller than threshold r , i.e., $1-c(t) < r \rightarrow c(t) > 1-r$, then, due to the model's assumptions, conformity cannot take place and changes are caused exclusively by independence. Therefore, for $c(0) \in (1-r, r)$ there are only random flips in both directions and as a result we should obtain stationary value $c_{st} = 0.5$, independently on p . Indeed we obtain such a result from simulations, as well as from analytical reasoning. For $c(0) > r$ only up spins can cause conformity and therefore with probability p spins flip randomly and with probability $1-p$ they flip up. This means that for $p=0$ the system will always reach ordered state with all spins up and thus $c_{st}=1$. On the other hand, for $p=1$ only random flips will occur, which leads to $c_{st}=1/2$. Expecting the linear dependence between c_{st} and p we can immediately draw the line, which crosses these two points $(p, c_{st}) = (0, 1)$ and $(p, c_{st}) = (1, 1/2)$; i.e., $c_{st} = 1 - p/2$. Analogous reasoning can be provided for $c(0) < 1-r$. In such a case the line $c_{st} = c_{st}(p)$ should cross points $(p, c_{st}) = (0, -1)$ and $(p, c_{st}) = (1, 1/2)$, which gives $c_{st} = 3p/2 - 1$. Alternative way to deduce the above relation is to realize that in general a fraction of p spins flips with probability $1/2$ competing with the complete order $c_{st}=1$, if only $c(0) > r$ and thus

$$c_{st} = \begin{cases} 1 - \frac{1}{2}p & \text{for } p \leq p^* \\ \frac{1}{2} & \text{for } p > p^*. \end{cases} \quad (26)$$

We obtain the value of p^* from the condition:

$$r = 1 - \frac{1}{2}p^* \rightarrow p^* = 2(1-r), \quad (27)$$

because, as written above, for $c(0) < r$ the system will reach disorder, i.e., $c = 1/2$. It should become clearer looking at Figure 4. Exactly the same results were obtained from the

Monte Carlo simulations, as well as the mean-field approach. However, this simple explanation helps to realize that the jump of c_{st} at $p^* = 2(1-r)$ is caused just because conformity cannot take place if $c(t) \in (1-r, r)$ and thus in this range the system is attracted to the disordered state with up-down symmetry.

For the model with anticonformity heuristic explanation is equally simple. If the fraction of up spins is smaller than threshold r , i.e., $c(0) < r$ and simultaneously the fraction of down spins is smaller than threshold r , i.e., $1-c(0) < r \rightarrow c(0) > 1-r$, then there is not enough social pressure for conformity, as well as for anticonformity. Therefore, for $c \in (1-r, r)$ there are no changes in the system and $\forall_t c(t) = c(0)$. For $c(0) > r$ only up spins drive changes in the system: with probability p a spin flips from \uparrow to \downarrow or with probability $1-p$ a spin flips from \downarrow to \uparrow , and thus

$$c = \begin{cases} 1 - p & \text{for } p \leq p^* \\ 1 - p^* & \text{for } p > p^*, \end{cases} \quad (28)$$

where p^* can be obtained analogously like for independence:

$$r = 1 - p^* \rightarrow p^* = 1 - r, \quad (29)$$

We can perform analogous reasoning for $c(0) < 1-r$; the only difference is that then only down spins drive changes in the system, so again the results will be symmetrical with respect to the line $c_{st} = 1/2$.

4. Discussion

The modification of the Watts threshold model that we have proposed here may be treated as a destruction of the model from the social point of view. However, our aim was not to propose a model describing properly some social phenomena but to understand the nature of the phase transitions observed within models of binary opinions with a single-flip dynamics and up-down symmetry.

It should be noticed that the Model A, proposed here, can be treated as the generalization of the original majority-vote model, which corresponds to $r = 1/2$. Within such a model only continuous phase transitions are observed, even in the presence of an additional noise [29, 39]. In [29] the model was studied via the mean-field approximation on the square lattice and it was suggested that maybe for larger number of neighbors discontinuous phase transitions would be observed. However, the same model was recently examined on various graphs and it was shown that the presence of independence does not change the type of the phase transition, which remains continuous even for highly connected networks [39]. Indeed we show here that for $r = 1/2$ transition is always continuous even in the limiting (the most connected) case of a complete graph. However, we have shown that discontinuous phase transition may appear within the model with independence for $r > 1/2$. This result agrees with those obtained for the threshold q -voter model, for which also discontinuous phase transition is possible only if $r > 1/2$ [21].

However, results obtained here help not only to understand the difference between the q -voter model and the majority-vote model, but additionally they help to understand what the difference between anticonformity and independence is. For both variants of the model proposed here, conformity cannot take place for $c(t) \in (1 - r, r)$ and thus ordering cannot occur. However, there is big difference between Model I and Model A, which cannot be visible for $r = 1/2$: independence can take place for $c(t) \in (1 - r, r)$, whereas anticonformity cannot. In result for Model I there is an attracting point $c_{st} = 1/2$ for any value of p , whereas freezing of the system, i.e., $\forall_t c(t) = c(0)$ within Model A. This causes jump between partially ordered state to the disordered state within Model I whereas freezing (and in consequence a lack of jump) within Model A.

Threshold $r > 1/2$ plays one more role, namely, introduces a kind inertia on the microscopic level. For $r = 1/2$ a spin always takes a position of majority, independently of its state, whereas for $r > 1/2$ it may happen that there is no majority above the threshold r and in such a case neighborhood does not influence a target spin. This point of view is particularly interesting if we recall recent results obtained in [47, 48]. It has been shown that inertia introduced on the microscopic level into the majority-vote model, which causes that spin-flip probability of a given spin depends not only on the states of its neighbors, but also on its own state, can change the type of the phase transition from continuous to discontinuous. Interestingly, in [48] the dependence between the order parameter, i.e., average magnetization $\langle m \rangle$, and the control parameter, i.e., the probability of anticonformity (denoted by f), was also nearly linear for $f < f^*$. Moreover $\langle m \rangle = 0$ was stable for $f \in (0, f^*)$, similarly as in our model.

Another possibility of obtaining a discontinuous phase transition has been recently suggested within the generalized threshold q -voter model, in which two types of nonconformity were introduced simultaneously [28]. It has been shown that discontinuous phase transition could be obtained even without independence if only the threshold for anticonformity would be smaller than for conformity. In the face of the reasoning carried out here, this result also becomes obvious, because the “forbidden” range for conformity is larger than for anticonformity and the jump will increase with the difference between these two thresholds.

We are aware of the fact that many people may wonder why to care about the type of the phase transition. Is there any reason, other than academic, to distinguish between continuous and discontinuous phase transitions? In the face of the social observations, and more recently also laboratory experiments, it seems that discontinuous phase transitions are particularly important, mainly because of the notion of the social hysteresis and the critical mass [49–53]. Both phenomena are strictly related to discontinuous phase transitions. There is no hysteresis within continuous phase transitions, which means that the state of the system is fully determined by the external conditions and does not depend on the history of the system. On the other hand, hysteresis, which is observed within discontinuous phase transitions, means that under the same external conditions

the system can be in different states depending on its previous states (history). The social hysteresis was observed in animal [49, 51, 52] as well as in human societies [50, 54, 55]. The second phenomenon, the so-called critical mass, which was recently observed experimentally in social convention [53], is also strongly related to the discontinuous phase transitions. Within the continuous phase transitions, there is no phase coexistence and the transition appears strictly at a given critical point due to the fluctuations and the infinite range of the correlations between them. Because of these correlations, the transition takes place immediately and simultaneously in the entire system. On the other hand, a seed (a “critical mass”) initiating the transition is needed to change the phase under discontinuous phase transition.

We realize that more interesting results could be obtained for different homogeneous and heterogeneous networks. Moreover, both noises could be introduced simultaneously as in [28, 29, 39]. However, the aim of this work was different—we wanted to understand the reason for the discontinuous phase transition in the simplest possible settings. Still, we believe that further studies of the model proposed here would be desirable task for the future, since it is a simple generalization of the majority-vote rule.

Data Availability

No data were used to support this study (no empirical data were used; only analytical calculations and Monte Carlo simulations were conducted).

Conflicts of Interest

The authors declare that they have no conflicts of interest.

Acknowledgments

This work was supported by funds from the National Science Center (NCN, Poland) through grant no. 2016/21/B/HS6/01256.

References

- [1] C. Castellano, S. Fortunato, and V. Loreto, “Statistical physics of social dynamics,” *Reviews of Modern Physics*, vol. 81, no. 2, pp. 591–646, 2009.
- [2] S. Galam, *Sociophysics: A Physicist’s Modeling of Psycho-Political Phenomena*, Springer-Verlag, New York, NY, USA, 2012.
- [3] P. Sen and B. K. Chakrabarti, *Sociophysics: An Introduction*, Oxford University Press, 2013.
- [4] A. Srba, V. Loreto, V. D. P. Servedio, and F. Tria, “Opinion dynamics: models, extensions and external effects,” in *Participatory Sensing, Opinions and Collective Awareness*, pp. 363–401, Springer, Cham, Switzerland, 2017.
- [5] G. Deffuant, D. Neau, F. Amblard, and G. Weisbuch, “Mixing beliefs among interacting agents,” *Advances in Complex Systems (ACS)*, vol. 3, pp. 87–98, 2000.
- [6] R. Hegselmann and U. Krause, “Opinion dynamics and bounded confidence: models, analysis and simulation,” *Journal of Artificial Societies and Social Simulation*, vol. 5, no. 3, 2002.

- [7] T. Krueger, J. Szwabiński, and T. Weron, “Conformity, anticonformity and polarization of opinions: insights from a mathematical model of opinion dynamics,” *Entropy*, vol. 19, no. 7, p. 371, 2017.
- [8] K. Sznajd-Weron, J. Szwabiński, R. Weron, and T. Weron, “Rewiring the network. What helps an innovation to diffuse?” *Journal of Statistical Mechanics: Theory and Experiment*, vol. 2014, no. 3, p. P03007, 2014.
- [9] K. Byrka, A. Jędrzejewski, K. Sznajd-Weron, and R. Weron, “Difficulty is critical: The importance of social factors in modeling diffusion of green products and practices,” *Renewable & Sustainable Energy Reviews*, vol. 62, pp. 723–735, 2016.
- [10] T. Weron, A. Kowalska-Pyzalska, and R. Weron, “The role of educational trainings in the diffusion of smart metering platforms: An agent-based modeling approach,” *Physica A: Statistical Mechanics and its Applications*, vol. 505, pp. 591–600, 2018.
- [11] S. Galam, “From 2000 Bush–Gore to 2006 Italian elections: voting at fifty-fifty and the contrarian effect,” *Quality & Quantity*, vol. 41, no. 4, pp. 579–589, 2007.
- [12] S. Galam, “The Trump phenomenon: an explanation from sociophysics,” *International Journal of Modern Physics B*, vol. 31, no. 10, 17 pages, 2017.
- [13] S. Galam, “Unavowed abstention can overturn poll predictions,” *Frontiers in Physics*, vol. 6, 24 pages, 2018, <https://www.frontiersin.org/article/10.3389/fphy.2018.00024>.
- [14] T. M. Liggett, *Interacting Particle Systems*, Springer, 1985.
- [15] T. Tome, M. J. Oliveira, and M. A. Santos, “Non-equilibrium Ising model with competing Glauber dynamics,” *Journal of Physics A: Mathematical and General*, vol. 24, no. 15, pp. 3677–3686, 1991.
- [16] M. J. de Oliveira, “Isotropic majority-vote model on a square lattice,” *Journal of Statistical Physics*, vol. 66, no. 1-2, pp. 273–281, 1992.
- [17] S. Galam, “Social paradoxes of majority rule voting and renormalization group,” *Journal of Statistical Physics*, vol. 61, no. 3-4, pp. 943–951, 1990.
- [18] K. Sznajd-Weron and J. Sznajd, “Opinion evolution in closed community,” *International Journal of Modern Physics C*, vol. 11, no. 6, pp. 1157–1165, 2000.
- [19] D. J. Watts, “A simple model of global cascades on random networks,” *Proceedings of the National Academy of Sciences of the United States of America*, vol. 99, no. 9, pp. 5766–5771, 2002.
- [20] C. Castellano, M. A. Muñoz, and R. Pastor-Satorras, “Pastor-Satorras, Nonlinear q-voter model,” *Physical Review E: Statistical, Nonlinear, and Soft Matter Physics*, vol. 80, no. 4, 2009.
- [21] P. Nyczka and K. Sznajd-Weron, “Anticonformity or independence?—insights from statistical physics,” *Journal of Statistical Physics*, vol. 151, no. 1-2, pp. 174–202, 2013.
- [22] A. R. Vieira and C. Anteneodo, “Threshold q-voter model,” *Physical Review E: Statistical, Nonlinear, and Soft Matter Physics*, vol. 97, no. 5, 2018.
- [23] J. P. Gleeson, “Binary-state dynamics on complex networks: pair approximation and beyond,” *Physical Review X*, vol. 3, no. 2, 2013.
- [24] M. Granovetter, “Threshold models of collective behavior,” *American Journal of Sociology*, vol. 83, no. 6, pp. 1420–1443, 1978.
- [25] A. Jędrzejewski and K. Sznajd-Weron, “Impact of memory on opinion dynamics,” *Physica A: Statistical Mechanics and its Applications*, vol. 505, pp. 306–315, 2018.
- [26] P. Nyczka, K. Sznajd-Weron, and J. Cislo, “Phase transitions in the q-voter model with two types of stochastic driving,” *Physical Review E: Statistical, Nonlinear, and Soft Matter Physics*, vol. 86, no. 1, 2012.
- [27] D. J. Watts and P. S. Dodds, “Influentials, networks, and public opinion formation,” *Journal of Consumer Research*, vol. 34, no. 4, pp. 441–458, 2007.
- [28] P. Nyczka, K. Byrka, P. R. Nail, K. Sznajd-Weron, and N. Fytas, “Conformity in numbers—Does criticality in social responses exist?” *PLoS ONE*, vol. 13, no. 12, p. e0209620, 2018.
- [29] A. R. Vieira and N. Crokidakis, “Phase transitions in the majority-vote model with two types of noises,” *Physica A: Statistical Mechanics and its Applications*, vol. 450, pp. 30–36, 2016.
- [30] S. Oh and M. A. Porter, “Complex contagions with timers,” *Chaos: An Interdisciplinary Journal of Nonlinear Science*, vol. 28, no. 3, p. 033101, 2018.
- [31] A. Jędrzejewski and K. Sznajd-Weron, “Statistical physics of opinion formation: is it a spoof?” 2019, <https://arxiv.org/abs/1903.04786>.
- [32] S. Galam, “Sociophysics: a review of galam models,” *International Journal of Modern Physics C*, vol. 19, no. 3, pp. 409–440, 2008.
- [33] S. Galam, “The drastic outcomes from voting alliances in three-party democratic voting (1990 → 2013),” *Journal of Statistical Physics*, vol. 151, no. 1-2, pp. 46–68, 2013.
- [34] P. R. Nail, G. MacDonald, and D. A. Levy, “Proposal of a four-dimensional model of social response,” *Psychological Bulletin*, vol. 126, no. 3, pp. 454–470, 2000.
- [35] P. R. Nail, S. I. Di Domenico, and G. MacDonald, “Proposal of a double diamond model of social response,” *Review of General Psychology*, vol. 17, no. 1, pp. 1–19, 2013.
- [36] A. Jędrzejewski, “Pair approximation for the q-voter model with independence on complex networks,” *Physical Review E: Statistical, Nonlinear, and Soft Matter Physics*, vol. 95, no. 1, 2017.
- [37] A. Chmiel and K. Sznajd-Weron, “Phase transitions in the q-voter model with noise on a duplex clique,” *Physical Review E: Statistical, Nonlinear, and Soft Matter Physics*, vol. 92, no. 5, 2015.
- [38] A. F. Peralta, A. Carro, M. San Miguel, and R. Toral, “Analytical and numerical study of the non-linear noisy voter model on complex networks,” *Chaos: An Interdisciplinary Journal of Nonlinear Science*, vol. 28, no. 7, p. 075516, 2018.
- [39] J. Encinas, H. Chen, M. M. de Oliveira, and C. E. Fiore, “Majority vote model with ancillary noise in complex networks,” *Physica A: Statistical Mechanics and its Applications*, vol. 516, pp. 563–570, 2019.
- [40] M. Mobilia, “Nonlinear q-voter model with inflexible zealots,” *Physical Review E: Statistical, Nonlinear, and Soft Matter Physics*, vol. 92, no. 1, 2015.
- [41] A. Mellor, M. Mobilia, and R. K. Zia, “Characterization of the nonequilibrium steady state of a heterogeneous nonlinear q-voter model with zealotry,” *EPL (Europhysics Letters)*, vol. 113, no. 4, p. 48001, 2016.
- [42] A. Mellor, M. Mobilia, and R. K. Zia, “Heterogeneous out-of-equilibrium nonlinear q-voter model with zealotry,” *Physical Review E: Statistical, Nonlinear, and Soft Matter Physics*, vol. 95, no. 1, 2017.
- [43] P. Nyczka, J. Cislo, and K. Sznajd-Weron, “Opinion dynamics as a movement in a bistable potential,” *Physica A: Statistical Mechanics and its Applications*, vol. 391, no. 1-2, pp. 317–327, 2012.

- [44] L. D. Landau, “On the theory of phase transitions,” *Journal of Experimental and Theoretical Physics*, vol. 7, pp. 19–32, 1937.
- [45] H. Hinrichsen, “Non-equilibrium critical phenomena and phase transitions into absorbing states,” *Advances in Physics*, vol. 49, no. 7, pp. 815–958, 2000.
- [46] P. L. Krapivsky, S. Redner, and E. Ben-Naim, *A Kinetic View of Statistical Physics*, Cambridge University Press, 2010.
- [47] H. Chen, C. Shen, H. Zhang, G. Li, Z. Hou, and J. Kurths, “First-order phase transition in a majority-vote model with inertia,” *Physical Review E: Statistical, Nonlinear, and Soft Matter Physics*, vol. 95, no. 4, 2017.
- [48] J. M. Encinas, P. E. Harunari, M. M. de Oliveira, and C. E. Fiore, “Fundamental ingredients for discontinuous phase transitions in the inertial majority vote model,” *Scientific Reports*, vol. 8, no. 1, 2018.
- [49] M. Beekman, D. J. Sumpter, and F. L. Ratnieks, “Phase transition between disordered and ordered foraging in Pharaoh’s ants,” *Proceedings of the National Academy of Sciences of the United States of America*, vol. 98, no. 17, pp. 9703–9706, 2001.
- [50] M. Scheffer, F. Westley, and W. Brock, “Slow Response of Societies to New Problems: Causes and Costs,” *Ecosystems*, vol. 6, no. 5, pp. 493–502, 2003.
- [51] J. N. Pruitt, A. Berdahl, C. Riehl et al., “Social tipping points in animal societies,” *Proceedings of the Royal Society B Biological Science*, vol. 285, no. 1887, p. 20181282, 2018.
- [52] G. N. Doering, I. Scharf, H. V. Moeller, and J. N. Pruitt, “Social tipping points in animal societies in response to heat stress,” *Nature Ecology & Evolution*, vol. 2, no. 8, pp. 1298–1305, 2018.
- [53] D. Centola, J. Becker, D. Brackbill, and A. Baronchelli, “Experimental evidence for tipping points in social convention,” *Science*, vol. 360, no. 6393, pp. 1116–1119, 2018.
- [54] J. Elster, “A note on hysteresis in the social sciences,” *Synthese*, vol. 33, no. 1, pp. 371–391, 1976.
- [55] A. Clark, “Unemployment as a social norm: psychological evidence from panel data,” *Journal of Labor Economics*, vol. 21, no. 2, pp. 323–351, 2003.

A.2 Article 2

Symmetrical threshold model with independence on random graphs

Symmetrical threshold model with independence on random graphs

Bartłomiej Nowak * and Katarzyna Sznajd-Weron †

Department of Theoretical Physics, Wrocław University of Science and Technology, Wrocław, Poland



(Received 28 February 2020; revised manuscript received 5 May 2020; accepted 7 May 2020; published 22 May 2020)

We study the homogeneous symmetrical threshold model with independence (noise) by pair approximation and Monte Carlo simulations on Erdős-Rényi and Watts-Strogatz graphs. The model is a modified version of the famous Granovetter's threshold model: with probability p a voter acts independently, i.e., takes randomly one of two states ± 1 ; with complementary probability $1 - p$, a voter takes a given state, if a sufficiently large fraction (above a given threshold r) of individuals in its neighborhood is in this state. We show that the character of the phase transition, induced by the noise parameter p , depends on the threshold r , as well as graph's parameters. For $r = 0.5$ only continuous phase transitions are observed, whereas for $r > 0.5$ discontinuous phase transitions also are possible. The hysteresis increases with the average degree $\langle k \rangle$ and the rewriting parameter β . On the other hand, the dependence between the width of the hysteresis and the threshold r is nonmonotonic. The value of r , for which the maximum hysteresis is observed, overlaps pretty well with the size of the majority used for the descriptive norms in order to manipulate people within social experiments. We put the results obtained within this paper into a broader picture and discuss them in the context of two other models of binary opinions: the majority-vote and the q -voter model. Finally, we discuss why the appearance of social hysteresis in models of opinion dynamics is desirable.

DOI: [10.1103/PhysRevE.101.052316](https://doi.org/10.1103/PhysRevE.101.052316)

I. INTRODUCTION

It is not surprising that binary opinion models are extremely popular among sociophysicists, given that the 1/2-spin Ising model is not only one of the most popular models of theoretical physics, but also absolutely fundamental for the theory of phase transitions. However, what is probably more surprising is that the binary-choice models have received considerably more theoretical attention than other choice models among social psychologists, sociologists, and economists [1,2]. One of the most important class of such models are the threshold models [3,4] taking root in the pioneering paper by Granovetter [5].

The idea behind these models is extremely simple—an agent takes state 1 (which can be interpreted as agree, adopt the innovation, join the riot, etc.) if a sufficiently large fraction (above a given threshold) of people in his or her neighborhood is in state 1. Originally the model was investigated under the assumption of perfect mixing (all-to-all interactions). However, in 2002 Watts adapted Granovetter's threshold model to a network framework [3]. We will use the same approach here, and therefore individuals will be influenced only by the nearest neighbors; i.e., interactions will take place only between agents that are directly linked.

There are two important differences between the Watts threshold model and other models of binary opinions, such as the Galam model [6–8], the majority-vote (MV) [9–20], the q -voter (qV) [21–28], or the threshold q -voter (TqV)

model [29–32]. The first difference, often considered the most important, is the heterogeneity—each agent is described by an individual threshold, and therefore some agents adopt a new state very easily, whereas others don't [3]. The second difference, which should be particularly important for physicists, is the lack of the up-down symmetry. Once an agent adopts a state 1 it cannot go back to the previous one. To make the threshold model comparable with other binary opinion models, we have introduced recently the homogeneous symmetrical threshold model [33]. Here we will call this model simply the symmetrical threshold (ST) model for brevity.

Previously we have studied two versions of the ST model, each with a different type of nonconformity (anticonformity or independence) on the complete graph [33]. Therefore we were able to obtain exact analytical results within the mean-field approach. Analogously as in other models of binary opinions, the introduction of nonconformity, whether in the form of anticonformity or in the form of independence, resulted in the appearance of the agreement-disagreement phase transitions. We have shown, that for the threshold $r = 0.5$, which corresponds to the majority-vote model, the phase transition is continuous, whereas for $r > 0.5$ discontinuous phase transitions appear within the model with independence. For the model with anticonformity, phase transitions are continuous for an arbitrary value of r . A similar phenomenon has been observed previously for the q -voter model—within the model with anticonformity, only continuous phase transitions are observed, whereas within the model with independence (known also as the nonlinear noisy voter model), discontinuous phase transitions appear for $q > 5$ [28,34,35].

In this paper we focus on the ST model with independence, because the hysteresis and tipping points, two signatures of

*bartłomiej.nowak@pwr.edu.pl

†katarzyna.weron@pwr.edu.pl

a discontinuous phase transitions, are common features of complex social systems [36–38]. We study the model on Erdős-Rényi (ER) and Watts-Strogatz (WS) graphs [39]. For the ER graph the pair approximation (PA) should give an accurate result, whereas the WS graph allows us to tune the structure from (1) the complete graph, for which the mean-field approximation (MFA) gives an exact result, through (2) random graphs for which the PA should work properly, to (3) small-world networks, which resemble the basic features of the real social networks. Because it has been shown recently that the size of the hysteresis may depend on the graph's properties, we focus on this issue and check to what extend results found within the MV model and the qV model are universal [14,15,19,20,28,40].

II. MODEL

We consider a system of N individuals placed in the nodes of an arbitrary graph. Each node represents exactly one individual (interchangeably called *an agent*, *a spin*, or *a voter*). We consider a model of binary opinions, beliefs, and decisions, and thus each voter at time t is described by a binary dynamical variable $S_i(t) = \pm 1(\uparrow / \downarrow)$. At each elementary update Δt :

- (1) A site i is randomly chosen from the entire graph,
- (2) An agent at site i acts independently with probability p , i.e., changes its opinion to the opposite one $S_i(t + \Delta t) = -S_i(t)$ with probability $\frac{1}{2}$,
- (3) With complementary probability $1 - p$ it conforms to its k_i neighbors if the fraction of its neighbors in the same state is larger than r :

- (a) $S_i(t + \Delta t) = 1$ if more than $r k_i$ neighbors are in the state 1 or
- (b) $S_i(t + \Delta t) = -1$ if more than $r k_i$ neighbors are in the state -1 .

As usual, a single Monte Carlo step consists of N updates, $\Delta t = 1/N$, which means that one time unit corresponds to the mean update time of a single individual. Under the above algorithm the following changes are possible in the system:

$$\begin{array}{c}
 \overbrace{\uparrow\uparrow \dots \uparrow}^{>\lfloor rk_i \rfloor} \downarrow \xrightarrow{1-p} \overbrace{\uparrow\uparrow \dots \uparrow}^{>\lfloor rk_i \rfloor} \uparrow, \\
 \downarrow \xrightarrow{1-p} \overbrace{\downarrow\downarrow \dots \downarrow}^{>\lfloor rk_i \rfloor} \uparrow, \\
 \text{any configuration} \xrightarrow{p/2} \text{any configuration} \\
 \downarrow \xrightarrow{p/2} \uparrow, \\
 \text{any configuration}
 \end{array} \quad (1)$$

where \downarrow and \uparrow denote states of a target agent, and $\lfloor rk_i \rfloor$ is the floor function of $r k_i$. In any other situation, the state of the system does not change.

In the Watts threshold model flipping from \uparrow to \downarrow , was forbidden [3]. Therefore, the model was asymmetrical contrary to the majority vote or the q voter.

In the original threshold model an arbitrary value of $r \in [0, 1]$ is possible, which is a reasonable assumption for the asymmetrical model describing the adoption to the new state. In the symmetrical case, the situation for $r < 0.5$ is less obvious. It can be easily seen within the following example: let the threshold $r < 0.5$ and the neighborhood of a target voter consist of 50% positive and 50% negative agents. It means that both opinions (positive and negative) could be adopted by the voter. Which one should be chosen in such a situation?

There are several possibilities to solve the above ambiguity, e.g., we can assume that (1) a voter prefers to change opinion and therefore will always change it to the opposite one whenever possible [30,32], (2) a voter prefers to keep an old opinion—this assumption overlaps $r \geq 0.5$ [29,33], or (3) a voter makes a random decision to flip or keep an old state. Each of these scenarios can be used. However, for modeling opinion or belief formation the second one, $r \geq 0.5$, seems to be the most justified from the social point of view [31].

III. ANALYTICAL APPROACH WITHIN PAIR APPROXIMATION

Our analytical approach is based on the pair approximation (PA), an improved version of the standard mean-field approximation (MFA), which already has been applied to various binary-state dynamics on complex networks [28,32,41,42].

Because at each elementary update only one voter can change his or her opinion, thus the number of agents with positive opinion N_\uparrow increases or decreases by 1 or remains constant. As in Ref. [34] we denote by $c = N_\uparrow/N$ the concentration of the positive opinion, which in an elementary time step increases or decreases by $\frac{1}{N}$ or remains constant. We also denote transition probabilities as in Ref. [22]:

$$\begin{aligned}
 \gamma^+ &= \text{Prob} \left[c(t + \Delta t) = c(t) + \frac{1}{N} \right], \\
 \gamma^- &= \text{Prob} \left[c(t + \Delta t) = c(t) - \frac{1}{N} \right], \\
 \gamma^0 &= \text{Prob} [c(t + \Delta t) = c(t)] = 1 - \gamma^+ - \gamma^-.
 \end{aligned} \quad (2)$$

For $N \rightarrow \infty$ we can safely assume that random variable c localizes to the expectation value, and we get the following continuous-time dynamical system:

$$\frac{dc}{dt} = \gamma^+ - \gamma^-, \quad (3)$$

in the rescaled time units t . The simplest and the most popular approach under which formulas for transition probabilities γ^\pm can be derived analytically is the simple mean-field approximation [21–23,29–31,33]. It gives very good agreement for the complete graph, but rarely for more complicated structures, because it neglects all fluctuations in the system by assuming that the local concentration of spins up is equal to the global one.

Another method, which works particularly well for random graphs with low clustering coefficient, is the pair

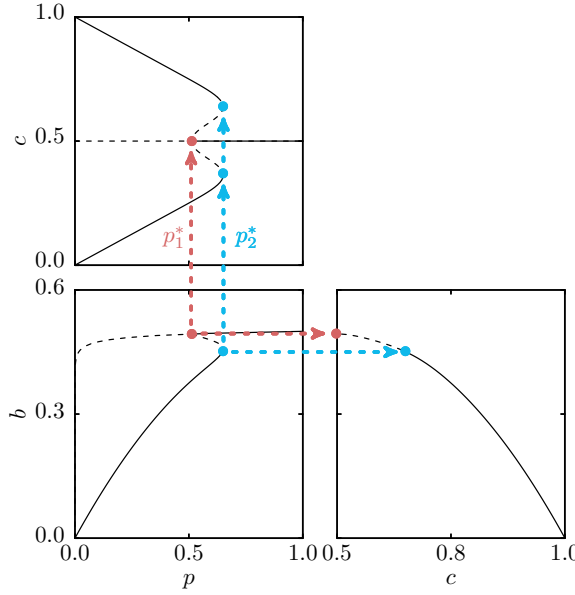


FIG. 1. Dependencies between the stationary value of the concentration of spins up c and active bonds b and the noise p obtained within the PA for sample values of parameters $\langle k \rangle = 80$ and $r = 0.6$. Results are presented in three phase-space projections: (c, p) , (b, p) , and (b, c) . For $p < p_1^*$ the only stable solution is the ordered phase, in which the symmetry between \uparrow and \downarrow states is broken, whereas for $p > p_2^*$ the only stable solution is the disordered phase.

approximation. Within the PA we describe the system by two differential equations—one for the time evolution of the concentration c of spins up and the second one for the time evolution of the concentration b of active bonds or links (bonds between two opposite spins) [2,28,41]:

$$\frac{dc}{dt} = - \sum_{j \in \{1, -1\}} c_j \sum_k P(k) \sum_{i=0}^k \binom{k}{i} \theta_j^i (1 - \theta_j)^{k-i} f(i, r, k, p) j, \quad (4)$$

$$\frac{db}{dt} = \frac{2}{\langle k \rangle} \sum_{j \in \{1, -1\}} c_j \sum_k P(k) \sum_{i=0}^k \binom{k}{i} \theta_j^i (1 - \theta_j)^{k-i} f(i, r, k, p) (k - 2i), \quad (5)$$

where c_j is the concentration of spins in state $j = \pm 1$ and thus $c_1 = c$, $c_{-1} = 1 - c$, $P(k)$ is the degree distribution of a graph and $\langle k \rangle$ is the average node degree. The parameter θ_j is the conditional probability of selecting a node that is in the opposite state to its neighbor in a state j , which is equivalent to the probability of choosing an active link from all links of a node in state j and can be approximated by [2,28]

$$\theta_j = \frac{b}{(2c_j)}, \quad (6)$$

where $f(i, r, k, p)$ is the flipping probability, i.e., the probability that a node in state j changes its state under the condition that exactly i from its k links are active.

Within our version of the threshold model, a voter flips with probability $1/2$ due to the independence, which takes place with probability p or due to the conformity, which takes place with probability $1 - p$ if more than $\lfloor rk \rfloor$ of its nearest neighbors are in the opposite state and thus

$$f(i, r, k, p) = \frac{p}{2} + (1 - p) \mathbb{1}_{\{i > \lfloor rk \rfloor\}}, \quad (7)$$

where $\mathbb{1}_{\{i > \lfloor rk \rfloor\}}$ is the indicator function, i.e. giving 1 for $i > \lfloor rk \rfloor$ and 0 otherwise.

In this paper, we focus mainly on the WS graph, because it allows us to tune the structure from the one with a high clustering coefficient and high average path length to the one with a low clustering coefficient and low average path length, by changing the parameter (rewiring probability) β without changing the average node degree $\langle k \rangle$. The degree probability $P(k)$ for such a network equals [43]

$$P(k) = \sum_{n=0}^{\min(k-\langle k \rangle/2, \langle k \rangle/2)} \binom{\langle k \rangle/2}{n} (1 - \beta)^n \beta^{k/2 - n} \times \frac{(\beta \langle k \rangle/2)^{k-\langle k \rangle/2-n}}{(k - \langle k \rangle/2 - n)!} e^{-\beta \langle k \rangle/2}. \quad (8)$$

The PA works properly for small clustering coefficients which correspond to large values of β . Moreover, under the assumption $\beta \rightarrow 1$, calculations simplify substantially, since Eq. (8) reduces to

$$P(k) = \frac{(\langle k \rangle/2)^{k-\langle k \rangle/2}}{(k - \langle k \rangle/2)!} e^{-\langle k \rangle/2}. \quad (9)$$

Therefore, we take in further calculations $P(k)$ given by Eq. (9), which is very close to the Poisson distribution centered at mean value $\langle k \rangle$ for the ER graph.

After inserting $f(i, r, k, p)$, given by Eq. (7), into Eqs. (4) and (5) we obtain

$$\begin{aligned} \frac{dc}{dt} = & - \sum_{j \in \{1, -1\}} c_j \sum_k P(k) \\ & \times \left[\frac{jp}{2} + j(1-p) \sum_{i=\lfloor rk \rfloor+1}^k \binom{k}{i} \theta_j^i (1 - \theta_j)^{k-i} \right], \end{aligned} \quad (10)$$

$$\begin{aligned} \frac{db}{dt} = & \frac{2}{\langle k \rangle} \sum_{j \in \{1, -1\}} c_j \sum_k P(k) \left[pk \left(\frac{1}{2} - \theta_j \right) \right. \\ & \left. + (1-p) \sum_{i=\lfloor rk \rfloor+1}^k \binom{k}{i} \theta_j^i (1 - \theta_j)^{k-i} (k - 2i) \right]. \end{aligned} \quad (11)$$

The steady states can be obtained by solving the following equations:

$$\frac{dc}{dt} = 0, \quad (12)$$

$$\frac{db}{dt} = 0. \quad (13)$$

Analogously as for the q -voter model with independence, we are not able to solve the above equations explicitly, but we can obtain inverse relation $p = p(c)$, instead of $c = c(p)$ [34]. For the concentration of active bonds we can present only an implicit solution.

One solution of Eq. (12), namely, $c = 1/2$, is straightforward because it is seen that for this value the right side of Eq. (10) equals zero, i.e., point $c = 1/2$ is the fixed point for all values of p . On the other hand, the right side of Eq. (11) is nonzero at $c = 1/2$ for arbitrary p ; thus from Eq. (13) for $c = 1/2$ we can derive the relation $p(b)$:

$$p = \frac{\sum_k P(k) \sum_{i=\lfloor rk \rfloor + 1}^k \binom{k}{i} b^i (1-b)^{k-i} (k-2i)}{-\langle k \rangle \left(\frac{1}{2} - b\right) + \sum_k P(k) \sum_{i=\lfloor rk \rfloor + 1}^k \binom{k}{i} b^i (1-b)^{k-i} (k-2i)}. \quad (14)$$

We see that $b \rightarrow 0$ gives $p = 0$ and $b \rightarrow 1/2$ gives $p = 1$.

To show the behavior of the system for $c \neq 1/2$ we insert Eq. (10) to Eq. (12), which allows us to derive the relation

$$p = \frac{\sum_k P(k) \sum_{i=\lfloor rk \rfloor + 1}^k \binom{k}{i} \left[c\theta_{\uparrow}^i (1-\theta_{\uparrow})^{k-i} - (1-c)\theta_{\downarrow}^i (1-\theta_{\downarrow})^{k-i} \right]}{\frac{1}{2} - c + \sum_k P(k) \sum_{i=\lfloor rk \rfloor + 1}^k \binom{k}{i} \left[c\theta_{\uparrow}^i (1-\theta_{\uparrow})^{k-i} - (1-c)\theta_{\downarrow}^i (1-\theta_{\downarrow})^{k-i} \right]}, \quad (15)$$

where we denote $\theta_{1/-1}$ by $\theta_{\uparrow/\downarrow}$ for clarity. Note that the above equation is in fact the relation $p = p(c, b)$, because both b and c are implicitly included in θ_{\uparrow} and θ_{\downarrow} according to Eq. (6). Thus, to solve the above equation we need the relation $b = b(c)$, which can be obtained by inserting the above equation into Eq. (13):

$$0 = \sum_k P(k) \sum_{i=\lfloor rk \rfloor + 1}^k \binom{k}{i} \{c\theta_{\uparrow}^i \times (1-\theta_{\uparrow})^{k-i} [\langle k \rangle (1-2b) + (1-2c)(k-2i)] + (1-c)\theta_{\downarrow}^i (1-\theta_{\downarrow})^{k-i} [(1-2c)(k-2i) - \langle k \rangle (1-2b)]\} \quad (16)$$

As we have noticed above, Eq. (15) gives the relation $p = p(c, b)$, which can be plotted in three different planes, as shown in Fig. 1. There are two critical points, seen in this plot: (1) $p = p_1^*$, in which the solution $c = 1/2$ loses stability (so-called lower spinodal) and (2) $p = p_2^*$, in which the solution $c = c(p) \neq 1/2$, given by Eq. (15), loses stability. There are several possibilities to calculate $p = p_1^*$ [22,28,31]. Here we use method based on the observation that $p = p_1^*$ corresponds to the point $c = 1/2$ in the relation $b = b(c)$ (right bottom panel of Fig. 1). Therefore, first we take a limit $c \rightarrow 1/2$ in Eq. (16), which gives

$$0 = \sum_k P(k) \sum_{i=\lfloor rk \rfloor + 1}^k \binom{k}{i} b^i (1-b)^{k-i} \times \left[k - \langle k \rangle (1-2b) \left(1 + \frac{kb}{1-b} \right) - 2i + \langle k \rangle (1-2b) \left(1 + \frac{b}{1-b} \right) i \right]. \quad (17)$$

and then derive b from the above equation. Finally we insert this value of b into Eq. (14), which gives $p = p_1^*$. The upper

spinodal, i.e., point $p = p_2^*$, where $p = p(c)$ has two maxima (see Fig. 1), can be calculated numerically from Eq. (15) by taking a maximum value of p .

IV. DISCUSSION OF THE PAIR APPROXIMATION RESULTS

It was shown that for the majority-vote model with inertia there are two ingredients responsible for the discontinuous phase transitions: (1) the level of inertia and (2) the average node degree $\langle k \rangle$ [15,19]. Similarly, for the q -voter model (1) the size of the influence group q and (2) $\langle k \rangle$ are key factors influencing the type of the phase transition [28,34,40]. The question is if the same can be seen within the ST model.

The first ingredient influencing the phase transition is studies in the previous paper already within the mean-field approach [33]. We have observed continuous phase transitions for $r = 0.5$ and discontinuous ones for $r > 0.5$. We have obtained a similar result within the PA, as shown in Fig. 2: for small values of r we observe a continuous phase transition, whereas for large r a discontinuous one. This result is similar to results obtained within the MV model with inertia and the qV model. In both models discontinuous phase transitions were observed only for the sufficiently large value of inertia θ [15,19] or the large size of the influence group q [28,34]. It should be noticed that both the large size of the influence group q and the high threshold r correspond to the high value of inertia:

qV model: it is unlikely that we find a unanimous group of size q if q is large

ST model: it is unlikely that we find a fraction of agents in the same state larger than r if r is large.

Therefore, in both cases a voter is unlikely influenced by neighbors, i.e., its inertia is larger.

Now it is time to investigate the second ingredient, namely, to check whether $\langle k \rangle$ influences phase transitions within the ST model. In Fig. 3 we present the dependence between the

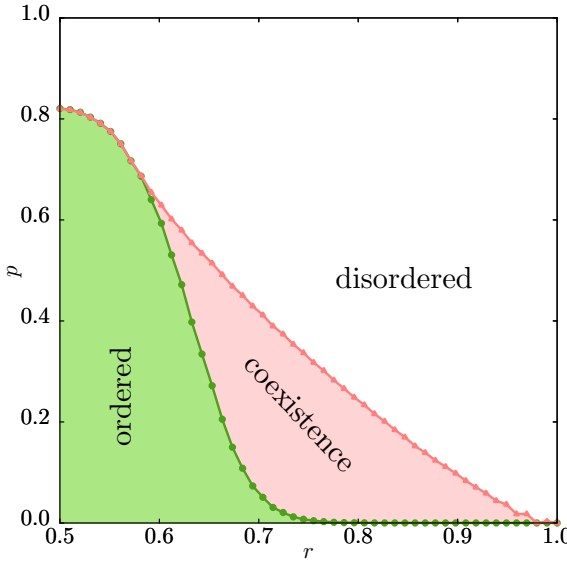


FIG. 2. Phase diagram for the average degree $\langle k \rangle = 50$. Lines with \bullet and \blacktriangle represent spinodals obtained within PA from Eqs. (15)–(17), i.e., limits of the region with metastability, in which the final state depends on the initial one.

stationary concentration of spins up c and the noise p for several values of the average node degree of the network $\langle k \rangle$ and two values of the threshold r . Again we see that for $r = 0.5$ only continuous phase transitions are observed independently of $\langle k \rangle$. However, for $r = 0.6$ the character of the phase transition changes with $\langle k \rangle$. Similarly as for the MV model with inertia and the qV model, the width of the hysteresis increases with $\langle k \rangle$ [15,19,40].

To the best of our knowledge, the dependence between the size of the hysteresis and $\langle k \rangle$ was not investigated precisely for the MV model with inertia. However, for the q -voter model it has been shown that $\langle k \rangle$ influences substantially the width of

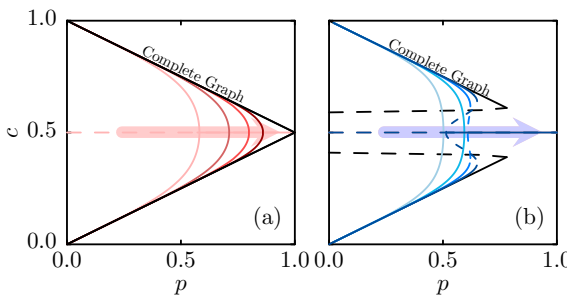


FIG. 3. Dependence between the stationary concentration of spins up c and the noise p for several values of the average node degree $\langle k \rangle$ and two values of the threshold: (a) $r = 0.5$ and (b) $r = 0.6$. Thin (red and blue colors online) lines refer to different values of $\langle k \rangle \in \{10, 20, 40, 80\}$ from left to right, whereas thick black lines represent the mean-field solution. Arrows indicate the direction in which $\langle k \rangle$ increases.

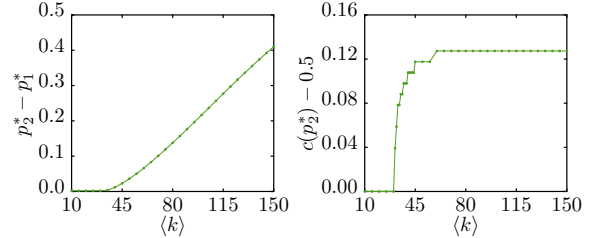


FIG. 4. The width of hysteresis $p_2^* - p_1^*$ (left panel) and the jump of the public opinion c (right panel) as a function of the average node degree $\langle k \rangle$ for threshold $r = 0.6$ obtained within PA.

the hysteresis and has almost no influence on the jump of the order parameter, defined as [40]

$$m = \frac{N_\uparrow - N_\downarrow}{N} = 2\frac{N_\uparrow}{N} - 1 = 2c - 1. \quad (18)$$

In this paper we did not introduce the order parameter m , because we made all calculations in terms of c . Of course, we could easily reformulate all results using the simple relation between m and c , given by Eq. (18).

In Ref. [40] the jump of m has been measured at upper spinodal. Therefore we also measure a jump of c at this point, i.e. $c(p_2^*) - 0.5$. As we see in Fig. 4 both hysteresis as well as the jump of c depend on $\langle k \rangle$. However, these dependencies are very different. There is only one common feature seen in both relations—below a certain value of $\langle k \rangle$ both $p_2^* - p_1^*$ as well as $c(p_2^*) - 0.5$ are equal zero, which indicates a continuous phase transition. Above this value the width of hysteresis increases almost linearly, for some intermediate values of $\langle k \rangle$, but then the growth significantly slows down and the hysteresis asymptotically approaches the limiting value, which is visible in Fig. 5. In result a hysteresis is an S-shaped curve, and the limiting value is given by mean-field size of the hysteresis [33]. On the other hand, the jump of concentration of spins up increases only slightly, but this growth is very rapid and takes place in a relatively small range of $\langle k \rangle$. For larger values of $\langle k \rangle$ the jump of c does not change, similarly as for the q -voter model [40].

Until now we have analyzed the influence of $\langle k \rangle$ on the phase transition only for $r = 0.6$. Of course, the same can be done for an arbitrary value of r , as shown in Fig. 5. We see that the width of the hysteresis indeed increases monotonically with $\langle k \rangle$. However, the dependence on the threshold r is much more interesting. There is an optimal value of r , which decreases with $\langle k \rangle$, for which the hysteresis has the maximum size.

Because empirical studies suggest that the mean number of friends varies typically from 5 to 150, depending on the rated emotional closeness between them [44], an optimal value of r is that for which the maximum size of hysteresis appear lies in $(0.65, 0.85)$. We find this result particularly interesting from the social point of view, which will be commented on in the Conclusions.

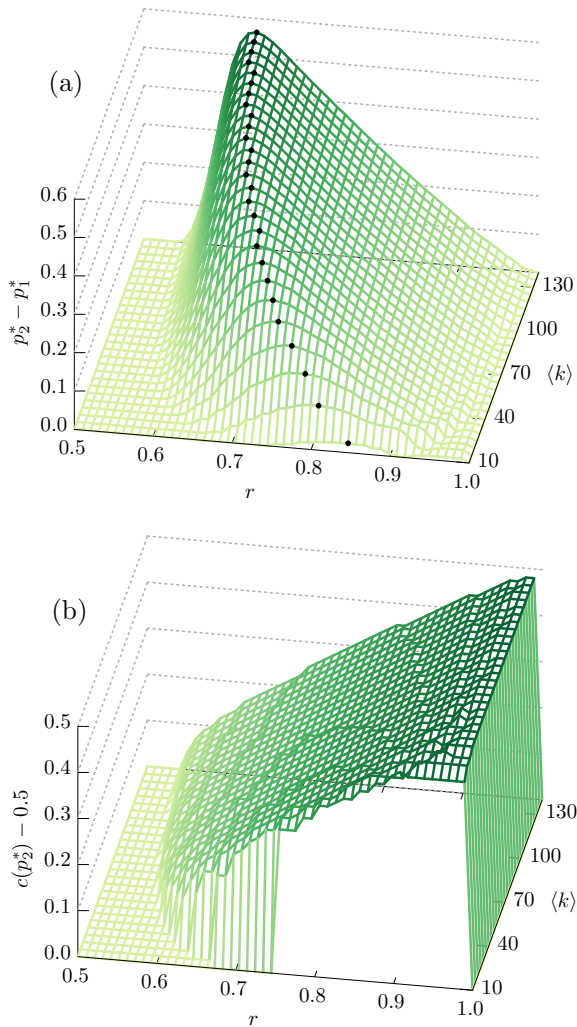


FIG. 5. The size of the hysteresis (a) and the jump of the concentration c at upper spinodal p_2^* (b) as a function of the threshold r and the average degree of a graph $\langle k \rangle$ obtained within the PA.

V. MONTE CARLO SIMULATIONS

We validate our analytical PA results with Monte Carlo (MC) simulations on ER and WS graphs [39]. We expect that the PA should give correct results for ER and WS graphs with $\beta = 1$. As we have observed in the Introduction, the WS algorithm allows us to tune the structure of the graph from a regular ($\beta = 0$) to a random one ($\beta = 1$). It also reduces to the complete graph for $\langle k \rangle = N - 1$. Moreover, in the whole spectrum of parameter β the average node degree is conserved. This makes the WS graph particularly interesting for our studies.

As expected, MC simulations for ER as well for WS graphs with $\beta = 1$ overlap the PA results, even for small values of $\langle k \rangle$; see Fig. 6. Moreover, this agreement is seen in all dependencies, namely, $c = c(p)$, $b = b(p)$, $b = b(c)$. The question is if and how the parameter β will influence results.

In Fig. 7 the parameter β varies from 0.1 to 1. The width of the hysteresis $p_2^* - p_1^*$ increases with β for $r > 0.5$ within the PA as well as MC simulations. To obtain the hysteresis from MC simulations we conduct simulations from two types of initial conditions: ordered ($c(0) = 1$) and disordered ($c(0) = 1/2$), as indicated in Fig. 7(a). As usual, in general the PA gives consistent results with MC simulations only for sufficiently large values of the rewiring probability β and big enough system size N , which is quite clear. First, within the PA we approximate all triangles, which are frequent in the case of high clustering coefficient, by pairs. Therefore, the higher clustering coefficient is (i.e., the lower β), the less accurate results are given by the PA. Second, PA equations are derived for the infinitively large system, and therefore the larger the system is, the better compatibility with the PA. Therefore to make a comparison with the PA we have chosen relatively large $N = 10^4$.

However, one may also ask how results scale with the system size. We have expected that our model will scale analogously to other binary models with up-down symmetry. Indeed, as shown in Fig. 8, critical exponents coincide with classical exponents for the Ising model, which have been also observed on various random networks [45], including Watts-Strogatz graphs [46]. Such a mean-field exponents have been also reported for various opinion dynamic models [47,48].

VI. CONCLUSIONS

The hysteresis and tipping points are common features of complex social and psychological systems [36,38,49–51]. For example, empirical studies suggest that public opinion exhibits both phenomena, which means that it remains seemingly resistant to change (which is related to hysteresis), and then a sudden, abrupt shift of opinion can be observed at the tipping point [36,38]. The notion of the tipping point, similar to the notion of the hysteresis, two signatures of discontinuous phase transitions, has been present in the social sciences for many years; for an early review of the importance of the notion of social hysteresis in social science see Ref. [50]. In the social sciences, the hysteresis is used to explain inelasticity of change and manifests as a slow response of societies to new problems, even if they are recognized by experts [36].

When it comes to the theoretical description of hysteresis in social science, different approaches are possible. One of the possibilities is Bourdieu's concept of the hysteresis effect [52], within which hysteresis is a consequence of interrelations between habitus (a property of actors, e.g., individuals, groups, or institutions) and field (social space); for a review see Ref. [53]. According to this concept, the hysteresis effect means that in the changed circumstances, individuals maintain their acquired dispositions, even when they are not suited to the new social context. Surprisingly, Bourdieu's concept is perfectly consistent with the idea of hysteresis appearing in the physics of phase transitions.

Although it may seem that the social hysteresis and the tipping point are just fancy buzzwords, empirical social studies have confirmed that they are not just abstract ideas [36,38,51].

These findings, among others, inspired researchers to look for the hysteresis in models of opinion dynamics [15,19,40]. For example, an additional noise has been introduced to the MV

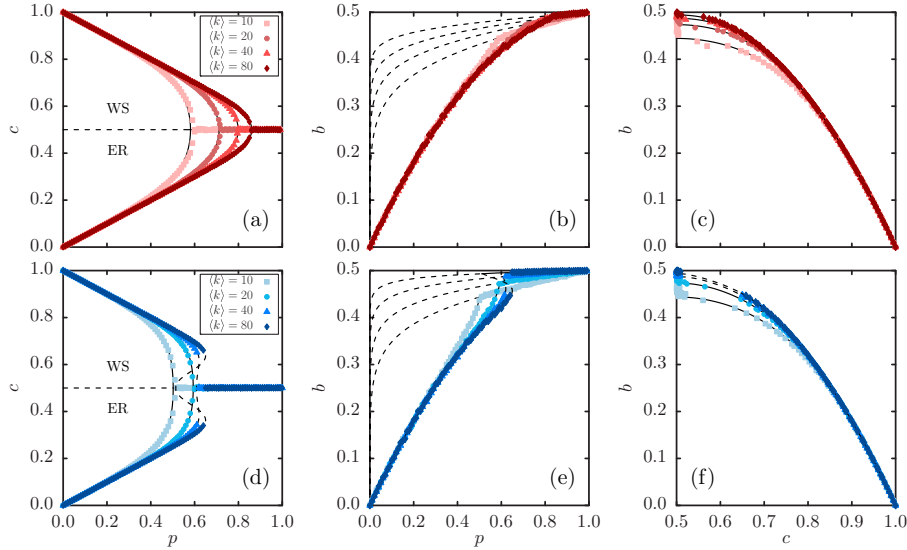


FIG. 6. Comparison between results obtained within the PA (denoted by lines) and Monte Carlo simulations (denoted by symbols) for $r = 0.5$ (upper panels) and $r = 0.6$ (bottom panels). In the left column [panels (a) and (d)] results for two types of graphs are presented: Watts-Strogatz with $\beta = 1$ [upper part, obtained from the initial condition $c(0) = 1$] and Erdős-Rényi [bottom part, obtained from the initial condition $c(0) = 0$]. In the remaining panels results for WS graphs with $\beta = 1$ are presented, but for ER graphs the results are the same. Solid lines correspond to stable, whereas dashed lines to unstable, solutions of Eqs. (12) and (13). For all diagrams the size of the system $N = 10^4$ and the thermalization time $t = 10^4$. Results are averaged only over five samples, but for this size of the system it is sufficient, as seen above.

model, but it was shown that it does not affect the type of the phase transition, and it remains continuous irrespective of the network degree and its distribution [14,20]. On the other hand it was shown that discontinuous phase transitions may appear in the MV model with inertia, when the inertia is above an appropriate level [15]. Later a question about the *fundamental ingredients for discontinuous phase transitions in the inertial majority vote model* was asked [19]. It was shown that low $\langle k \rangle$ leads to the suppression of the phase coexistence. A similar result has been also reported for the q -voter model [40].

This motivated us to check if the same behavior will be observed within the ST model introduced in Ref. [33]. We have shown, using PA and MC simulations, that indeed the type of the phase transition within ST model depends on threshold r , as well as the properties of the network $\langle k \rangle$ and β ; i.e., hysteresis increases with $\langle k \rangle$ and β . On the other hand, the dependence on r is nonmonotonic, which will be commented on below.

We discuss ST in the context of MV and qV models, because they have much in common, which has been already discussed in Ref. [33]. In particular, ST model with anticonformity is the generalization of the basic majority-vote model, which corresponds to $r = 0.5$. Moreover, the ST model with $r = 1$ reduces to the q -voter model on the random regular graph with degree q , i.e., if $\forall i k_i = k = q$. Finally, the ST model with an arbitrary value of r corresponds to the threshold q -voter model on the random regular graph with $\forall i k_i = k = q$ [29–32].

Moreover, as we have noticed in Sec. IV, the parameters that are mainly responsible for the discontinuous phase transitions, namely, the level of inertia θ in the MV model with inertia, the size of the influence group q in the qV model,

and the threshold r needed for the social influence in the ST model, play in a sense a similar role. The larger q or r is, the harder it is to influence a voter, which as a result increases inertia on the microscopic level.

Because the hysteresis can be viewed as an inertia of the system on the macroscopic level, it would not be surprising that the inertia on the microscopic level supports the hysteresis. However, as shown in Fig. 5, the relation between the size of the hysteresis and parameter r is not that trivial, i.e., it is nonmonotonic, having the maximum value for a given value of r , which depends on $\langle k \rangle$. This is a particularly interesting result from the social point view and worth discussions here.

It is known that social influence increases with the size of the influence group as well as the unanimity of the group. However, this dependence is far from being trivial. First, it increases only up to a certain level. The social influence is stronger if the group of influence consists of four, instead of two, people. However, above a certain threshold it remains on the same level. Moreover, above this threshold, around 7–11 people, the social influence decreases [54].

Therefore, in social experiments, in which descriptive norms are used to influence people, social psychologists use neither unanimity nor a simple majority. Instead they use a certain supermajority, often around 75%. For example, they manipulate people to reuse towels in hotels with the fake descriptive norm saying something like: “75% of our guests are reusing towels.” There is no strong evidence that 75% is the magic number, and in some other experiments larger majorities were used, as briefly reviewed in Ref. [31]. The main message we want to convey here is that the larger majority does not always result in stronger social influence. It seems that some optimal values exist, and these values probably

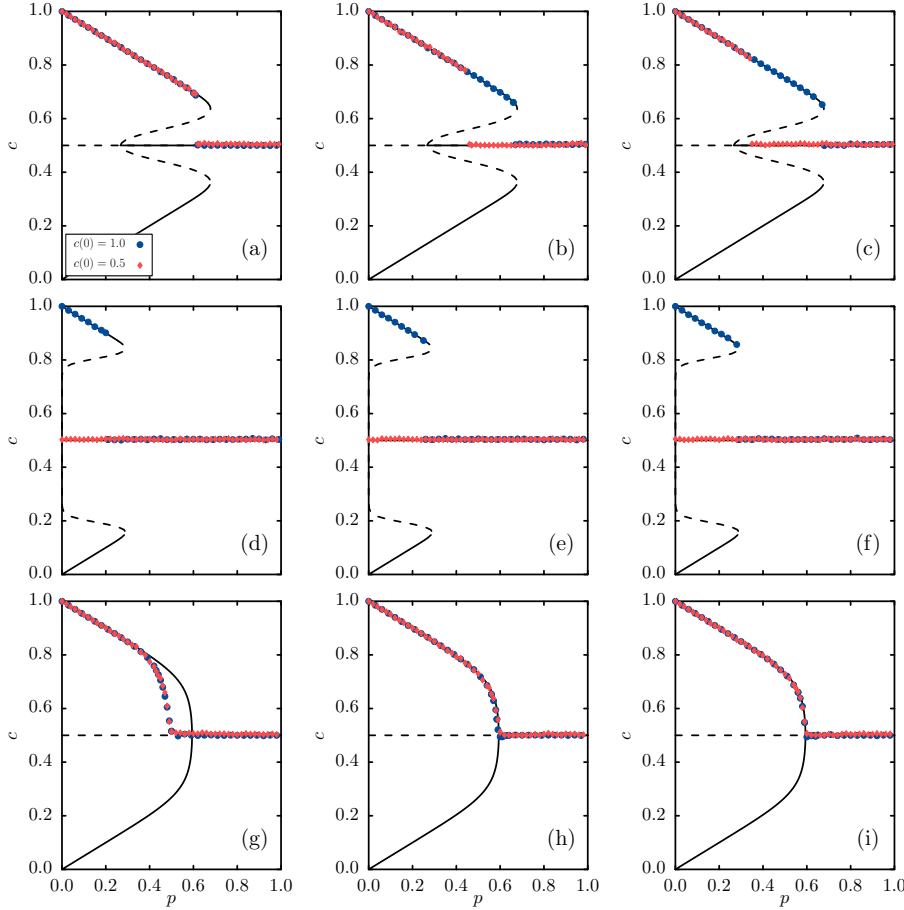


FIG. 7. Dependence between the stationary concentration of spins up c and the noise p for $r = 0.6$, $\langle k \rangle = 150$ (upper row), $r = 0.8$, $\langle k \rangle = 150$ (middle row), $r = 0.6$, $\langle k \rangle = 20$ (bottom row), and several values of the rewriting parameter: (a), (d), and (g) $\beta = 0.1$, (b), (e), and (h) $\beta = 0.5$, (c), (f), and (i) $\beta = 1$. Monte Carlo results for two types of initial conditions [as indicated in panel (a)] and $N = 10^4$ are denoted by symbols, whereas lines correspond to PA results. The thermalization time $t = 10^6$ for initial condition $c(0) = 0.5$ and $t = 2 \times 10^4$ for initial condition $c(0) = 1$. Results are averaged over five samples.

depend on the size of the influence group: for small groups unanimity is needed but for large groups some threshold value is more appropriate, significantly larger than 50%, but smaller than 100%. How is this related with the results obtained here?

As we have observed in Sec. IV, it was found empirically that in real social networks $\langle k \rangle \in (5, 150)$. This finding may seem surprising if we realize that, for example, on Facebook the current limit for the number of friends is 5000 people. Indeed, the growth of online communication raises a question about the scalability of the number of friends with the size of a social network. However, it seems that it is not a matter of the size of the whole social network that matters but rather the cognitive limits of our brain. As shown by Dunbar, the typical size of social groups correlates closely with the size of the neocortex. As a result *the structure of online social networks mirrors* the offline network of face-to-face contacts and consists of layers at 5, 15, 50, and 150 individuals [44]. For these values the optimal threshold of r , for which the largest social hysteresis is observed, lies in the range (0.65,0.85), depending on the average size of the influence group $\langle k \rangle$. We admit

that what we measure is not the power of social influence, but the size of the hysteresis. However, having in mind that the hysteresis is usually observed in social systems, we can speculate that there are some optimal values in the level of social influence and these values influence the hysteresis that is usually observed in social systems.

We are aware that it maybe merely intriguing but the meaningless coincident. However, we believe that this finding deserves more attention and studies within other models of opinion dynamics.

Data sharing is not applicable to this article as no new data were created or analyzed in this study.

ACKNOWLEDGMENTS

This work is supported by funds from the National Science Centre (NCN, Poland) through Grant no. 2016/21/B/HS6/01256 and by PLGrid Infrastructure.

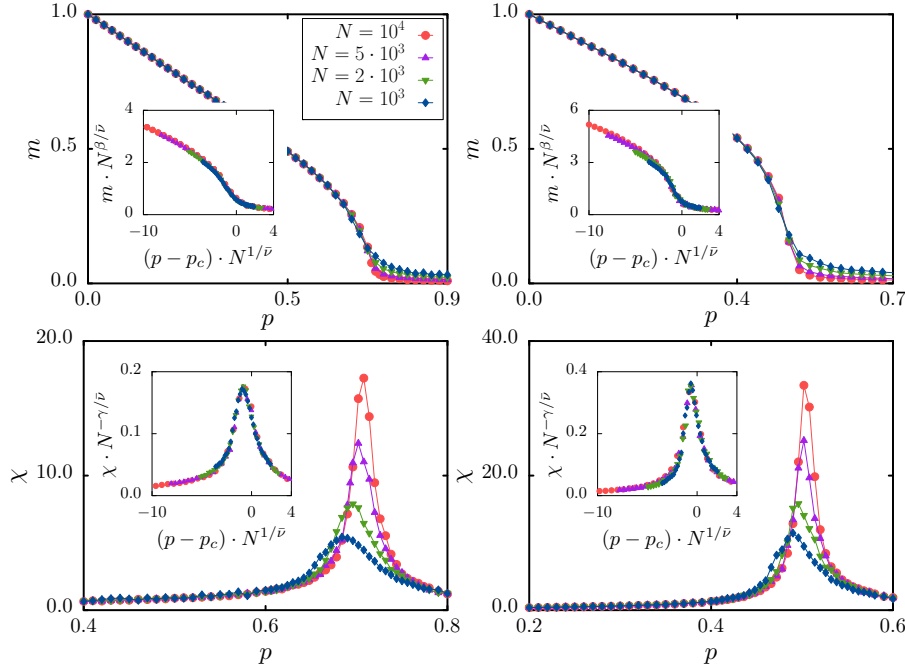


FIG. 8. Order parameter m (upper panels) and susceptibility χ (bottom panels) for $r = 0.5$, $\langle k \rangle = 20$ (left column), and $r = 0.6$, $\langle k \rangle = 10$ (right column) and different population sizes N , indicated in the left top panel. The corresponding scaling plots are shown in the respective insets. Presented data were obtained for $\beta \sim 1/2$, $\bar{v} \sim 2$, $\gamma \sim 1$, and $p_c \sim 0.714$ (left column) and $p_c \sim 0.512$ (right column).

- [1] D. Watts and P. Dodds, in *Threshold Models of Social Influence*, edited by P. Bearman and P. Hedström, (Oxford University Press, Oxford, 2017), pp. 475–497.
- [2] A. Jędrzejewski and K. Sznajd-Weron, *C. R. Phys.* **20**, 244 (2019).
- [3] D. J. Watts, *Proc. Nat. Acad. Sci. USA* **99**, 5766 (2002).
- [4] M. Grabisch and F. Li, *Dyn. Games Appl.* **10**, 444 (2019).
- [5] M. Granovetter, *Am. J. Sociol.* **83**, 489 (1978).
- [6] S. Galam, *J. Stat. Phys.* **61**, 943 (1990).
- [7] S. Galam, *Intl. J. Modern Phys. C* **19**, 409 (2008).
- [8] S. Galam, *Sociophysics: A Physicist's Modeling of Psycho-Political Phenomena* (Springer-Verlag, New York, 2012).
- [9] T. M. Liggett, *Interacting Particle Systems* (Springer, Berlin, 1985).
- [10] T. Tome, M. De Oliveira, and M. Santos, *J. Phys. A: Gen. Phys.* **24**, 3677 (1991).
- [11] M. de Oliveira, *J. Stat. Phys.* **66**, 273 (1992).
- [12] F. Lima and K. Malarz, *Intl. J. Mod. Phys. C* **17**, 1273 (2006).
- [13] J. Santos, F. Lima, and K. Malarz, *Physica A* **390**, 359 (2010).
- [14] A. Vieira and N. Crokidakis, *Physica A* **450**, 30 (2016).
- [15] H. Chen, C. Shen, H. Zhang, G. Li, Z. Hou, and J. Kurths, *Phys. Rev. E* **95**, 042304 (2017).
- [16] A. Fronczak and P. Fronczak, *Phys. Rev. E* **96**, 012304 (2017).
- [17] A. Krawiecki, *Eur. Phys. J. B* **91**, 50 (2018).
- [18] A. Krawiecki and T. Gradowski, *Acta Phys. Pol. B: Proc. Suppl.* **12**, 91 (2019).
- [19] J. Encinas, P. Harunari, M. De Oliveira, and C. Fiore, *Sci. Rep.* **8**, 9338 (2018).
- [20] J. Encinas, H. Chen, M. de Oliveira, and C. Fiore, *Physica A* **516**, 563 (2019).
- [21] C. Castellano, M. A. Muñoz, and R. Pastor-Satorras, *Phys. Rev. E* **80**, 041129 (2009).
- [22] P. Nyczka, K. Sznajd-Weron, and J. Cisło, *Phys. Rev. E* **86**, 011105 (2012).
- [23] P. Moretti, S. Liu, C. Castellano, and R. Pastor-Satorras, *J. Stat. Phys.* **151**, 113 (2013).
- [24] M. Mobilia, *Phys. Rev. E* **92**, 012803 (2015).
- [25] M. A. Javarone and T. Squartini, *J. Stat. Mech.: Theory Exp.* (2015) P10002.
- [26] A. Mellor, M. Mobilia, and R. Zia, *Europhys. Lett.* **113**, 48001 (2016).
- [27] A. Mellor, M. Mobilia, and R. K. P. Zia, *Phys. Rev. E* **95**, 012104 (2017).
- [28] A. Jędrzejewski, *Phys. Rev. E* **95**, 012307 (2017).
- [29] P. Nyczka and K. Sznajd-Weron, *J. Stat. Phys.* **151**, 174 (2013).
- [30] A. R. Vieira and C. Anteneodo, *Phys. Rev. E* **97**, 052106 (2018).
- [31] P. Nyczka, K. Byrka, P. R. Nail, and K. Sznajd-Weron, *PLoS ONE* **13**, e0209620 (2018).
- [32] A. Vieira, A. F. Peralta, R. Toral, M. San Miguel, and C. Anteneodo, *arXiv:2002.04715v1* (2020).
- [33] B. Nowak and K. Sznajd-Weron, *Complexity* **2019**, 5150825 (2019).
- [34] P. Nyczka, J. Cisło, and K. Sznajd-Weron, *Physica A* **391**, 317 (2012).

- [35] A. Peralta, A. Carro, M. San Miguel, and T. R., *Chaos* **28**, 075516 (2018).
- [36] M. Scheffer, F. Westley, and W. Brock, *Ecosystems* **6**, 493 (2003).
- [37] R. Vallacher, S. Read, and A. Nowak (Eds.), *Computational Social Psychology* (Routledge Taylor & Francis Group, New York, 2017).
- [38] D. Centola, J. Becker, D. Brackbill, and A. Baronchelli, *Science* **360**, 1116 (2018).
- [39] D. J. Watts and S. H. Strogatz, *Nature (London)* **393**, 440 (1998).
- [40] A. Abramiuik and K. Sznajd-Weron, *Entropy* **22**, 120 (2020).
- [41] J. P. Gleeson, *Phys. Rev. X* **3**, 021004 (2013).
- [42] A. Peralta, A. Carro, M. San Miguel, and R. Toral, *New J. Phys.* **20**, 103045 (2018).
- [43] A. Barrat and M. Weigt, *Eur. Phys. J. B* **13**, 547 (2000).
- [44] R. Dunbar, V. Arnaboldi, M. Conti, and A. Passarella, *Soc. Netw.* **43**, 39 (2015).
- [45] H. Hong, M. Ha, and H. Park, *Phys. Rev. Lett.* **98**, 258701 (2007).
- [46] H. Hong, B. Kim, and M. Choi, *Phys. Rev. E* **66**, 018101 (2002).
- [47] R. Toral and C. Tessone, *Commun. Comput. Phys.* **2**, 177 (2007).
- [48] N. Crokidakis and C. Anteneodo, *Phys. Rev. E* **86**, 061127 (2012).
- [49] E. Wolf, *J. Am. Plan. Assoc.* **29**, 217 (1963).
- [50] J. Elster, *Synthese* **33**, 371 (1976).
- [51] G. Doering, I. Scharf, H. Moeller, and J. Pruitt, *Nat. Ecol. Evol.* **2**, 1298 (2018).
- [52] P. Bourdieu, *The Logic of Practice* (Stanford University Press, Stanford, CA, 1990).
- [53] C. Hardy, *Pierre Bourdieu: Key Concepts* (Routledge Taylor & Francis Group, New York, 2012), p. 126–145.
- [54] S. E. Asch, *Sci. Am.* **193**, 31 (1955).

A.3 Article 3

The threshold model with anticonformity under random sequential updating

Threshold model with anticonformity under random sequential updating

Bartłomiej Nowak^{1,*}, Michel Grabisch^{2,†}, and Katarzyna Sznajd-Weron^{1,‡}

¹*Department of Theoretical Physics, Faculty of Fundamental Problems of Technology, Wrocław University of Science and Technology,
50-370 Wrocław, Poland*

²*University of Paris I Panthéon-Sorbonne, Paris School of Economics, 106-112 Boulevard de l'Hôpital, 75013 Paris, France*

(Received 7 February 2022; accepted 15 May 2022; published 31 May 2022)

We study an asymmetric version of the threshold model of binary decision making with anticonformity under an asynchronous update mode that mimics continuous time. We analyze this model on a complete graph using three different approaches: the mean-field approximation, Monte Carlo simulation, and the Markov chain approach. The latter approach yields analytical results for arbitrarily small systems, in contrast to the mean-field approach, which is strictly correct only for an infinite system. We show that, for sufficiently large systems, all three approaches produce the same results, as expected. We consider two cases: (1) homogeneous, in which all agents have the same tolerance threshold, and (2) heterogeneous, in which thresholds are given by a beta distribution parametrized by two positive shape parameters α and β . The heterogeneous case can be treated as a generalized model that reduces to a homogeneous model in special cases. We show that particularly interesting behaviors, including social hysteresis and critical mass reported in innovation diffusion, arise only for values of α and β that yield the shape of the distribution observed in reality.

DOI: [10.1103/PhysRevE.105.054314](https://doi.org/10.1103/PhysRevE.105.054314)

I. INTRODUCTION

Within the broad class of two-state dynamics [1], threshold models are particularly useful for describing various social and economic phenomena [2–4]. As in other binary-state opinion dynamics [5], the threshold model describes the social influence in decision making for the choice between precisely two alternatives, often denoted by 1 (agree, adopt, be active, etc.) and 0 (disagree, refuse, be inactive, etc.). Although a binary decision framework seems to be oversimplified, it is relevant for surprisingly many complex problems [3].

In the original threshold models of collective behavior proposed by Schelling [6] and Granovetter [2], an agent takes action 1 if the proportion of his neighbors in state 1 exceeds some threshold, otherwise action 0 is taken. It means that an agent in state 1 may return to state 0, because not enough neighbors are active. On the other hand, in many other threshold models, the transition from state 1 to state 0 is forbidden [3,7,8].

Here, we will use the original formulation, in which a transition from 1 to 0 is possible, as in [2,9,10], but additionally in the presence of anticonformity. Such a model has been already studied from a mathematical point of view under the synchronous update mode [10], considering a complete network or a random neighborhood. The study focused on finding absorbing classes, cycles, etc. In this paper, we investigate the same model but under random sequential updating (asynchronous updating), which mimics continuous time, and

restricting to the complete network. Quick analysis shows that the two models behave very differently. Under the complete network assumption, the synchronous updating is a deterministic model and causes the appearance of cycling phenomena, in a way which is very dependent on the parameters chosen. In contrast, asynchronous updating is probabilistic and prevents the appearance of cycles. We show that it behaves similarly to a random-walk process. The appropriate tools in this situation are the phase transitions and phase diagrams under the mean-field approximation, which are typical for statistical physics of opinion formation [11–15], and also the Markov chain approach. It should be noted that phase transition diagrams cannot be used in the case of cycling, as only steady states can be studied.

We study the model on a complete graph since in this case the mean-field method allows us to obtain rigorous results. Independently, we conducted Monte Carlo simulations to validate the theoretical approach. Finally, we present a Markov chain approach, which allows us not only to obtain results for arbitrary small systems but also to derive the stationary distribution of visited states.

II. MODEL

We consider a society of n agents placed at the vertices of an arbitrary graph $G = (N, E)$, where $N = \{1, \dots, n\}$ is a set of vertices (agents) and E is the set of undirected edges. Each agent i has a set of neighbors $K_i = \{j \in N : \{i, j\} \in E\}$, and the cardinality of this set $|K_i| = k_i$ is the degree of agent i . Here we assume that each agent belongs to its own neighborhood to avoid the unrealistic effect that the agent does not consider its own state at all. However, this assumption is only relevant when the neighborhood is small, which is

*bartłomiej.nowak@pwr.edu.pl

†michel.grabisch@univ-paris1.fr

‡katarzyna.weron@pwr.edu.pl

obviously not the case for an infinite complete graph. As in many other models, an agent can be in one of two alternative states: 1 (agree, adopt, be active, etc.) or 0 (disagree, refuse, be inactive, etc.). Following [10], we use the term “active” for agents in state 1, and “inactive” for agents in state 0, and denote by $a_i(t)$ the state (action) taken by agent i at time t .

We consider two types of social response, anticonformity and conformity, which occur with complementary probabilities p and $1 - p$ respectively. In both cases, an agent can change its state if the ratio of active neighbors is above its tolerance threshold $r_i \in [0, 1]$. The threshold r_i of each agent is the realization of the random variable R with arbitrary distribution function $F_R(r)$ and does not change over time. In case of conformity, an agent follows the others, whereas in case of anticonformity he takes an opposite state to others. Therefore, the dynamics of the agent’s state in the case of conformity can be written as [10]

$$a_i(t + \Delta t) = \begin{cases} 1 & \text{if } \frac{1}{k_i} \sum_{j \in K_i} a_j(t) \geq r_i, \\ 0 & \text{otherwise,} \end{cases} \quad (1)$$

whereas in case of anticonformity [10]

$$a_i(t + \Delta t) = \begin{cases} 0 & \text{if } \frac{1}{k_i} \sum_{j \in K_i} a_j(t) \geq r_i, \\ 1 & \text{otherwise.} \end{cases} \quad (2)$$

In this paper, we use the random sequential update mode, which means that an elementary update consists of

- (1) random drawing of agent i from all n agents;
- (2) with probability p agent i anticonforms to the neighborhood, that is, takes action $a_i(t + \Delta t)$ according to Eq. (2);
- (3) with complementary probability $1 - p$ agent i conforms to the neighborhood, that is, takes action $a_i(t + \Delta t)$ according to Eq. (1);
- (4) time is updated: $t := t + \Delta t$.

As usual, $\Delta t = 1/n$ which means that the time unit consists of n elementary updates, which corresponds to one Monte Carlo step (MCS).

III. TRANSITION PROBABILITIES

Since we limit our study to the complete graph, we can fully describe the state of the system using a single random variable:

$$c = \frac{n_1}{n}, \quad (3)$$

where n_1 is the number of agents in the state 1 and thus c is the ratio of active agents. Therefore, there are $n + 1$ possible states of the system: $0, \frac{1}{n}, \frac{2}{n}, \dots, 1$.

Because we use the sequential (asynchronous) update mode, at most one agent can change its state at a time, and thus we can introduce the following transition probabilities:

$$\begin{aligned} \gamma^+(c) &= \Pr\left(c(t + \Delta t) = c(t) + \frac{1}{n}\right), \\ \gamma^-(c) &= \Pr\left(c(t + \Delta t) = c(t) - \frac{1}{n}\right). \end{aligned} \quad (4)$$

For our model, the explicit form of these probabilities can be written, according to the algorithm described in the

previous section, as follows:

$$\begin{aligned} \gamma^+(c) &= (1 - p)(1 - c)\Pr(R \leq c) + p(1 - c)\Pr(R > c), \\ \gamma^-(c) &= (1 - p)c\Pr(R > c) + pc\Pr(R \leq c), \end{aligned} \quad (5)$$

where $\Pr(R \leq c)$ is the probability that the concentration c of the active agents is greater than or equal to the threshold R of the considered agent. This probability is simply the value of the cumulative distribution function $F_R(r)$ at $r = c$. Similarly, $\Pr(R > c)$ is the probability that the concentration of active voters does not exceed the threshold of considered agents, and thus it is equal to $1 - F_R(c)$. Therefore, we obtain

$$\begin{aligned} \gamma^+(c) &= (1 - p)(1 - c)F_R(c) + p(1 - c)[1 - F_R(c)], \\ \gamma^-(c) &= (1 - p)c[1 - F_R(c)] + pcF_R(c). \end{aligned} \quad (6)$$

As can be seen from Eq. (4), the concentration of active agents c is a random variable. However, we can easily write the evolution equation for the expected value of c . Moreover, for $n \rightarrow \infty$ we can assume that c is localized to the expectation value. Therefore, we can write [5]

$$\frac{dc}{dt} = \gamma^+(c) - \gamma^-(c) \equiv f(c), \quad (7)$$

where $f(c)$ can be interpreted as an effective force acting on the system. Such a force will later allow us to introduce a potential that helps visualize the dynamics of the system [16]. As usual, we focus on the steady states, i.e., those for which

$$\frac{dc}{dt} = 0. \quad (8)$$

In the next two sections, we will use condition (8) to calculate the stationary concentration of active agents for two cases: (1) homogeneous, in which all agents have the same tolerance threshold, and (2) heterogeneous, in which the distribution of thresholds $F_R(r)$ is given by the beta distribution. We will compare the analytical results with the results of Monte Carlo simulations for the system of size $n = 10^4$, averaged over ten independent runs collected after 10^4 Monte Carlo steps. For the Monte Carlo simulations, two types of initial conditions will be used to reproduce all stable solutions of Eq. (8): (1) all agents initially active, which will be denoted by $c(0) = 1$, and (2) all agents initially inactive, which will be denoted by $c(0) = 0$.

IV. ONE THRESHOLD

In this case, the random variable R takes one value for all agents in the system, that is, all voters have the same threshold r :

$$\begin{aligned} F_R(c) &= \mathbf{1}_{\{r \leq c\}}, \\ 1 - F_R(c) &= \mathbf{1}_{\{r > c\}}, \end{aligned} \quad (9)$$

where $\mathbf{1}_{\{r \leq c\}} = 1$ when $r \leq c$ and 0 otherwise. Inserting (9) into Eq. (6) and then into Eq. (7) we obtain

$$\begin{aligned} \frac{dc}{dt} &= (1 - p)[(1 - c)\mathbf{1}_{\{r \leq c\}} - c\mathbf{1}_{\{r > c\}}] \\ &\quad + p[(1 - c)\mathbf{1}_{\{r > c\}} - c\mathbf{1}_{\{r \leq c\}}]. \end{aligned} \quad (10)$$

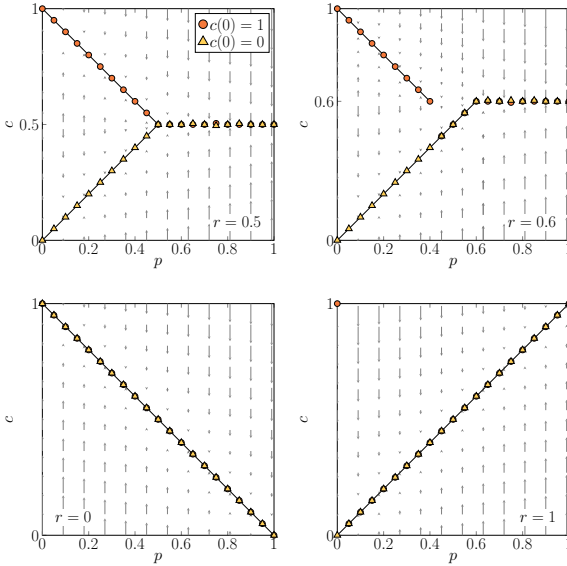


FIG. 1. Dependency between the stationary concentration of active agents c and the probability of anticonformity p for the model with one threshold for different values of the parameter r (indicated in the plots). Solid lines represent stable fixed points obtained analytically from Eq. (16). Symbols represent Monte Carlo simulations from two initial conditions indicated in the legend. Arrows indicate the flow in the system. The length of each arrow corresponds to the value of velocity $\frac{dc}{dt}$ given by Eq. (10).

From (10), we obtain several trivial fixed points:

$$(p = 0, c = 0) \quad \forall r \neq 0, \quad (11)$$

$$(p = 1, c = 0) \quad r = 0, \quad (12)$$

$$(p = 0, c = 1) \quad \forall r \in [0, 1], \quad (13)$$

$$(p = 0.5, c = 0.5) \quad \forall r \in [0, 1], \quad (14)$$

$$(p = 1 - r, c = r) \quad \forall r \in [0, 1]. \quad (15)$$

The remaining solutions can be obtained by solving Eq. (8), which leads to

$$p = \frac{\mathbf{1}_{\{r \leq c\}} - c}{\mathbf{1}_{\{r \leq c\}} - \mathbf{1}_{\{r > c\}}}, \quad (16)$$

which is equivalent to the following cases:

$$\forall c < r \quad p = c, \quad \forall c \geq r \quad p = 1 - c. \quad (17)$$

From the above analysis, we do not obtain the steady state for any value of $r \in [0, 1]$ if $p \geq r$ for $r > 0.5$ or $p > 1 - r$ for $r \leq 0.5$. However, from the evolution of Eq. (10), represented by solid lines in Fig. 1, and from Monte Carlo simulations, represented by symbols in Fig. 1, we see that the system approaches the state $c = r$ for $p > r$. This raises the question of what the evolution of the system actually looks like. To

answer this question we can provide at least three alternative approaches. We decided to present all three because we believe that there is value in showing the different possibilities of system analysis, especially given the interdisciplinary nature of the work. The composition of the authors themselves is also interdisciplinary, and each of us found a different method more compelling/intuitive.

The first, which is the most basic technique used to analyze dynamical systems, consists of interpreting a differential equation as a vector field [16]. Within this graphical way of thinking, we draw the arrows representing the flow dc/dt in the plane of model parameters, as shown in Fig. 1. The second method is based directly on the transition probabilities $\gamma^+(c), \gamma^-(c)$. If we split the transition probabilities into cases,

$$\begin{aligned} \forall c < r \quad \gamma^+(c) &= p(1 - c) \wedge \gamma^-(c) = (1 - p)c, \\ \forall c \geq r \quad \gamma^+(c) &= (1 - p)(1 - c) \wedge \gamma^-(c) = pc. \end{aligned} \quad (18)$$

we easily observe that they do not cross at any point, when $\forall r > 0.5 \quad p \geq r$ or $\forall r \leq 0.5 \quad p > 1 - r$; see the fourth column of Fig. 2. This implies no steady state. On the other hand, for $p < r$ transition probabilities $\gamma^-(c)$ and $\gamma^+(c)$ cross each other, as shown in the first three columns of Fig. 2, i.e., the steady state $\gamma^-(c) = \gamma^+(c)$ exists.

The third method is based on the idea of potential $V(c)$ [16]:

$$V(c) = - \int f(c) dc. \quad (19)$$

From Eq. (18) we see that the effective force $f(c)$ defined in Eq. (7) takes the following form:

$$f(c) = \gamma^+(c) - \gamma^-(c) = \begin{cases} p - c & \text{for } c < r, \\ 1 - p - c & \text{for } c \geq r, \end{cases} \quad (20)$$

and thus

$$V(c) = \begin{cases} - \int (p - c) dc = \frac{c^2}{2} - cp & \text{for } c < r, \\ - \int (1 - p - c) dc = \frac{c^2}{2} - c(1 - p) & \text{for } c \geq r. \end{cases} \quad (21)$$

Using such an approach, we draw a ball sliding down the walls of a potential well [16], as shown in Fig. 2. It should be noted that potentials given by Eq. (21) are determined up to a constant. Therefore, the size of the jump at the border $c = r$ is not unambiguously defined. Here, we have assumed that both constants are equal to zero, but this does not influence the dynamics of the system since the system cannot jump from one to the other potential minima, as presented in Fig. 2. This is because the point $c = r$ belongs only to one area and thus the dynamics from this point is uniquely defined no matter what jump is at $c = r$.

The steady states are the local extrema of $V(c)$. From Eq. (21) we see that the potential has a discontinuity at $c = r$, which implies no maximum (unstable steady state). Still,

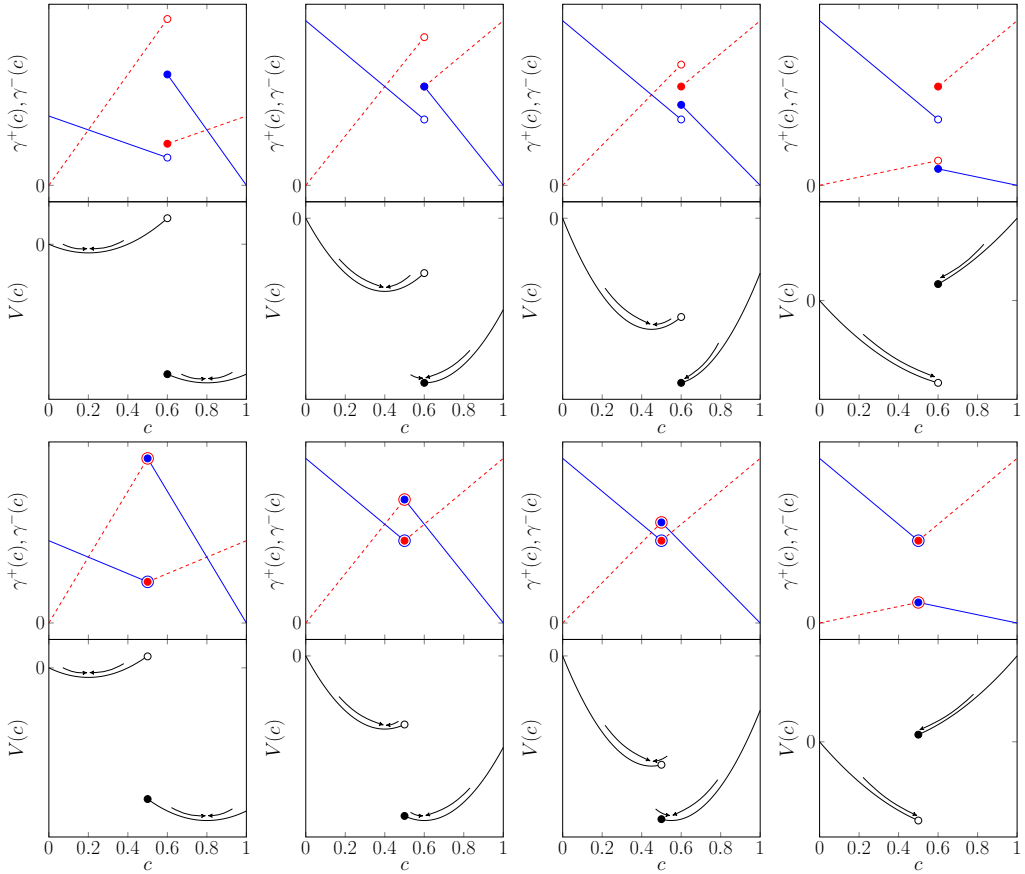


FIG. 2. Analysis of the steady states and the stability of the system for two values of threshold $r = 0.6$ (two first rows) and $r = 0.5$ (two last rows) and four values of $p = 0.2$ (first column), $p = 0.4$ (second column), $p = 0.45$ (third column), $p = 0.8$ (fourth column). In first and third rows, solid lines represents values of γ^+ and dotted lines stands for γ^- obtained with Eq. (18). Potentials $V(c)$ (second and fourth rows) are obtained with Eq. (21). In all subplots, filled circles denote continuity, while empty circles denote lack of continuity at this point.

at most two minima (stable steady states) are possible. In general, the number of minima, denoted by $M(r, p)$, can be described as follows:

$$\forall r > 0.5 \quad M(r, p) = \begin{cases} 2 & \text{for } p \leq 1 - r, \\ 1 & \text{for } 1 - r < p < r, \\ 0 & \text{for } p \geq r, \end{cases} \quad (22)$$

$$\forall r \leq 0.5 \quad M(r, p) = \begin{cases} 2 & \text{for } p < r, \\ 1 & \text{for } r \leq p \leq 1 - r, \\ 0 & \text{for } p > 1 - r. \end{cases} \quad (23)$$

In conclusion, despite the lack of steady state in the case $M(r, p) = 0$ we can observe that the flow of the system is towards the point $c = r$. It reaches an asymptotic minimum at this point because from both the left and right boundaries, the system flow is towards this minimum. This explains the behavior shown in Fig. 1, which was at first incomprehensible and inspired the above analysis.

V. BETA DISTRIBUTION

In the previous section, we studied the homogeneous system, in which all agents had the same value of the tolerance

threshold r . However, we can also consider more general distributions of thresholds, allowing for heterogeneity. The most useful are distributions whose support values $r \in [0, 1]$ and show a variety of shapes. This is the case of the beta distribution with two parameters α and β , previously considered, for the models of tolerance without anticonformity [4]. It has a well-defined cumulative distribution function:

$$F_R(r) = I_r(\alpha, \beta) = \frac{B(r, \alpha, \beta)}{B(\alpha, \beta)}, \quad (24)$$

where $I_r(\alpha, \beta)$ is the regularized incomplete beta function, which can be defined in terms of the incomplete beta function $B(r, \alpha, \beta)$ and the complete beta function $B(\alpha, \beta)$. Inserting $F_R(r)$ given by Eq. (24) into (6) we obtain the transition probabilities $\gamma^+(c), \gamma^-(c)$. Then inserting them to Eq. (7) we get

$$\begin{aligned} \frac{dc}{dt} = & (1-p)[(1-c)I_c(\alpha, \beta) - c(1-I_c(\alpha, \beta))] \\ & + p[(1-c)(1-I_c(\alpha, \beta)) - cI_c(\alpha, \beta)]. \end{aligned} \quad (25)$$

Again, we can point out the obvious steady states ($p = 0, c = 0$), ($p = 0, c = 1$) for arbitrary values of α and β . For

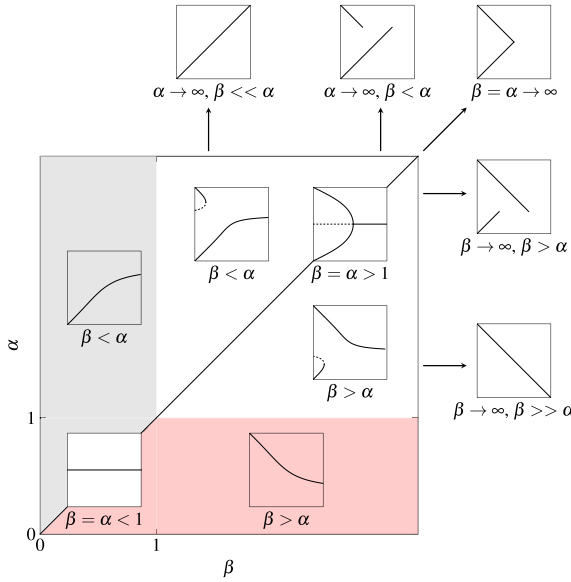


FIG. 3. Phase diagram for the heterogeneous model with thresholds described by the beta distribution parametrized by two shape parameters α and β . Each inset shows representative behavior of $c(p)$ for a given area of the phase diagram. Solid lines in the insets correspond to stable stationary states, whereas dashed lines correspond to unstable stationary states.

$c = 1/2$ formula (25) boils down to

$$\frac{dc}{dt} \Big|_{c=\frac{1}{2}} = \left(I_{\frac{1}{2}}(\alpha, \beta) - \frac{1}{2} \right) (1 - 2p), \quad (26)$$

which has two roots. The first one $p = 1/2$ gives the fixed point ($p = \frac{1}{2}$, $c = \frac{1}{2}$). The other root $I_{\frac{1}{2}}(\alpha, \beta) = \frac{1}{2}$ exists if the beta distribution is symmetric around the value $\frac{1}{2}$. This happens for $\alpha = \beta$, which leads to the conclusion that the value $c = \frac{1}{2}$ is a fixed point for all values of p if $\alpha = \beta$. For all remaining solutions we have the following relation:

$$p = \frac{I_c(\alpha, \beta) - c}{2I_c(\alpha, \beta) - 1}. \quad (27)$$

The information about the stability of the steady state is given by the sign of the derivative

$$\frac{dF}{dc} = \frac{c^{\alpha-1}(1-c)^{\beta-1}\Gamma(\alpha+\beta)}{\Gamma(\alpha)\Gamma(\beta)}(1-2p) - 1. \quad (28)$$

The state is stable if the above derivative is negative and unstable otherwise. The overall behavior of the model is summarized in Fig. 3. In the insets of this figure the dependence between the stationary value of c and parameter p is shown. Two shaded areas in Fig. 3 correspond to the situation in which at least one of the parameters α, β is smaller than 1. In this case, for $p > 0$ there is always only one steady state and c is monotonically increasing ($\beta < \alpha$), monotonically decreasing ($\beta > \alpha$), or constant ($\beta = \alpha$) function of p .

Recalling the shape of the probability density function (PDF) of the beta distribution, we can draw some conclusions. If the PDF of the tolerance threshold is a monotonically decreasing function of the threshold r , then the concentration of active agents decreases with the probability of anticonformity p , and vice versa. If the PDF has the highest values at $r = 0$ and $r = 1$, being a convex function of r , then for all values of $p > 0$ the stationary value of active agents is 0.5.

The most complex behavior is seen if both shape parameters α, β are greater than 1 but not infinitely large, which corresponds to a unimodal PDF, with zero probabilities at both end of the interval range, i.e., at $r = 0$ and $r = 1$. This case corresponds to moderate tolerance [4], and it is a typical shape of the distribution of actual trait manifestations in behavior, as reported by psychologists [17]. In such a case, the phase transitions appear, as shown in Fig. 3. As long as $\beta = \alpha$, which corresponds to the symmetric PDF, there is a continuous phase transition between the phase in which one type of agent (active or inactive) dominates, and the symmetrical phase without the domination. The critical point, at which this transition occurs, can be calculated by solving the equation

$$\frac{dF}{dc} \Big|_{c=\frac{1}{2}} = 0, \quad (29)$$

which gives

$$p_1^* = \frac{1}{2} - \frac{\Gamma^2(\alpha)}{2^{3-2\alpha}\Gamma(2\alpha)}. \quad (30)$$

For $\alpha \neq \beta$, as long as shape parameters are finite and at least one of them is larger than 1, we obtain an interesting behavior, with the jump at some value of $p = p^*$ and hysteresis, as shown in Fig. 3. This can be especially useful to describe the innovation diffusion. For example, if $\beta > \alpha$ then for the small value of $p < p^*$ there is possibility of high adoption if the initial fraction of adopted is above the critical mass. However, if the initial fraction of adopted is too low, i.e., below the critical mass, the innovation cannot spread in the society. Similar behavior has been recently reported for the completely different mathematical model of the collective decision making with social learners for unequal merit options [18].

It is worth noticing that for $\alpha, \beta \rightarrow \infty$ we can recover the solution for the model with one threshold, as shown in Fig. 3. We are able to do that by recalling the formula giving the mode of the beta distribution with $\alpha, \beta > 1$:

$$m = \frac{\alpha - 1}{\alpha + \beta - 2}. \quad (31)$$

While $\alpha, \beta \rightarrow \infty$, the beta distribution is a one-point degenerate distribution with probability 1 at the midpoint m and 0 elsewhere. Thus, to obtain the case with the mode at the point $m = r$, i.e., recover the distribution for one threshold, parameters α and β should follow the formula

$$\beta = \frac{(1-r)\alpha - 1 + 2r}{r} \quad (32)$$

for $\alpha, \beta \rightarrow \infty$.

All results obtained analytically for beta distribution can be also obtained by Monte Carlo simulations, as shown in Fig. 4.

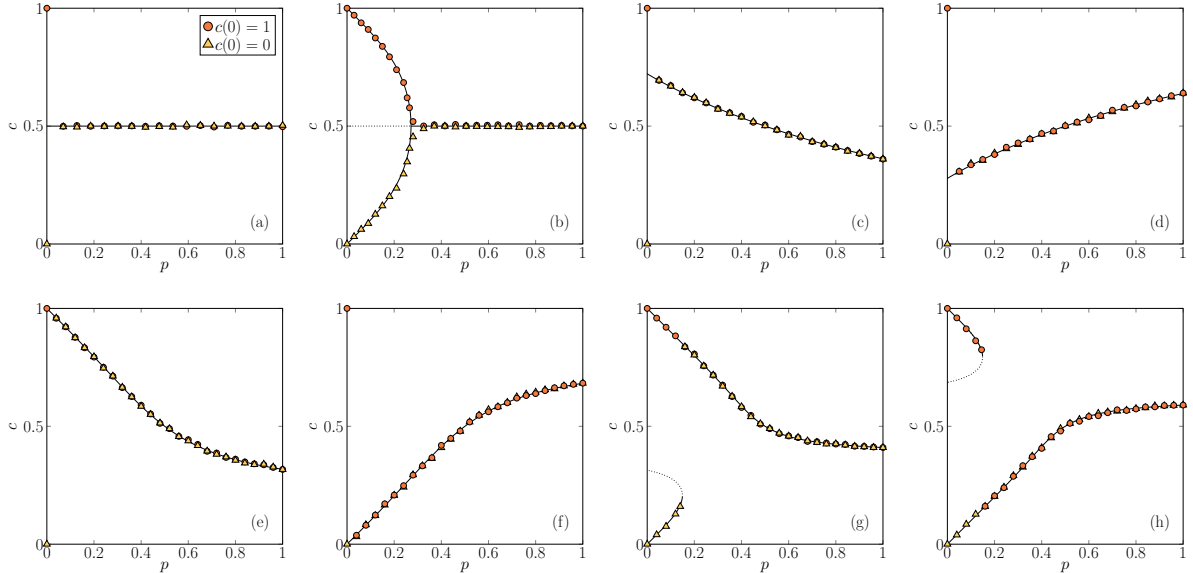


FIG. 4. Representative dependencies between the stationary concentration of spins up and the probability of anticonformity for model with beta distribution for different values of the parameters α and β : (a) $\alpha = \beta \leq 1$, (b) $\alpha = \beta > 1$, (c) $\alpha < \beta < 1$; α close to β , (d) $1 > \alpha > \beta$; α close to β , (e) $\alpha \leq 1 \wedge \alpha < \beta$, (f) $\beta \leq 1 \wedge \alpha > \beta$, (g) $1 < \alpha < \beta$, (h) $\alpha > \beta > 1$. Solid and dotted lines represent stable and unstable steady states respectively, obtained with Eq. (27). The exact values of parameters in the plots are as follows: (a) $\alpha = \beta = 0.9$; (b) $\alpha = \beta = 4$; (c) $\alpha = 0.1, \beta = 0.2$; (d) $\alpha = 0.2, \beta = 0.1$; (e) $\alpha = 1, \beta = 3$; (f) $\alpha = 3, \beta = 1$; (g) $\alpha = 5, \beta = 8$; (h) $\alpha = 8, \beta = 5$. Symbols represent Monte Carlo simulations from two initial conditions, denoted in the legend. The results are averaged over ten runs and collected after 10^4 MCS for system of size 10^4 .

VI. MARKOV CHAIN APPROACH

Previously, we were assuming that the size of the system is infinite, i.e., $n \rightarrow \infty$. However, such an assumption is not very realistic for social systems. Actually, social scientists are often interested in small systems. Therefore, in this section, we make analysis of the convergence of c in the long run using Markov chains for arbitrary small systems. The advantage

of the Markov chain approach in the context of agent-based modeling of opinion dynamics has been already reported in [19].

Transition probabilities given by Eq. (4) allows us to write the $(n+1) \times (n+1)$ transition matrix, whose general term (i, j) indicates the probability of transition from state i to state j . Due to the asynchronous update mode, \mathbf{P} is a tridiagonal row-stochastic matrix:

$$\mathbf{P} = \begin{bmatrix} \gamma^0(0) & \gamma^+(0) & 0 & 0 & \dots & 0 \\ \gamma^-(\frac{1}{n}) & \gamma^0(\frac{1}{n}) & \gamma^+(\frac{1}{n}) & 0 & \dots & 0 \\ 0 & \gamma^-(\frac{2}{n}) & \gamma^0(\frac{2}{n}) & \gamma^+(\frac{2}{n}) & \dots & 0 \\ 0 & \dots & \ddots & \ddots & \ddots & 0 \\ 0 & \dots & 0 & \gamma^-(\frac{n-1}{n}) & \gamma^0(\frac{n-1}{n}) & \gamma^+(\frac{n-1}{n}) \\ 0 & \dots & 0 & 0 & \gamma^-(1) & \gamma^0(1) \end{bmatrix} \quad (33)$$

with $\gamma^0(c) = 1 - \gamma^+(c) - \gamma^-(c)$. This process is a random walk process. Its transition graph is strongly connected and aperiodic, hence \mathbf{P} is a primitive matrix, i.e., the only absorbing class is the set of all states. This means that in the long run, the system at time t can be in any of the $n+1$ states, and there is no stabilization [20,21].

From Markov chain theory, the limit vector $\pi = [\pi(0), \dots, \pi(c), \dots, \pi(1)]^T$ giving the probability $\pi(c)$ to be

in state c in the long run is obtained as the left normalized eigenvector of \mathbf{P} associated with eigenvalue 1, i.e., π is the solution of the linear system in variable z

$$(\mathbf{P}^T - I)z = 0, \quad \mathbf{1}^T z = 1 \quad (34)$$

with $\mathbf{1} = (1, \dots, 1)^T$. From now on, to avoid heavy notation, we denote $\gamma^+(k/n)$ by $\gamma^+(k)$, and similarly for $\gamma^-(k/n)$,

$\pi(k/n)$, etc. We obtain

$$\mathbf{P}^T - \mathbf{I} = \begin{bmatrix} -\gamma^+(0) & \gamma^-(1) & 0 & 0 & 0 & \cdots & 0 \\ \gamma^+(0) & -\gamma^-(1) - \gamma^+(1) & \gamma^-(2) & 0 & 0 & \cdots & 0 \\ 0 & \ddots & \ddots & \ddots & 0 & \cdots & 0 \\ 0 & \cdots & \gamma^+(k-1) & -\gamma^-(k) - \gamma^+(k) & \gamma^-(k+1) & \cdots & 0 \\ 0 & \cdots & 0 & \ddots & \ddots & \ddots & 0 \\ 0 & \cdots & 0 & 0 & \gamma^+(n-2) & -\gamma^-(n-1) - \gamma^+(n-1) & \gamma^-(n) \\ 0 & \cdots & 0 & 0 & 0 & \gamma^+(n-1) & -\gamma^-(n) \end{bmatrix}. \quad (35)$$

Solving the system yields

$$\begin{aligned} \pi(0) &= \frac{\gamma^-(1)}{\gamma^+(0)} \pi(1), \\ \pi(1) &= \frac{\gamma^-(2)}{\gamma^+(1)} \pi(2), \\ &\vdots \\ \pi(k) &= \frac{\gamma^-(k+1)}{\gamma^+(k)} \pi(k+1), \\ &\vdots \\ \pi(n-1) &= \frac{\gamma^-(n)}{\gamma^+(n-1)} \pi(n). \end{aligned} \quad (36)$$

This yields

$$\pi(k) = \frac{\gamma^+(k-1)}{\gamma^-(k)} \frac{\gamma^+(k-2)}{\gamma^-(k-1)} \cdots \frac{\gamma^+(0)}{\gamma^-(1)} \pi(0) \quad (k = 1, \dots, n). \quad (37)$$

In the case of one threshold we are able to derive the above formulas analytically. Using Eq. (18) we obtain

$$\begin{aligned} \pi(k) &= \frac{(1-p)(k+1)}{p(n-k)} \pi(k+1) \quad (k < rn-1), \\ \pi(k) &= \frac{k+1}{n-k} \pi(k+1) \quad (rn-1 \leq k < rn), \\ \pi(k) &= \frac{p(k+1)}{(1-p)(n-k)} \pi(k+1) \quad (k \geq rn). \end{aligned}$$

Let us find when $\pi(k)$ is increasing or decreasing. Supposing $k < rn-1$, we have

$$\begin{aligned} \frac{(1-p)(k+1)}{p(n-k)} \leq 1 &\Leftrightarrow (1-p)(k+1) \leq p(n-k) \\ &\Leftrightarrow k \leq p(n+1)-1. \end{aligned}$$

When $k \geq rn$, we obtain

$$\frac{p(k+1)}{(1-p)(n-k)} \leq 1 \Leftrightarrow k \leq n - p(n+1).$$

Therefore,

(1) For states below r , the peak is attained at

$$\hat{c}_1 = \frac{\hat{k}_1}{n}, \text{ with } \hat{k}_1 = \lceil p(n+1) \rceil - 1.$$

Observe that when n is large, this yields $\hat{c}_1 \approx p$.

(2) For states above r , the peak is attained at

$$\hat{c}_2 = \frac{\hat{k}_2}{n}, \text{ with } \hat{k}_2 = n - \lfloor p(n+1) \rfloor.$$

When n is large, we obtain $\hat{c}_2 \approx 1-p$.

Depending on the relative positions of p and r , there can be one or two peaks, as summarized as follows:

- If $r \leq p, r \leq 1-p$: peak at \hat{c}_2 ,
- if $p \leq r \leq 1-p$: two peaks at \hat{c}_1, \hat{c}_2 ,
- if $1-p \leq r \leq p$: peak at $\frac{\lceil rn \rceil}{n}$,
- $p \leq r, 1-p \leq r$: peak at \hat{c}_1 .

In the case where there are two peaks, i.e., $p \leq r \leq 1-p$, let us find the relative heights of the peaks. From (37), we find, assuming $rn \notin \mathbb{N}$,

$$\begin{aligned} \pi(\lceil rn \rceil) &= \pi(\hat{k}_1) \left(\frac{p}{1-p} \right)^{\lceil rn \rceil - \lceil p(n+1) \rceil + 1} \\ &\quad \times \frac{(n - \lceil rn \rceil + 1) \cdots (n - \lceil p(n+1) \rceil + 1)}{\lceil rn \rceil \cdots \lceil p(n+1) \rceil}, \\ \pi(\lceil rn \rceil + 1) &= \pi(\hat{k}_2) \left(\frac{p}{1-p} \right)^{n - \lceil p(n+1) \rceil - \lceil rn \rceil - 1} \\ &\quad \times \frac{(\lceil rn \rceil + 2) \cdots (n - \lceil p(n+1) \rceil)}{(n - \lceil rn \rceil - 1) \cdots (\lceil p(n+1) \rceil + 1)}, \\ \pi(\lceil rn \rceil + 1) &= \pi(\lceil rn \rceil) \frac{n - \lceil rn \rceil}{\lceil rn \rceil + 1}. \end{aligned}$$

Hence, assuming $p(n+1) \notin \mathbb{N}$,

$$\frac{\pi(\hat{k}_2)}{\pi(\hat{k}_1)} = \left(\frac{p}{1-p} \right)^{2\lceil rn \rceil - n + 1}. \quad (38)$$

When n is large, we obtain

$$\frac{\pi(\hat{k}_2)}{\pi(\hat{k}_1)} \approx \left(\frac{p}{1-p} \right)^{n(2r-1)+1}. \quad (39)$$

Observe that the peaks have equal heights when $p = 0.5$, and when $r = 0.5$ the ratio is equal to $p/(1-p)$.

Besides, we have solved numerically by SCILAB the system of equations (34), which is possible for reasonable values of n , and obtained its solution $\pi(k)$, $k = 0, \dots, n$. Table I shows the value of the ratio of the two peaks for various values of p, r as given by Eq. (38), compared to the output of SCILAB. Figure 5 shows the computed distribution π for $n = 100$ for the one-threshold case and also the case of the beta distribution, compared to the histograms obtained from Monte Carlo simulations.

TABLE I. Example of results for $n = 10$ for different values of p and r under the condition $p \leq r \leq 1 - p$. In the table are presented the theoretical ratio given by Eq. (38) (left column), as well as the values $\pi(\hat{k}_1)$ and $\pi(\hat{k}_2)$ computed numerically and the ratio between them (three rightmost columns).

p	r	$\pi(\hat{k}_2)/\pi(\hat{k}_1)$	$\pi(\hat{k}_1)$	$\pi(\hat{k}_2)$	Ratio
0.21	0.41	3.7619048	0.064177	0.241429	3.7619052
0.21	0.61	0.0187835	0.2966234	0.005572	0.0187834
0.25	0.5	0.3333333	0.218683	0.0728942	0.3333334

We comment on these results. The Markov approach permits to obtain the stationary probability distribution of the different states, for any value of n , without approximation. It is found that in the long run, even if any state has a nonzero probability to be reached, some states have a much higher probability than the others to appear. In the case of one threshold, we have analytically proved the presence of one or two peaks, and their positions when n is large perfectly coincides with what was predicted by the mean-field approach. It is complementary to the results given by the mean-field approach, since the Markov approach is able to give the probability of occurrence of each stationary state. On the other hand, the complexity of the system of linear equations (34) induced by the Markov chain makes this approach not always tractable (e.g., with the beta distribution). Nevertheless, we

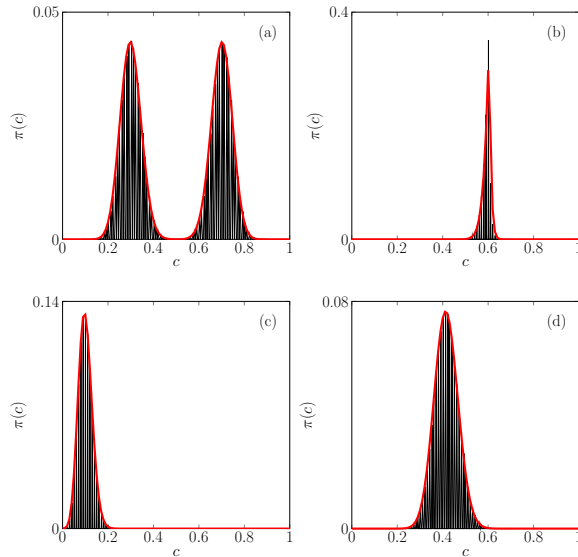


FIG. 5. Stationary distributions of visited states for model with one threshold (upper row) with parameters (a) $r = 0.5$, $p = 0.3$; (b) $r = 0.6$, $p = 0.7$ and model with beta distribution (bottom row) with parameters (c) $\alpha = 8$, $\beta = 5$, $p = 0.1$; (d) $\alpha = 3$, $\beta = 1$, $p = 0.4$. Solid red lines are distributions obtained with Markov approach, black histograms are obtained with trajectories from Monte Carlo simulations for system of size $n = 100$ and thermalization time $t = 2 \times 10^6$ MCS from 100 initial conditions evenly distributed on interval $[0,1]$, averaged over 1000 independent runs.

have shown that for reasonably large values of n (e.g., $n = 100$), this linear system can be solved numerically, giving a perfect fit with theoretical values, as shown by Table I and with Monte Carlo simulations as well, see Fig 5.

VII. SUMMARY AND RESEARCH DIRECTIONS FOR THE FUTURE

In this paper, we investigated the threshold model with anticonformity under asynchronous update mode, which mimics continuous time. We considered two cases: (1) homogeneous, in which all agents had the same threshold, and (2) heterogeneous, in which the thresholds are given by the beta distribution function. The homogeneous case with $r = 0.5$ is identical to the homogeneous symmetrical threshold model with anticonformity [22]. Moreover, it is almost identical to the majority-vote process [23,24]. The only difference between the models is when the number of active and inactive agents in the neighborhood of a chosen agent is equal. In such a case, the state of the system does not change within the majority-vote model, whereas within the threshold model the change is possible. From this point of view, the threshold model with anticonformity under asynchronous updating can be treated as a generalization of a majority-vote model.

On the complete graph, the homogeneous threshold model does not give particularly interesting results. The relationship between the stationary ratio of active agents and the probability of anticonformity consists of linear dependencies, similarly to the homogeneous symmetrical threshold model [22,25]. The only interesting feature of this model is the discontinuity that appears at $c = r = 1 - p$ for $r > 0.5$ and at $c = r = p$ for $r < 0.5$. In the result, the system reaches one of two different steady states, depending on the initial conditions. Much richer behavior is observed in the heterogeneous model with thresholds given by the beta distribution function, parametrized by α, β , which allows tuning the model to the homogeneous one ($\alpha, \beta \rightarrow \infty$) and to the maximally heterogeneous one (i.e., described by the uniform distribution function).

A particularly interesting behavior is obtained if at least one of the shape parameters α or β is larger than 1 and both parameters are finite. In this case the PDF has a shape that resembles those of actual trait manifestation in behavior, as reported by psychologists [17], i.e., unimodal, not necessarily symmetrical, function with maximum at the value $0 < r < 1$. In such a case a phase transition appears, which is continuous for $\alpha = \beta$, and discontinuous otherwise. In the latter case, the transition involves phenomena typical of social systems, such as social hysteresis [26] and the critical mass [27–29].

The future research on the model can be conducted in several directions, related to the following questions:

(1) How would the results change if the threshold for anticonformity were different than that for conformity? This question is inspired by the work on the q -voter model with generalized anticonformity [30]. In the q -voter model such a generalization resulted in switching from continuous to discontinuous phase transitions for some values of parameters. The question is, are the same phenomena observed for the threshold model?

(2) How would the structure of a network influence the results? This question is inspired by the work on the symmetrical threshold [25]. It was shown that on random graphs with the degree observed empirically for social networks, the largest social hysteresis is observed for $r \in (0.65, 0.85)$. This was a meaningful result from the social point of view and thus it would be desirable to check if it appears also in the asymmetric model studied here.

(3) How would the results change if the quenched approach to anticonformity were used? In this version of the model, we used the annealed approach, in the sense that each agent could anticonform (with probability p) or conform (with probability $1 - p$). However, we could use also the quenched

approach, in which a fraction p of agents are permanently anticonformists. This question is inspired by the work on the q -voter model with nonconformity under quenched and annealed approaches [31]. It was shown that on the complete graph both approaches give the same result for the q -voter model with anticonformity, but different results for the model with independence. The question is, to what extend is this result universal?

ACKNOWLEDGMENTS

This research was supported by the National Science Center (NCN, Poland) Grant No. 2019/35/B/HS6/02530.

-
- [1] J. P. Gleeson, Binary-State Dynamics on Complex Networks: Pair Approximation and Beyond, *Phys. Rev. X* **3**, 021004 (2013).
 - [2] M. Granovetter, Threshold models of collective behavior, *Am. J. Sociol.* **83**, 1420 (1978).
 - [3] D. Watts, A simple model of global cascades on random networks, *Proc. Natl. Acad. Sci. USA* **99**, 5766 (2002).
 - [4] V. V. Breer, Models of tolerant threshold behavior (from T. Schelling to M. Granovetter), *Autom. Remote Control* **78**, 1304 (2017).
 - [5] A. Jędrzejewski and K. Sznajd-Weron, Statistical physics of opinion formation: Is it a SPOOF? *C. R. Phys.* **20**, 244 (2019).
 - [6] T. C. Schelling, *Micromotives and Macrobbehavior* (Norton, New York, 1978).
 - [7] P. S. Dodds and D. J. Watts, Universal Behavior in a Generalized Model of Contagion, *Phys. Rev. Lett.* **92**, 218701 (2004).
 - [8] J. S. Juul and M. A. Porter, Hipsters on networks: How a minority group of individuals can lead to an antiestablishment majority, *Phys. Rev. E* **99**, 022313 (2019).
 - [9] E. Lee and P. Holme, Social contagion with degree-dependent thresholds, *Phys. Rev. E* **96**, 012315 (2017).
 - [10] M. Grabisch and F. Li, Anti-conformism in the threshold model of collective behavior, *Dynamic Games and Applications* **10**, 444 (2020).
 - [11] C. Castellano, S. Fortunato, and V. Loreto, Statistical physics of social dynamics, *Rev. Mod. Phys.* **81**, 591 (2009).
 - [12] S. Galam and A. Martins, Two-dimensional Ising transition through a technique from two-state opinion-dynamics models, *Phys. Rev. E* **91**, 012108 (2015).
 - [13] T. Raducha, M. Wilinski, T. Gubiec, and H. Stanley, Statistical mechanics of a coevolving spin system, *Phys. Rev. E* **98**, 030301(R) (2018).
 - [14] M. Calvelli, N. Crokidakis, and T. J. Penna, Phase transitions and universality in the Sznajd model with anticonformity, *Physica A* **513**, 518 (2019).
 - [15] A. R. Vieira, A. F. Peralta, R. Toral, M. S. Miguel, and C. Anteneodo, Pair approximation for the noisy threshold q -voter model, *Phys. Rev. E* **101**, 052131 (2020).
 - [16] S. H. Strogatz, *Nonlinear Dynamics and Chaos: With Applications to Physics, Biology, Chemistry, and Engineering*, 2nd ed. (CRC, Boca Raton, FL, 2015).
 - [17] W. Fleeson and P. Gallagher, The implications of Big Five standing for the distribution of trait manifestation in behavior: Fifteen experience-sampling studies and a meta-analysis, *J. Pers. Soc. Psychol.* **97**, 1097 (2009).
 - [18] V. Yang, M. Galesic, H. McGuinness, and A. Harutyunyan, Dynamical system model predicts when social learners impair collective performance, *Proc. Nat. Acad. Sci. USA* **118**, e2106292118 (2021).
 - [19] S. Banisch, R. Lima, and T. Araújo, Agent based models and opinion dynamics as markov chains, *Soc. Netw.* **34**, 549 (2012).
 - [20] J. G. Kemeny and J. L. Snell, *Finite Markov Chains* (Springer, Berlin, 1976).
 - [21] E. Seneta, *Non-negative Matrices and Markov Chains* (Springer, Berlin, 2006).
 - [22] B. Nowak and K. Sznajd-Weron, Homogeneous symmetrical threshold model with nonconformity: Independence versus anticonformity, *Complexity* **2019**, 14 (2019).
 - [23] T. M. Liggett, *Interacting Particle Systems* (Springer, Berlin, 1985).
 - [24] M. de Oliveira, Isotropic majority-vote model on a square lattice, *J. Stat. Phys.* **66**, 273 (1992).
 - [25] B. Nowak and K. Sznajd-Weron, Promoting discontinuous phase transitions by the quenched disorder within the multistate q -voter model, *arXiv:2106.11238*.
 - [26] M. Scheffer, F. Westley, and W. Brock, Slow response of societies to new problems: Causes and costs, *Ecosystems* **6**, 493 (2003).
 - [27] D. Centola, J. Becker, D. Brackbill, and A. Baronchelli, Experimental evidence for tipping points in social convention, *Science* **360**, 1116 (2018).
 - [28] C. Van Slyke, V. Ilie, H. Lou, and T. Stafford, Perceived critical mass and the adoption of a communication technology, *Eur. J. Inf. Syst.* **16**, 270 (2007).
 - [29] A. Mahler and E. M. Rogers, The diffusion of interactive communication innovations and the critical mass: The adoption of telecommunications services by German banks, *Telecomm. Policy* **23**, 719 (1999).
 - [30] A. Abramuk-Szurlej, A. Lipiecki, J. Pawłowski, and K. Sznajd-Weron, Discontinuous phase transitions in the q -voter model with generalized anticonformity on random graphs, *Sci. Rep.* **11**, 17719 (2021).
 - [31] A. Jędrzejewski and K. Sznajd-Weron, Person-situation debate revisited: Phase transitions with quenched and annealed disorders, *Entropy* **19**, 415 (2017).

A.4 Article 4

**Discontinuous phase transitions in the multi-state noisy
 q -voter model: quenched vs. annealed disorder**

scientific reports



OPEN

Discontinuous phase transitions in the multi-state noisy q -voter model: quenched vs. annealed disorder

Bartłomiej Nowak¹, Bartosz Stoiń & Katarzyna Sznajd-Weron^{1,2}

We introduce a generalized version of the noisy q -voter model, one of the most popular opinion dynamics models, in which voters can be in one of $s \geq 2$ states. As in the original binary q -voter model, which corresponds to $s = 2$, at each update randomly selected voter can conform to its q randomly chosen neighbors only if they are all in the same state. Additionally, a voter can act independently, taking a randomly chosen state, which introduces disorder to the system. We consider two types of disorder: (1) annealed, which means that each voter can act independently with probability p and with complementary probability $1 - p$ conform to others, and (2) quenched, which means that there is a fraction p of all voters, which are permanently independent and the rest of them are conformists. We analyze the model on the complete graph analytically and via Monte Carlo simulations. We show that for the number of states $s > 2$ the model displays discontinuous phase transitions for any $q > 1$, on contrary to the model with binary opinions, in which discontinuous phase transitions are observed only for $q > 5$. Moreover, unlike the case of $s = 2$, for $s > 2$ discontinuous phase transitions survive under the quenched disorder, although they are less sharp than under the annealed one.

It might seem that determining the type of a given phase transition is interesting only from the physics point of view. However, it has been reported that the hysteresis appears in real social systems^{1–5}, which means that this issue is important also from the social point of view. Because hysteresis cannot appear within the continuous phase transition, researchers working in the field of opinion dynamics try to determine conditions under which discontinuous phase transitions appear^{6–14}.

In this paper we focus on two factors that are known to influence the type of transition, namely the type of disorder (quenched vs. annealed) and the number of states. It is known, that discontinuous phase transitions can be rounded (become less sharp) or even totally forbidden in the presence of the quenched disorder^{15–18}. On the other hand, the larger number of states supports discontinuous phase transitions. The classical example is the Potts model: in two dimensions discontinuous phase transitions are observed for the number of states larger than 4, whereas continuous ones for the smaller values of states¹⁹. Similar situation has been reported for the majority-vote model. For the binary model only continuous phase transitions are observed^{7,11,20}, whereas for more than two states the model undergoes a discontinuous order-disorder phase transition^{21,22}.

In this paper we introduce the generalized version of the noisy q -voter model, in which each agent can be in one of several discrete states, similarly as it was done already for the linear voter^{23–28}, majority-vote^{21,22,29–32} or other models of opinion dynamics^{33,34}. We show that already for the 3-state model only discontinuous phase transitions are possible. Moreover, we consider the model under two approaches, the quenched and the annealed one, and we show that discontinuous phase transitions can survive under the quenched disorder, similarly as in³⁵. Only for the binary opinions, which were studied originally, the quenched disorder forbids discontinuous phase transition¹⁸.

The model

In this paper we propose a generalization of the original binary q -voter model (qVM) with independence⁶, known also as the noisy nonlinear voter³⁶ or the noisy q -voter model³⁷. Therefore, we consider a system of N agents placed in the vertices of an arbitrary graph. In this paper we will focus on the complete graph, for which exact analytical calculations can be provided. In the generalized model, each agent i is described by a dynamical

Department of Theoretical Physics, Faculty of Fundamental Problems of Technology, Wrocław University of Science and Technology, 50-370 Wrocław, Poland. email: katarzyna.weron@pwr.edu.pl

www.nature.com/scientificreports/

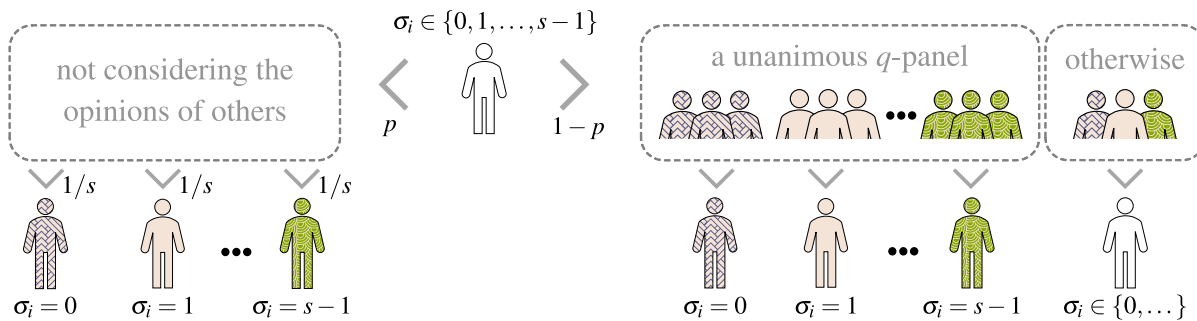


Figure 1. Visualization of an elementary update for the multi-state q -voter model with independence. Within the annealed approach two alternative social responses, independence and conformity, appear with complementary probabilities p and $1 - p$. Whereas, within the quenched approach, a fraction p of agents is permanently independent, whereas others are always conformists.

s -state variable $\sigma_i(t) \in \{0, 1, 2, 3, \dots, s - 1\}$. As in the original q -voter model³⁸, which corresponds to $s = 2$, a voter can be influenced by its neighbors only if the group of q agents, chosen randomly out of the neighborhood of a given voter, is unanimous. Additionally, a voter can change its opinion to a random one, independently of others, as proposed by Nyczka et al.⁶.

These two competitive processes—conformity to others (ordering) and independence (disordering), were originally introduced as alternatives appearing with complementary probabilities $1 - p$ and p , respectively. Such an annealed approach led to two types of phase transitions in the original q -voter model: continuous for $q \leq 5$ and discontinuous for $q > 5$. Later on, it was shown that replacing the annealed disorder by the quenched one reduced all transitions to continuous ones¹⁸.

In this paper we consider both types of disorder, annealed and quenched, and corresponding elementary updates are the following:

- **Annealed approach**

1. site i is randomly chosen from the entire graph,
2. a voter at site i acts independently with probability p , i.e. changes its opinion to randomly chosen state (each state can be chosen with the same probability $1/s$),
3. with complementary probability $1 - p$ a group of q neighbors is randomly selected (without repetitions) and if all q neighbors are in the same state, the voter at site i copies their state.

- **Quenched approach**

1. site i is randomly chosen from the entire graph,
2. if the voter is independent (a fraction p of all agents is permanently independent), then it changes its opinion to randomly chosen state (each state can be chosen with the same probability $1/s$),
3. if the agent is conformist (a fraction $1 - p$ of all agents is permanently conformists), a group of q neighbors is randomly selected (without repetitions) and if all q neighbors are in the same state, the voter at site i copies their state.

As usually time is measured in Monte Carlo Steps (MCS), and a single time step consists of N elementary updates, visualized in Fig. 1. It means that one time unit corresponds to the mean update time of a single individual.

Methods

In this section, we are going to analyze the annealed and quenched formulations of the multi-state q -voter model (MqVM). We use both the analytical as well as the Monte Carlo approach. We focus on the mean-field description of the model, which corresponds to the fully connected graph. This approach was already applied to various binary-state^{6,18,39,40} and multi-state^{21,25} dynamics. We are aware that Monte Carlo (MC) simulations can be carried out only for the finite system, whereas analytical results correspond to the infinite one. However, it occurs that already for systems of size $N = 10^5$ simulation results overlap the analytical ones.

The main goal of our study is to check how the number of states and the type of disorder influence the phase transition, observed in the original q -voter model with independence⁶. Therefore, we need to find the relation between stationary values of the concentration c_α of agents with a given opinion $\alpha = 0, 1, 2, 3, \dots, s - 1$ and model's parameters p and q . The concentration c_α is defined as:

$$c_\alpha = \frac{N_\alpha}{N}, \quad (1)$$

where N_α denotes the number of agents with opinion α . As usually, concentrations of all states sum up to one:

www.nature.com/scientificreports/

$$\sum_{\alpha=0}^{s-1} c_{\alpha} = \frac{N_0 + N_1 + \dots + N_{s-1}}{N} = 1. \quad (2)$$

Based on the values of c_{α} we distinguish the following phases:

- The disordered phase, in which all opinions are equinumerous i.e. $c_0 = c_1 = \dots = c_{s-1} = \frac{1}{s}$.
- The ordered phase, in which one or more opinions dominate over the others. A special case within this phase is the state of consensus, i.e. when all voters share the same opinion $c_{\alpha} = 1, c_{\beta} = c_{\gamma} = \dots = 0$.
- The coexistence phase (possible only in case of discontinuous phase transitions), if both ordered and disordered phases can be reached depending on the initial state of the system.

Our model is based on the random sequential updating, i.e. in a single update only one agent can change its state. Thus, the concentration c_{α} can increase or decrease by $1/N$ or remain constant with the respective probabilities:

$$\begin{aligned} \gamma^+(s, c_{\alpha}, q, p) &= \text{Prob}\left\{c_{\alpha} \rightarrow c_{\alpha} + \frac{1}{N}\right\} \equiv \gamma_{\alpha}^+, \\ \gamma^-(s, c_{\alpha}, q, p) &= \text{Prob}\left\{c_{\alpha} \rightarrow c_{\alpha} - \frac{1}{N}\right\} \equiv \gamma_{\alpha}^-, \\ \gamma^0(s, c_{\alpha}, q, p) &= \text{Prob}\{c_{\alpha} \rightarrow c_{\alpha}\} = 1 - \gamma^+(s, c_{\alpha}, q) - \gamma^-(s, c_{\alpha}, q) \equiv 1 - \gamma_{\alpha}^+ - \gamma_{\alpha}^-. \end{aligned} \quad (3)$$

The dynamics of our model in the mean-field limit is given by the rate equation:

$$\frac{dc_{\alpha}}{dt} = \gamma_{\alpha}^+ - \gamma_{\alpha}^- = F(s, c_{\alpha}, q, p), \quad (4)$$

where $F(s, c_{\alpha}, q, p)$ can be interpreted as the effective force acting on the system^{6,38}.

Annealed approach. Within the annealed approach a system is homogeneous, i.e. all agents are identical and transition rates can be expressed as:

$$\begin{aligned} \gamma_{\alpha}^+ &= \sum_{i \neq \alpha} P(i) \left[(1-p)P^q(\alpha|i) + \frac{p}{s} \right], \\ \gamma_{\alpha}^- &= \sum_{i \neq \alpha} P(\alpha) \left[(1-p)P^q(i|\alpha) + \frac{p}{s} \right], \end{aligned} \quad (5)$$

where $P(i)$ is the probability of choosing a voter in i -th state and $P(\alpha|i)$ is the conditional probability of picking a neighbor in state α given that a target voter is in state i . Inserting γ_{α}^{\pm} to Eq. (4) we obtain:

$$F(s, c_{\alpha}, q, p) = \sum_{i \neq \alpha} \left[P(i) \left((1-p)P^q(\alpha|i) + \frac{p}{s} \right) - P(\alpha) \left((1-p)P^q(i|\alpha) + \frac{p}{s} \right) \right]. \quad (6)$$

When events of picking a voter in state i and a neighbor in state α are independent, which is true in case of a complete graph, then $P(\alpha|i) = P(\alpha)$. If we additionally assume that $\forall_{\alpha} P(\alpha) = c_{\alpha}$, which is also true for a complete graph, we end up with the simple formula:

$$F(s, c_{\alpha}, q, p) = \frac{dc_{\alpha}}{dt} = \sum_{i \neq \alpha} \left[c_i \left((1-p)c_{\alpha}^q + \frac{p}{s} \right) - c_{\alpha} \left((1-p)c_i^q + \frac{p}{s} \right) \right]. \quad (7)$$

Stationary states of Eq. (4) are those for which

$$\frac{dc_{\alpha}}{dt} = F(s, c_{\alpha}, q, p) = 0. \quad (8)$$

The obvious solution of the above equation, which is valid for arbitrary value of p , is $c_0 = c_1 = \dots = c_{s-1} = \frac{1}{s}$. The other solutions can be obtained by solving numerically Eq. (8). However, independently we can provide also the general analytical solution based on the analogy to the Potts model¹⁹. In our model opinions are equivalent and there is no external field so we deal with Z_s symmetry that can be broken due to the noise. Because we have such a noise, introduced by independence, we expect an order-disorder phase transition. At the critical value of the noise (temperature in the Potts model and independence here), the Z_s symmetry is broken and the system choose spontaneously one of s states as a dominant one. From the mathematical point of view, such a transition corresponds to the bifurcation, at which fixed point $c_0 = c_1 = \dots = c_{s-1} = \frac{1}{s}$ loses stability⁴¹. However, because it is a fixed point, although unstable, if initially the system is exactly at this point, it will stay in this point forever. It shows how important the initial state is, if we analyze a system of an infinite size.

If initially one opinion dominates over the others, i.e. $c_{\alpha}(0) > c_{\beta}(0), c_{\gamma}(0), c_{\delta}(0), \dots$, where $\alpha, \beta, \gamma, \delta, \dots \in \{0, 1, \dots, s-1\}$ the system reaches an absorbing state in which this opinion still dominates over the others and the concentrations of all the others are equal $c_{\alpha} > c_{\beta} = c_{\gamma} = c_{\delta} = \dots$, see Fig. 2. Similarly,

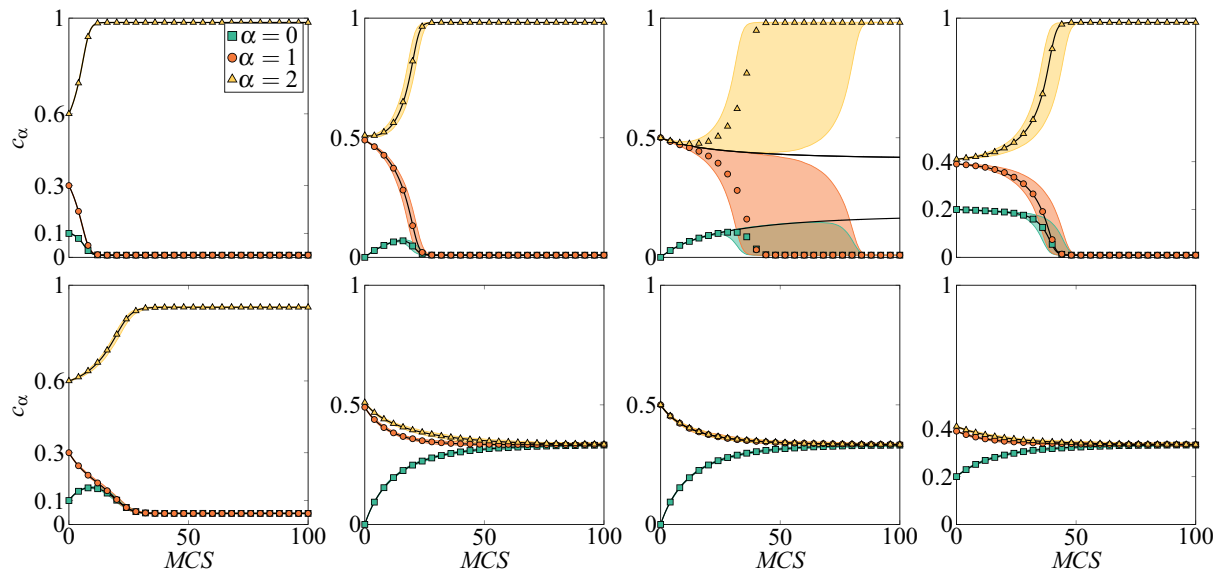


Figure 2. Trajectories for the multi-state annealed q -voter model on the complete graph of size $N = 10^5$ with the size of the influence group $q = 5$ and $s = 3$ states. Upper and lower panels differ by the amount of noise: $p = 0.025$ at the top row and $p = 0.09$ at the bottom one. Markers and color areas represent the outcome of Monte Carlo simulations and thick solid black lines are results of analytical prediction obtained from Eq. (7). Symbols represent median trajectory over 50 samples. The shaded color areas show the range of trajectories, i.e. are limited by 0 and 100th quantiles. Note that Monte Carlo simulations show a good agreement with analytical solutions in all panels, except of the third one in the upper row. The reason for this inconsistency is that in this case we are dealing with the hyperbolic (saddle) fixed point, i.e., a stable, as well as an unstable manifold exist⁴¹. Therefore, within MC simulations the system always eventually leaves such a state due to the finite-size fluctuations.

if initially two or more equinumerous states dominate over the others the system reaches an absorbing state in which concentrations for these states are still equal and larger than the concentrations of others:

$$\begin{aligned} c_\alpha &= c_\beta > c_\gamma = c_\delta = c_\epsilon = \dots \\ c_\alpha &= c_\beta = c_\gamma > c_\delta = c_\epsilon = \dots \\ c_\alpha &= c_\beta = c_\gamma = c_\delta > c_\epsilon = \dots \\ &\vdots \\ c_\alpha &= c_\beta = c_\gamma = c_\delta = c_\epsilon = \dots = \frac{1}{s}. \end{aligned} \quad (9)$$

It means that in the final state at most two values of opinion's concentrations are possible. This observation, together with the normalizing condition (2) indicates that all solutions can be written in terms of a single variable c , which describes the concentration of a one given state. Because in our model all states are equivalent, we can choose any of them as a representative one. Therefore, let us denote the concentration of state 0 by c and then the concentrations of all remaining states can be expressed with c by using condition (2):

$$\begin{aligned} c_0 &= \dots = c_{s-(\xi+1)} = c, \\ c_{s-\xi} &= \dots = c_{s-1} = \frac{1 - (s - \xi)c}{\xi}, \end{aligned} \quad (10)$$

where $\xi = 1, 2, \dots, s - 1$ and $\xi = 0$ indicates solution, where all states are equinumerous: $c_0 = c_1 = \dots = c_{s-1} = \frac{1}{s}$.

Inserting Eq. (10) to Eq. (7) we obtain

$$F(s, c, q, \xi) = (1 - p) \left[(1 - (s - \xi)c)c^q - c\xi \left(\frac{1 - (s - \xi)c}{\xi} \right)^q \right] + \frac{p}{s}(1 - sc). \quad (11)$$

The stationary solutions different than $c = \frac{1}{s}$ are not that easy to derive in the simple form $c = c(p)$. However, since above equation is linear with the parameter p , we can derive the opposite relation from $F(s, c_{st}, q, \xi) = 0$, i.e. $p = p(c_{st})$ ⁶:

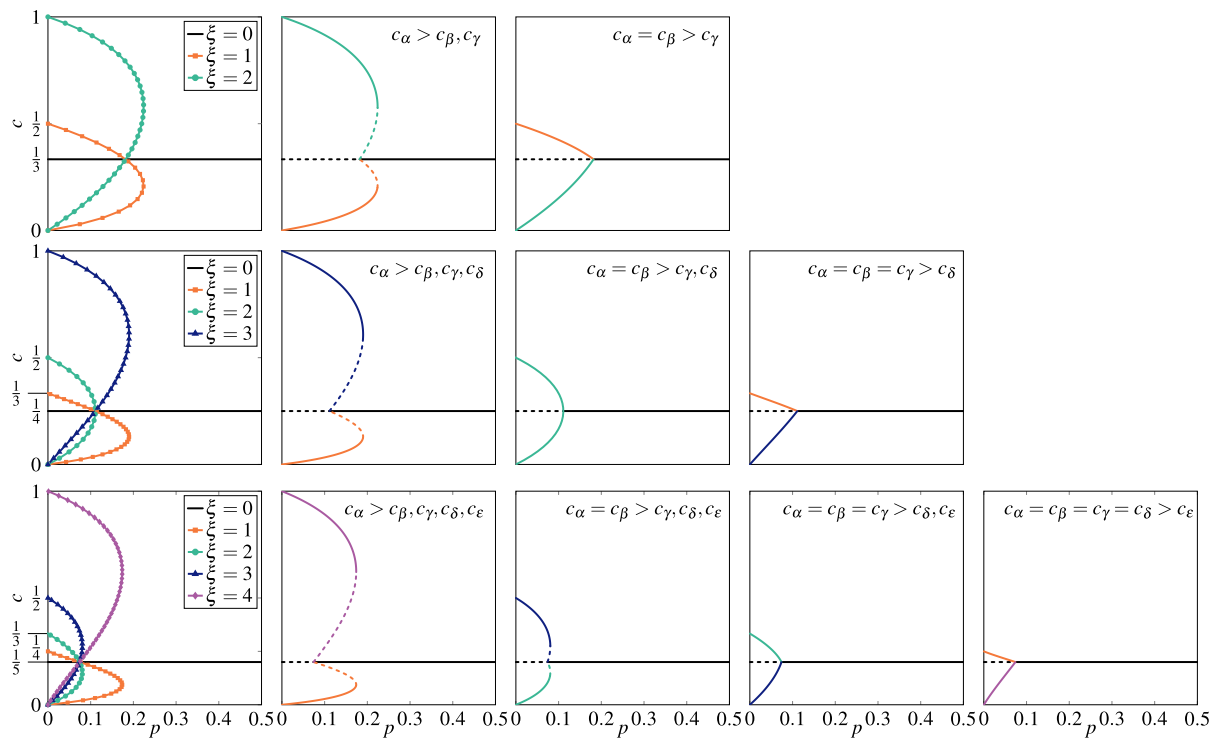


Figure 3. Steady states, given by the solution of Eq. (12), for the annealed model with $q = 3$. Each row corresponds to a different number of states: $s = 3$ (top panels), $s = 4$ (middle panels), $s = 5$ (bottom panels). The first column represents all possible solutions indexed with different values of ξ without the distinction between the stable and unstable solutions. The remaining columns represent stationary states for initial conditions indicated in the top right corner of each panel, where $\alpha, \beta, \gamma, \delta, \epsilon \in \{0, 1, \dots, s - 1\}$. Stable solutions are denoted by the solid lines, whereas the unstable ones are marked with the dashed lines.

$$p = \frac{s \left[c_{st}^q - (s - \xi) c_{st}^{q+1} - \xi c_{st} \left(\frac{1 - (s - \xi) c_{st}}{\xi} \right)^q \right]}{s \left[c_{st}^q - (s - \xi) c_{st}^{q+1} - \xi c_{st} \left(\frac{1 - (s - \xi) c_{st}}{\xi} \right)^q \right] - 1 + c_{st}s}. \quad (12)$$

For $s = 2$ and $\xi = 1$ the above equation correctly reproduces the analytical solution for the original binary q -voter model with noise⁶. For more states, namely $s > 2$, the above relation produces $s - 1$ stationary solutions for $\xi = 1, 2, \dots, s - 1$ respectively, see Fig. 3.

The information about the stability of these states is given by the sign of the first derivative of the effective force with respect to the concentration c at the steady point:

$$F'(s, c, q, \xi) = \left. \frac{dF(s, c, q, \xi)}{dc} \right|_{c=c_{st}}. \quad (13)$$

The state is stable if $F'(s, c_{st}, q, \xi) < 0$ and unstable if $F'(s, c_{st}, q, \xi) > 0$. Based on this analysis, two critical points can be identified: $p = p_1^*$ in which solution $c_{st} = 1/s$ loses stability (so called a lower spinodal) and $p = p_2^*$ in which steady state given by Eq. (12) loses stability (so called an upper spinodal).

At $c_{st} = 1/s$ we can determine the stability analytically, i.e. we are able to derive a formula for the lower spinodal. To do so we calculate the derivative of the effective force

$$F'(s, c, q, \xi) = (1 - p) \left[c^{q-1} q (1 - c(s - \xi)) - c^q (s - \xi) - \xi \left(\frac{1 - c(s - \xi)}{\xi} \right)^q + (s - \xi) c q \left(\frac{1 - c(s - \xi)}{\xi} \right)^{q-1} \right] - p, \quad (14)$$

which for $c_{st} = \frac{1}{s}$ gives

$$F' \left(s, \frac{1}{s}, q, \xi \right) = (1 - p) \left(\frac{1}{s} \right)^q s(q - 1) - p. \quad (15)$$

From the above equation we see that $c_{st} = \frac{1}{s}$ is stable for $p > p_1^*$ and unstable otherwise, where

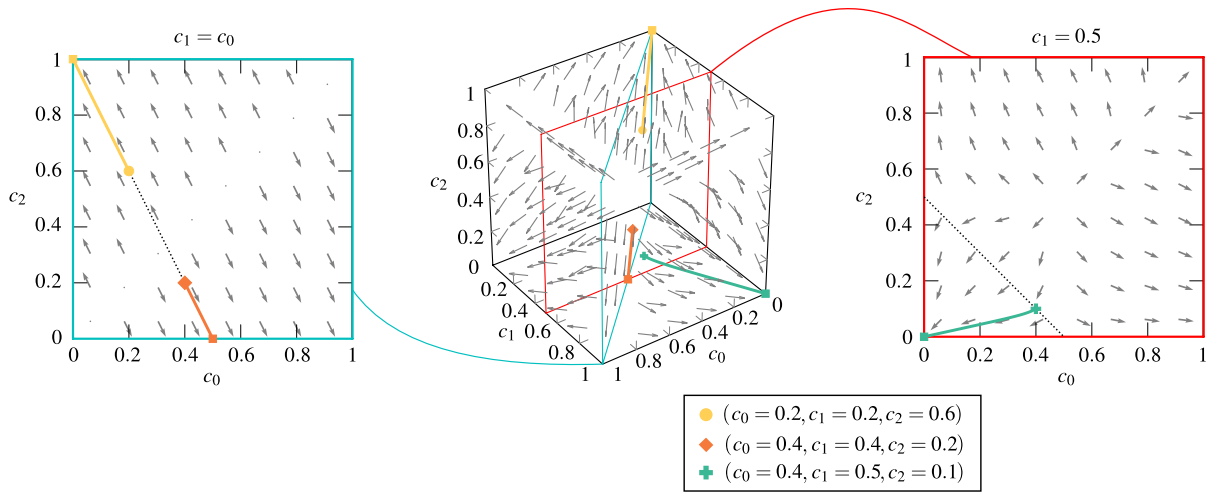


Figure 4. Flow diagrams for the annealed model with $s = 3$ states, the group of influence $q = 5$ and probability of independence $p = 0$ obtained from Eq. (7). Arrows indicate the direction of the flow in the system. Squares refer to stationary points, whereas other markers represent initial points, as indicated in the legend. Lines that connect them represent trajectories. Space for clarity is presented for $c_0, c_1, c_2 \in [0, 1]$ as independent variables, whereas dotted lines on insets represent possible initial conditions $c_0 + c_1 + c_2 = 1$.

$$p_1^* = \frac{q-1}{q-1+s^{q-1}}. \quad (16)$$

The same result can be obtained in several different ways^{6,42}, for example by taking the limit $c \rightarrow 1/s$ in Eq. (12). As expected, for $s = 2$ the result for p_1^* agrees with the one for the original q -voter model with independence⁶. We see in Eq. (16) that, the transition point depends on the size of the influence group q and number of states s . However, it does not depend on the value of ξ , which means that all stationary solutions intersect in the same point p_1^* , as clearly seen in Fig. 3.

The stability of other solutions of Eq. (12) can be determined numerically. In Fig. 4 we present the flow diagram for $s = 3$ and the noise parameter $p = 0$ as an example. It is visible that the states with only one dominant opinion are attractive. It means that from almost all initial conditions the system reaches the stationary state in which one opinion significantly dominates over the others. However, also another type of solution, namely the hyperbolic (saddle)⁴¹ fixed point appears with more than one dominating opinion. In this case a stable, as well as an unstable manifold exist: the point is reached only from the initial state in which two or more equinumerous opinions dominate over the others but it cannot be reached from any other state. This type of solution has been observed also for the multi-state majority-vote model²¹.

The steady state related to the saddle point in which several equinumerous opinions dominate over the others is visible only within the analytical approach but not within the MC simulations. In the latter case, the system initially seems to go towards the saddle point. However, after some time fluctuations push the system into the attractive steady state with only one dominant opinion, as shown in the third (from left) upper panel of Fig. 2.

Quenched approach. Under the quenched approach, we have two types of agents¹⁸: independent and conformists. For each type we introduce the concentration of agents in a given state, similarly as for the annealed model. The only difference in respect to the annealed approach is that this time we consider separately $c_{(I,\alpha)}$ and $c_{(C,\alpha)}$ for independent and conformist voters in state α , respectively. As a result the total concentration of voters in state α is

$$c_\alpha = pc_{(I,\alpha)} + (1-p)c_{(C,\alpha)}. \quad (17)$$

Therefore, now the mean-field dynamics is given by two equations instead of one:

$$\frac{dc_{(I,\alpha)}}{dt} = F_I(s, c_{(I,\alpha)}, q, p), \quad (18)$$

$$\frac{dc_{(C,\alpha)}}{dt} = F_C(s, c_{(C,\alpha)}, q, p). \quad (19)$$

Similarly as for the annealed approach we have

$$F_I(s, c_{(I,\alpha)}, q, p) = \gamma_I^+(s, c_{(I,\alpha)}, q) - \gamma_I^-(s, c_{(I,\alpha)}, q) \equiv \gamma_{(I,\alpha)}^+ - \gamma_{(I,\alpha)}^-, \quad (20)$$

$$F_C(s, c_{(C,\alpha)}, q, p) = \gamma_{(C,\alpha)}^+ - \gamma_{(C,\alpha)}^-, \quad (21)$$

where $\gamma_{(I,\alpha)}^+$ and $\gamma_{(I,\alpha)}^-$ are probabilities that the number of independent agents in state α increases and decreases respectively in a single update. The probabilities $\gamma_{(C,\alpha)}^+$ and $\gamma_{(C,\alpha)}^-$ describe the same, but for conformist agents. These probabilities can be expressed analogously as in the annealed approach:

$$\gamma_{(I,\alpha)}^+ = \sum_{i \neq \alpha} \frac{P_I(i)}{s}, \quad (22)$$

$$\gamma_{(I,\alpha)}^- = \sum_{i \neq \alpha} \frac{P_I(\alpha)}{s}, \quad (23)$$

$$\gamma_{(C,\alpha)}^+ = \sum_{i \neq \alpha} P_C(i) P^q(\alpha|i), \quad (24)$$

$$\gamma_{(C,\alpha)}^- = \sum_{i \neq \alpha} P_C(\alpha) P^q(i|\alpha), \quad (25)$$

where $P(i)$ is the probability of choosing a voter with i -th state, $P_I(i)/P_C(i)$ is the probability of choosing a independent/conformist voter with i -th state and $P(\alpha|i)$ is the conditional probability of picking the neighbor in state α given that a target voter is in state i .

As previously, $P(\alpha|i) = P(\alpha)$, and $\forall_\alpha P(\alpha) = c_\alpha$, and $\forall_\alpha P_I(\alpha) = c_{(I,\alpha)}$, $\forall_\alpha P_C(\alpha) = c_{(C,\alpha)}$, for the complete graph. Therefore:

$$\begin{aligned} F_I(s, c_{(I,\alpha)}, q) &= \frac{dc_{(I,\alpha)}}{dt} = \gamma_{(I,\alpha)}^+ - \gamma_{(I,\alpha)}^- = \sum_{i \neq \alpha} \left[\frac{c_{(I,i)}}{s} - \frac{c_{(I,\alpha)}}{s} \right], \\ F_C(s, c_{(C,\alpha)}, q) &= \frac{dc_{(C,\alpha)}}{dt} = \gamma_{(C,\alpha)}^+ - \gamma_{(C,\alpha)}^- = \sum_{i \neq \alpha} [c_{(C,i)} c_\alpha^q - c_{(C,\alpha)} c_i^q]. \end{aligned} \quad (26)$$

Similarly as in the annealed approach the system can reach the steady state in which all opinions are equinumerous or the one in which some states dominate over the others. Again, we can express all stationary states by c , which denotes the concentration of an arbitrarily chosen state, and by c_I and c_C , which denote the concentration of independent and conformist agents in this state respectively:

$$\begin{aligned} c_0 = \dots = c_{s-(\xi+1)} &= c, \quad c_{s-\xi} = \dots = c_{s-1} = \frac{1 - (s - \xi)c}{\xi}, \\ c_{(I,0)} = \dots = c_{(I,s-(\xi+1))} &= c_I, \quad c_{(I,s-\xi)} = \dots = c_{(I,s-1)} = \frac{1 - (s - \xi)c_I}{\xi}, \\ c_{(C,0)} = \dots = c_{(C,s-(\xi+1))} &= c_C, \quad c_{(C,s-\xi)} = \dots = c_{(C,s-1)} = \frac{1 - (s - \xi)c_C}{\xi}, \\ c &= pc_I + (1 - p)c_C. \end{aligned} \quad (27)$$

where $\xi = 1, 2, \dots, s - 1$ and $\xi = 0$ indicates solution, where all states are equinumerous.

Hence Eq. (26) reduces to:

$$\begin{aligned} F_I(s, c_I, q, \xi) &= \frac{1}{s} - c_I, \\ F_C(s, c_C, q, \xi) &= \xi \left[\frac{1 - (s - \xi)c_C}{\xi} c^q - c_C \left(\frac{1 - (s - \xi)c}{\xi} \right)^q \right]. \end{aligned} \quad (28)$$

Because in the steady state $F_I(s, c_{I,st}, q, \xi) = 0$ and $F_C(s, c_{C,st}, q, \xi) = 0$ we obtain:

$$\begin{aligned} c_{I,st} &= \frac{1}{s}, \\ c_{C,st} &= \frac{c^q}{c^q(s - \xi) + \xi \left(\frac{1 - (s - \xi)c}{\xi} \right)^q}. \end{aligned} \quad (29)$$

By inserting the above formulas to the last formula of Eq. (27), we obtain:

$$p = \frac{s \left[c_{st} \xi \left(\frac{1 - (s - \xi)c_{st}}{\xi} \right)^q - c_{st}^q [1 - (s - \xi)c_{st}] \right]}{\xi \left(\frac{1 - (s - \xi)c_{st}}{\xi} \right)^q - \xi c_{st}^q}. \quad (30)$$

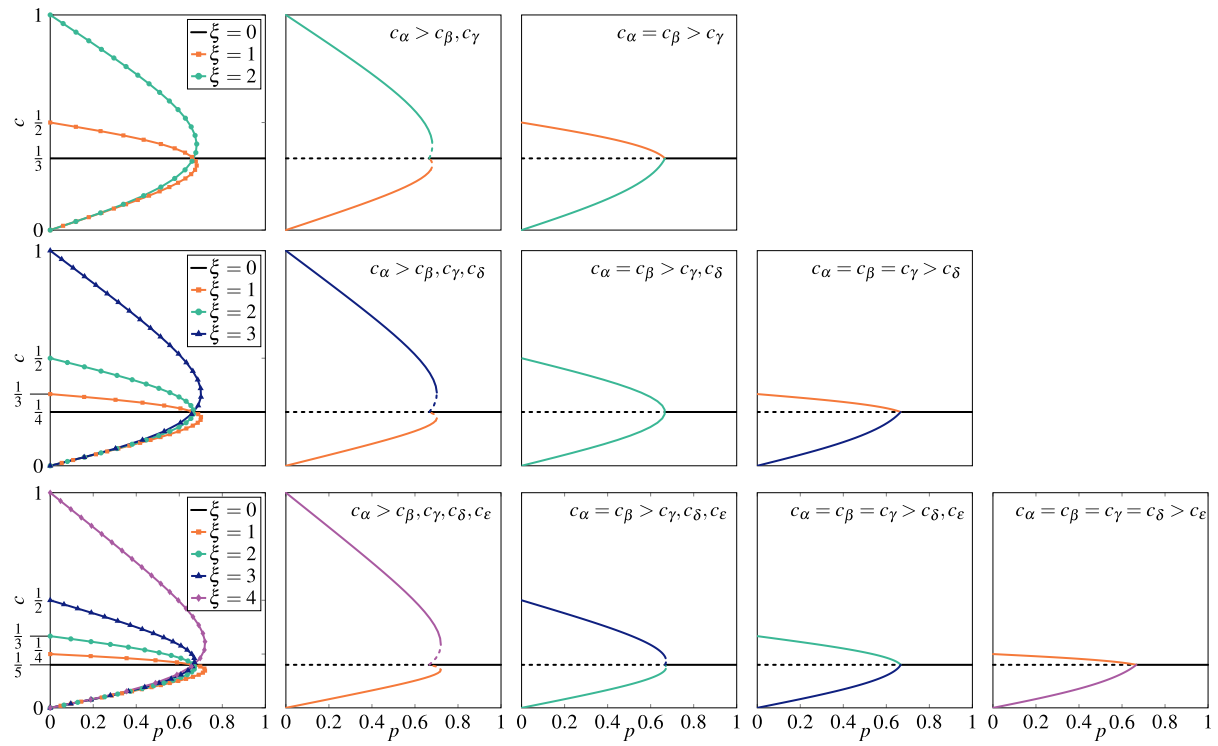


Figure 5. Steady states, given by the solution of Eq. (30), for the quenched model with $q = 3$. The distribution of opinions is the same for Independent and Conformist agents. Each row corresponds to a different number of states: $s = 3$ (top panels), $s = 4$ (middle panels), $s = 5$ (bottom panels). The first column represents all possible solutions indexed with different values of ξ without the distinction between the stable and unstable solutions. The remaining columns represent stationary states for initial conditions indicated in the top right corner of each panel, where $\alpha, \beta, \gamma, \delta, \epsilon \in \{0, 1, \dots, s - 1\}$. Stable solutions are denoted by the solid lines, whereas the unstable ones are marked with the dashed lines.

It is easy to notice that the above equation for $s = 2$ and $\xi = 1$ reproduces the analytical result for the quenched binary q -voter model¹⁸. For more states, namely $s > 2$, above relation produces $s - 1$ stationary solutions, for $\xi = 1, 2, \dots, s - 1$ in the same way as for annealed model, see Fig. 5.

The stability of a steady point is given by determinant and trace of the Jacobian matrix at this point^{21,39}

$$\mathbf{J}_{(c_{I,st}, c_{C,st})} = \begin{bmatrix} \frac{\partial F_I}{\partial c_I} & \frac{\partial F_I}{\partial c_C} \\ \frac{\partial F_C}{\partial c_I} & \frac{\partial F_C}{\partial c_C} \end{bmatrix}_{(c_I, c_C) = (c_{I,st}, c_{C,st})}, \quad (31)$$

where

$$\frac{\partial F_I}{\partial c_I} = -1, \quad (32)$$

$$\frac{\partial F_C}{\partial c_C} = 0, \quad (33)$$

$$\frac{\partial F_C}{\partial c_I} = qp \left[c^{q-1} - (s - \xi)c_C c^{q-1} + (s - \xi)c_C \left(\frac{1 - (s - \xi)c}{\xi} \right)^{q-1} \right], \quad (34)$$

$$\frac{\partial F_C}{\partial c_C} = q(1 - p) \left[c^{q-1} - (s - \xi)c_C c^{q-1} + (s - \xi)c_C \left(\frac{1 - (s - \xi)c}{\xi} \right)^{q-1} \right] - (s - \xi)c^q - \xi \left(\frac{1 - (s - \xi)c}{\xi} \right)^q. \quad (35)$$

The state is stable if $\det[\mathbf{J}_{(c_{I,st}, c_{C,st})}] > 0$ and $\text{tr}[\mathbf{J}_{(c_{I,st}, c_{C,st})}] < 0$. For the steady state $(c_{I,st}, c_{C,st}) = (\frac{1}{s}, \frac{1}{s})$ we are able to determine the stability analytically as for the annealed version of the model:

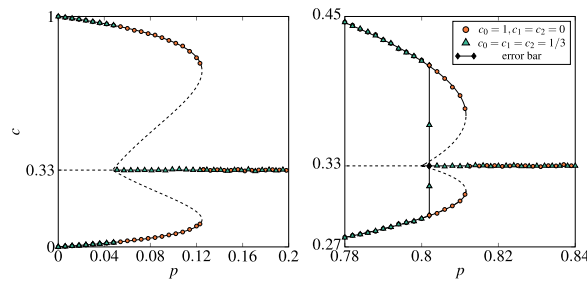


Figure 6. Dependence between the stationary concentration of agents in state 0 and probability of independence p within the annealed (left panel) and the quenched (right panel) approach for $q = 5$ and $s = 3$. Lines represent the solutions of Eqs. (12) and (30): solid and dashed lines correspond to stable and unstable steady states, respectively. Symbols represent the outcome from MC simulations for the system size $N = 5 \times 10^5$. The results are averaged over ten runs and collected after $t = 10^5$ MCS. Simulations are performed from two different initial conditions indicated in the legend. To compare analytical with MC results we plotted also error bars, but for almost all values of p they are invisible, i.e. smaller than the symbols representing results.

$$\det[\mathbf{J}_{\frac{1}{s}, \frac{1}{s}}] = \left(\frac{1}{s}\right)^{q-1} (1 - q + qp) \quad (36)$$

$$\text{tr}[\mathbf{J}_{\frac{1}{s}, \frac{1}{s}}] = \left(\frac{1}{s}\right)^{q-1} (q(1-p) - 1) - 1. \quad (37)$$

Thus the steady state is stable for $p > p_1^*$ and unstable otherwise, where

$$p_1^* = \frac{q-1}{q}. \quad (38)$$

We see that, the critical point p_1^* depends only on the size of the group of influence q , but not on the number of states s , contrary to the annealed model.

Discussion of the results. In the above sections, several aspects of the multi-state qVM was analyzed, namely the role of the parameters: q being the size of the group of influence, s being the number of states, as well as the type of the disorder. The model was considered on the complete graph, which allowed for the mean-field approach. However, all analytical results were also confirmed by the Monte Carlo simulations. In particular, we observe very good agreement between Eqs. (12), (16), (30), (38) and numerical results for the critical points, see Figs. 6 and 7.

It was shown previously that under the quenched disorder only continuous phase transitions are possible within the original (binary) q -voter model with noise¹⁸. Moreover, even under the annealed approach, the appropriate size of the influence group $q > 5$ is required to obtain discontinuous phase transition^{6,36,37}.

Here we have shown that already for the 3-state opinions, the model displays discontinuous phase transitions for any $q > 1$, as presented in Fig. 7. An analogous result was obtained for the majority-vote model, in which agents are not influenced by the unanimous group of q neighbors but by the absolute majority of all agents in the neighborhood. Within such a model with binary opinions, only continuous phase transitions appear⁴³, even if an additional noise is introduced^{7,11,20}. However, for more than two states the majority-vote model displays discontinuous order-disorder phase transitions^{21,32}.

In Fig. 7 it is also seen that discontinuous phase transitions are observed even under the quenched disorder if only the number of states is larger than two, although indeed they are less sharp. This result cannot be compared directly with the analogous one for the majority-vote model, because to our best knowledge multi-state majority-vote model was not studied with the quenched noise. However, the 3-state majority-vote model was studied on the quenched networks and in such a case only a continuous phase transitions were observed as in the binary model^{21,30}.

Although discontinuous phase transitions are observed under both types of disorder, there is a huge difference between two approaches, clearly seen in Figs. 6, 7 and 8:

1. For an arbitrary number of states s , spinodals p_1^* and p_2^* are non-monotonic functions of q within the annealed approach (left panel in Fig. 8), whereas monotonically increasing ones under the quenched approach.
2. While the parameter q affects the lower spinodal p_1^* under both approaches (differently as stayed above), parameter s influences p_1^* only in the case of the annealed approach, see Eq. (16) for the annealed approach and Eq. (38) for the quenched one.
3. Hysteresis, and simultaneously coexistence phase, appears under both approaches for $s > 2$ but it is much larger under the annealed approach than under the quenched one.

www.nature.com/scientificreports/

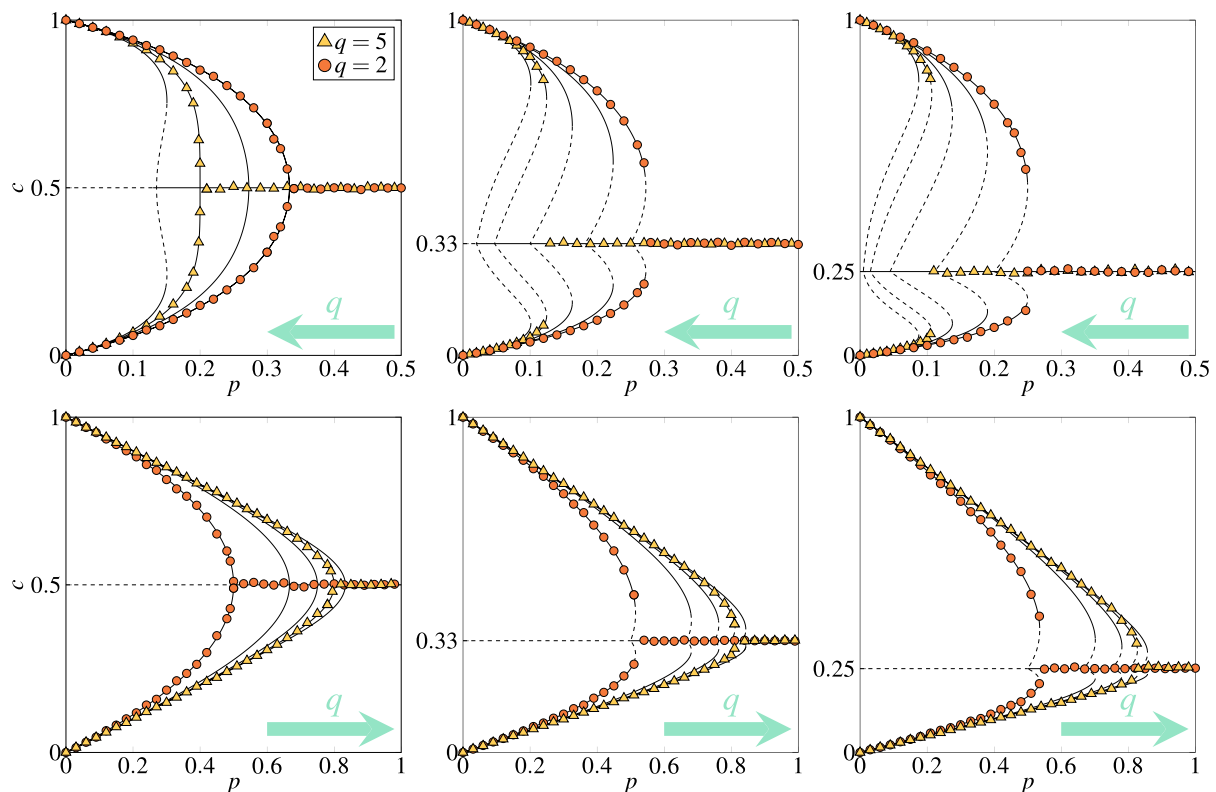


Figure 7. Dependence between the stationary concentration of agents in state 0 and probability of independence p within the annealed (upper panels) and quenched (bottom panels) approach for different values of the influence group size $q = \{2, 3, 4, 5, 6\}$. Arrows in the right corners of subplots indicate the direction in which q increases. The number of states: $s = 2$ (left column), $s = 3$ (middle column) and $s = 4$ (right column). Lines represent the solutions of Eqs. (12) and (30): solid and dashed lines correspond to stable and unstable steady states, respectively. Note that for $s = 2$ we have only four curves, the reason for that is that for $q = 2$ and $q = 3$ exactly the same results are obtained. Symbols represent the outcome from MC simulations for the system size $N = 5 \times 10^5$ performed from initial condition $c_0 = 1, c_1 = c_2 = 0$. The results are averaged over ten runs and collected after $t = 2 \times 10^4$ MCS. Symbols above the line $c = 1/s$ correspond to the concentration of state 0, whereas symbols below the line $c = 1/s$ represent concentration of all others.

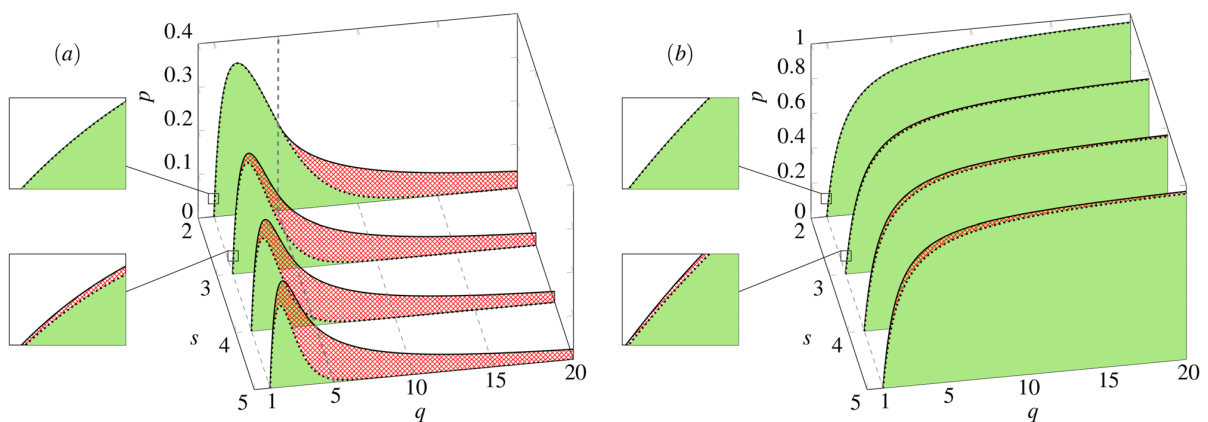


Figure 8. Phase diagram of the multi-state q -voter model under (a) the annealed and (b) the quenched approach. The ordered phases are marked by solid fill-color (green). The coexistence regions are marked by crosshatched pattern (red). The disordered phases are shown as no-fill-color regions (white). Lower and upper spinodals are marked by dotted and solid thick line respectively.

Conclusions

Binary opinions are probably the most frequently used microscopic dynamical variables in models of opinion dynamics, such as the linear voter^{23,44–47} and non-linear voter^{6,13,18,36–40,48–50} models, or the majority-vote model^{7,8,10,11,20,43,51–55}. However, it seems that the binary opinion format is not always sufficient and thus the multi-state versions of the voter^{23–28}, as well as majority-vote model^{21,22,29–32} was introduced.

In this paper we proposed the generalized version of the noisy q -voter model, in which agents are described by the s -state dynamical variables. In our model all opinions are equivalent and agents can switch between any of them. Hence, it is not the best model for opinions that can be measured within the Likert psychometric scale, used to scaling responses in survey research. Such a scale is often used to measure the level of agreement/disagreement, e.g., a typical five-level scale would be: Strongly disagree, Disagree, Neither agree nor disagree, Agree, Strongly agree. One may argue that going in one step from one extreme to another would be not very realistic. Therefore, the multi-state model introduced here would me more appropriate for making a choice between equivalent items. A good example of such a situation is a choice between equivalent products or services on the oligopoly market, such as the choice of the Cable Television and Cellular Phone Services or Automobiles. The model, which could describe opinions on the Likert scale requires in our opinion additional assumptions, such as bounded confidence, and will be studied in the future.

We have investigated the model under two types of approaches, the annealed and the quenched one, to check how the type of disorder influences the model for $s > 2$. Previously it was shown that for $s = 2$ quenched disorder forbids discontinuous phase transitions¹⁸. However, it occurs that for $s > 2$ discontinuous phase transitions are possible even for the quenched disorder. Moreover, they appear for any $q > 1$, on contrary to the original binary q -voter model for which discontinuous phase transitions appear only for $q > 5$ within the annealed approach.

Physicists always look for universalities and this is also the case in this paper. If we compare two popular, yet very different, binary models of opinion dynamics, such as the majority-vote and the q -voter model we clearly see such a universality. In both models introducing only one additional (third) state results in discontinuous phase transitions for the annealed approach. The universality of the second result obtained here, namely the survival of the discontinuous phase transition under the quenched approach would be an interesting task for the future.

Received: 12 January 2021; Accepted: 24 February 2021

Published online: 17 March 2021

References

- Scheffer, M., Westley, F., Brock, W.: Slow response of societies to new problems: Causes and costs. *Ecosystems* **6**, 493–502 (2003). <https://doi.org/10.1007/s10021-002-0146-0>
- Bissell, J., Caiado, C., Curtis, S., Goldstein, M., Straughan, B.: *Tipping Points: Modelling Social Problems and Health*. (Wiley, 2015).
- Strand, M., Lizardo, O.: The hysteresis effect: Theorizing mismatch in action. *J. Theory Soc. Behav.* **47**, 164–194 (2017). <https://doi.org/10.1111/jtsb.12117>
- Pruett, J., et al.: Social tipping points in animal societies. *Proc. R. Society B Biol. Sci.* (2018). <https://doi.org/10.1098/rspb.2018.1282>
- Centola, D., Becker, J., Brackbill, D., Baronchelli, A.: Experimental evidence for tipping points in social convention. *Science* **360**, 1116–1119 (2018). <https://doi.org/10.1126/science.aas8827>
- Nyczka, P., Sznajd-Weron, K., Cislo, J.: Phase transitions in the q -voter model with two types of stochastic driving. *Phys. Rev. E* **86**, 011105 (2012). <https://doi.org/10.1103/PhysRevE.86.011105>
- Vieira, A., Crokidakis, N.: Phase transitions in the majority-vote model with two types of noises. *Physica A Stat. Mech. Appl.* **450**, 30–36 (2016). <https://doi.org/10.1016/j.physa.2016.01.013>
- Chen, H., et al.: First-order phase transition in a majority-vote model with inertia. *Phys. Rev. E* (2017). <https://doi.org/10.1103/PhysRevE.95.042304>
- Tuzón, P., Fernández-Gracia, J., Eguíluz, V.: From continuous to discontinuous transitions in social diffusion. *Front. Phys.* (2018). <https://doi.org/10.3389/fphy.2018.00021>
- Encinas, J., Harunari, P., De Oliveira, M., Fiore, C.: Fundamental ingredients for discontinuous phase transitions in the inertial majority vote model. *Sci. Rep.* (2018). <https://doi.org/10.1038/s41598-018-27240-4>
- Encinas, J., Chen, H., de Oliveira, M., Fiore, C.: Majority vote model with ancillary noise in complex networks. *Physica A Stat. Mech. Appl.* **516**, 563–570 (2019). <https://doi.org/10.1016/j.physa.2018.10.055>
- Nowak, B., Sznajd-Weron, K.: Homogeneous symmetrical threshold model with nonconformity: Independence versus anticonformity. *Complexity*. (2019). <https://doi.org/10.1155/2019/5150825>
- Abramiuk, A., Pawłowski, J., Sznajd-Weron, K.: Is independence necessary for a discontinuous phase transition within the q -voter model? *Entropy*. (2019). <https://doi.org/10.3390/e21050521>
- Chmiel, A., Sienkiewicz, J., Fronczak, A., Fronczak, P.: A veritable zoology of successive phase transitions in the asymmetric q -voter model on multiplex networks. *Entropy*. (2020). <https://doi.org/10.3390/e22091018>
- Aizenman, M., Wehr, J.: Rounding of first-order phase transitions in systems with quenched disorder. *Phys. Rev. Lett.* **62**, 2503–2506 (1989). <https://doi.org/10.1103/PhysRevLett.62.2503>
- Borile, C., Maritan, A., Muñoz, M.: The effect of quenched disorder in neutral theories. *J. Stat. Mech. Theory Exp.* (2013). <https://doi.org/10.1088/1742-5468/2013/04/P04032>
- Martin, P.V., Bonachela, J., & Muñoz, M.: Quenched disorder forbids discontinuous transitions in nonequilibrium low-dimensional systems. *Phys. Rev. E. Stat. Nonlinear Soft. Matter. Phys.* <https://doi.org/10.1103/PhysRevE.89.012145> (2014).
- Jędrzejewski, A., Sznajd-Weron, K.: Person-situation debate revisited: Phase transitions with quenched and annealed disorders. *Entropy* **19**, 415 (2017). <https://doi.org/10.3390/e19080415>
- Wu, F.Y.: The potts model. *Rev. Modern Phys.* **54**, 253–268 (1982)
- Vilela, A.L.M., Moreira, F.G.B.: Majority-vote model with different agents. *Physica A Stat. Mech. Appl.* **388**, 4171–4178 (2009). <https://doi.org/10.1016/j.physa.2009.06.046>
- Li, G., Chen, H., Huang, F., Shen, C.: Discontinuous phase transition in an annealed multi-state majority-vote model. *J. Stat. Mech. Theory Exp.* (2016). <https://doi.org/10.1088/1742-5468/2016/07/073403>
- Oesterreich, A., Pires, M., Crokidakis, N.: Three-state opinion dynamics in modular networks. *Phys. Rev. E* (2019). <https://doi.org/10.1103/PhysRevE.100.032312>
- Redner, S.: Reality-inspired voter models: A mini-review. *Comptes Rendus Physique* **20**, 275–292 (2019). <https://doi.org/10.1016/j.crhy.2019.05.004>
- N., K. & T., G.: Zealots in multi-state noisy voter models (2020). [arXiv:2007.07535](https://arxiv.org/abs/2007.07535).

www.nature.com/scientificreports/

25. Vazquez, F., Loscar, E.S., Baglietto, G.: Multistate voter model with imperfect copying. *Phys. Rev. E* **100**, 042301 (2019). <https://doi.org/10.1103/PhysRevE.100.042301>
26. Böhme, G. & Gross, T.: Fragmentation transitions in multistate voter models. *Phys. Rev. E Stat. Nonlinear Soft. Matter. Phys.* <https://doi.org/10.1103/PhysRevE.85.066117> (2012).
27. Herrerías-Azcué, F., Gallá, T.: Consensus and diversity in multistate noisy voter models. *Phys. Rev. E.* (2019). <https://doi.org/10.1103/PhysRevE.100.022304>
28. Starnini, M., Baronchelli, A., Pastor-Satorras, R.: Ordering dynamics of the multi-state voter model. *J. Stat. Mech. Theory Exp.* **2012**, P10027 (2012). <https://doi.org/10.1088/1742-5468/2012/10/p10027>
29. Chen, P., Redner, S.: Consensus formation in multi-state majority and plurality models. *J. Phys. A Math. General* **38**, 7239–7252 (2005). <https://doi.org/10.1088/0305-4470/38/33/003>
30. Melo, D., Pereira, L., Moreira, F.: The phase diagram and critical behavior of the three-state majority-vote model. *J. Stat. Mech. Theory Exp.* (2010). <https://doi.org/10.1088/1742-5468/2010/11/P11032>
31. Vilela, A., et al.: Three-state majority-vote model on scale-free networks and the unitary relation for critical exponents. *Sci. Rep.* (2020). <https://doi.org/10.1038/s41598-020-63929-1>
32. Chen, H., Li, G.: Phase transitions in a multistate majority-vote model on complex networks. *Phys. Rev. E.* (2018). <https://doi.org/10.1103/PhysRevE.97.062304>
33. Baicerowski, P., Malarz, K.: Multi-choice opinion dynamics model based on latané theory. *Eur. Phys. J. B.* (2019). <https://doi.org/10.1140/epjb/e2019-90533-0>
34. Sznaid-Weron, K., Sznaid, J., Weron, T.: A review on the sznaid model—20 years after. *Physica A Stat. Mech. Appl.* **565**, 125537 (2021). <https://doi.org/10.1016/j.physa.2020.125537>
35. Neto, M., Brigatti, E.: Discontinuous transitions can survive to quenched disorder in a two-dimensional nonequilibrium system. *Phys. Rev. E.* (2020). <https://doi.org/10.1103/PhysRevE.101.022112>
36. Peralta, A., Carro, A., San Miguel, M., Toral, R.: Analytical and numerical study of the non-linear noisy voter model on complex networks. *Chaos* **28**, 075516 (2018). <https://doi.org/10.1063/1.5030112>
37. Vieira, A., Peralta, A., Toral, R., Miguel, M., Anteneodo, C.: Pair approximation for the noisy threshold q-voter model. *Phys. Rev. E.* (2020). <https://doi.org/10.1103/PhysRevE.101.052131>
38. Castellano, C., Muñoz, M.A., Pastor-Satorras, R.: Nonlinear q-voter model. *Phys. Rev. E* **80**, 041129 (2009). <https://doi.org/10.1103/PhysRevE.80.041129>
39. Jedrzejewski, A., Sznaid-Weron, K.: Nonlinear q-voter model from the quenched perspective. *Chaos*. (2020). <https://doi.org/10.1063/1.5134684>
40. Moretti, P., Liu, S., Castellano, C., Pastor-Satorras, R.: Mean-field analysis of the q-voter model on networks. *J. Stat. Phys.* **151**, 113–130 (2013). <https://doi.org/10.1007/s10955-013-0704-1>
41. Strogatz, S.: *Nonlinear Dynamics and Chaos: With Applications to Physics, Biology, Chemistry, and Engineering*. (Perseus Books Publishing, 1994)
42. Nowak, B., Sznaid-Weron, K.: Symmetrical threshold model with independence on random graphs. *Phys. Rev. E.* (2020). <https://doi.org/10.1103/PhysRevE.101.052316>
43. de Oliveira, M.: Isotropic majority-vote model on a square lattice. *J. Stat. Phys.* **66**, 273–281 (1992). <https://doi.org/10.1007/BF01060069>
44. Holley, R.A., Liggett, T.M.: Ergodic theorems for weakly interacting infinite systems and the voter model. *Ann. Probab.* (1975). <https://doi.org/10.1214/aop/1176996306>
45. Castellano, C., Fortunato, S., Loreto, V.: Statistical physics of social dynamics. *Rev. Modern Phys.* **81**, 591–646 (2009). <https://doi.org/10.1103/RevModPhys.81.591>
46. Mobilia, M.: Does a single zealot affect an infinite group of voters? *Phys. Rev. Lett.* **91**, 028701 (2003). <https://doi.org/10.1103/PhysRevLett.91.028701>
47. Peralta, A., Khalil, N., Toral, R.: Ordering dynamics in the voter model with aging. *Physica A Stat. Mech. Appl.* (2020). <https://doi.org/10.1016/j.physa.2019.122475>
48. Gradowski, T., Krawiecki, A.: Pair approximation for the q-voter model with independence on multiplex networks. *Phys. Rev. E.* (2020). <https://doi.org/10.1103/PhysRevE.102.022314>
49. Mukhopadhyay, A., Mazumdar, R., Roy, R.: Voter and majority dynamics with biased and stubborn agents. *J. Stat. Phys.* **181**, 1239–1265 (2020). <https://doi.org/10.1007/s10955-020-02625-w>
50. Tanabe, S., Masuda, N.: Complex dynamics of a nonlinear voter model with contrarian agents. *Chaos Interdiscip. J. Nonlinear Sci.* **23**, 043136 (2013). <https://doi.org/10.1063/1.4851175>
51. Krawiecki, A.: Ferromagnetic and spin-glass-like transition in the majority vote model on complete and random graphs. *Eur. Phys. J. B.* (2020). <https://doi.org/10.1140/epjb/e2020-10288-9>
52. Krawiecki, A.: Spin-glass-like transition in the majority-vote model with anticonformists. *Eur. Phys. J. B.* (2018). <https://doi.org/10.1140/epjb/e2018-80551-9>
53. Krawiecki, A.: Stochastic resonance in the majority vote model on regular and small-world lattices. *Int. J. Modern Phys. B.* (2017). <https://doi.org/10.1142/S0217979217502149>
54. Vilela, A.L., Wang, C., Nelson, K.P., Stanley, H.E.: Majority-vote model for financial markets. *Physica A Stat. Mech. Appl.* **515**, 762–770 (2019). <https://doi.org/10.1016/j.physa.2018.10.007>
55. Krapivsky, P.L., Redner, S.: Dynamics of majority rule in two-state interacting spin systems. *Phys. Rev. Lett.* **90**, 238701 (2003). <https://doi.org/10.1103/PhysRevLett.90.238701>

Acknowledgements

This work has been partially supported by the National Science Center (NCN, Poland) through Grants no. 2016/21/B/HS6/01256 and 2019/35/B/HS6/02530.

Author contributions

B.N. conducted extensive Monte Carlo simulations and analytical calculations for both versions of the model and wrote the original draft, B.S. conducted preliminary studies of the 3-state annealed version of the model consisting of the Monte Carlo simulations and analytical calculations for selected types of initial conditions, K.Sz-W. developed the model, designed and supervised the research. All authors reviewed and edited the manuscript.

Competing interests

The authors declare no competing interests.

Additional information

Correspondence and requests for materials should be addressed to K.S.-W.

www.nature.com/scientificreports/

Reprints and permissions information is available at www.nature.com/reprints.

Publisher's note Springer Nature remains neutral with regard to jurisdictional claims in published maps and institutional affiliations.



Open Access This article is licensed under a Creative Commons Attribution 4.0 International License, which permits use, sharing, adaptation, distribution and reproduction in any medium or format, as long as you give appropriate credit to the original author(s) and the source, provide a link to the Creative Commons licence, and indicate if changes were made. The images or other third party material in this article are included in the article's Creative Commons licence, unless indicated otherwise in a credit line to the material. If material is not included in the article's Creative Commons licence and your intended use is not permitted by statutory regulation or exceeds the permitted use, you will need to obtain permission directly from the copyright holder. To view a copy of this licence, visit <http://creativecommons.org/licenses/by/4.0/>.

© The Author(s) 2021

A.5 Article 5

Switching from a continuous to a discontinuous phase transition under quenched disorder

Switching from a continuous to a discontinuous phase transition under quenched disorder

Bartłomiej Nowak* and Katarzyna Sznajd-Weron†

Department of Theoretical Physics, Wrocław University of Science and Technology, 50-370 Wrocław, Poland

(Dated: July 18, 2022)

Discontinuous phase transitions are particularly interesting from a social point of view because of their relationship to social hysteresis and critical mass. In this paper, we show that the replacement of a time-varying (annealed, situation-based) disorder by a static (quenched, personality-based) one can lead to a change from a continuous to a discontinuous phase transition. This is a result beyond the state of the art, because so far numerous studies on various complex systems (physical, biological, and social) have indicated that the quenched disorder can round or destroy the existence of a discontinuous phase transition. To show the possibility of the opposite behavior, we study a multistate q -voter model, with two types of disorder related to random competing interactions (conformity and anticonformity). We confirm, both analytically and through Monte Carlo simulations, that indeed discontinuous phase transitions can be induced by a static disorder.

I. INTRODUCTION

The study of complex systems, for which the 2021 Nobel Prize was awarded, is arguably the most interdisciplinary field of science, influencing many seemingly unrelated disciplines. For example, it may seem that physics and the social sciences have little in common, yet a huge number of papers have been published in recent decades using statistical physics methods to model various social systems [1–4].

Someone might ask why physicists are concerned with social systems. Probably the first answer that comes to mind is that the methods and concepts of statistical physics can also be useful in the social sciences. But is feedback possible? Can problems and concepts from the social sciences trigger the development of physics itself? The very birth of statistical physics shows that this is what can happen [5]. However today, as sometimes claimed, *physicists are completing the circle by applying physical methods (often times those of statistical physics) to quantify social phenomena* [4]. This is undeniably true, but does this mean that nowadays research at the intersection of physics and social science no longer contributes anything new to physics? There are several examples, which suggest the opposite [6, 7].

In this paper, we also show that the result obtained within the model originally proposed to describe social opinion dynamics can go beyond the state of the art in physics. This result will address the effects of two types of approaches, so-called quenched and annealed, on phase transitions. Before we get to the point, let us clarify the terms *quenched* and *annealed* in the context of disorder in complex systems, because, in our experience, they are not widely known to the general audience. Within the quenched approach various randomness (heterogeneity) associated with interactions, topol-

ogy, etc. are fixed in time. In the context of opinion dynamics, a good example of such an approach are inflexible agents [8] or zealots [9]. On the other hand, within the annealed approach all these randomnesses are changed at each time step [10]. A good example of this type of approach is a contrarian behavior introduced by Galam [11]. In the context of social systems, inspired by the long-standing person-situation debate [12], we related quenched to the personality-oriented, while annealed to the situation-oriented approach [13, 14]. Therefore, the analysis of differences resulting from the given approach (quenched versus annealed) is interesting in the context of social systems. But is this topic of interest in the context of physics itself? Looking at the literature it definitely does.

The role of the quenched disorder in shaping the type of the phase transitions (PTs) have been intensively studied from experimental and theoretical points of view, and applied to understand the behavior of various complex systems [15]. In particular, it has been found that in low-dimensions quenched randomness results in rounding, smearing or completely destroying discontinuous PTs [16–21]. The early prediction of this effect was given heuristically by Imry and Ma [16], and later proven by Aizenman and Wehr [17]. More recently, it was found to be true also in genuinely nonequilibrium systems [22, 23]. Another possibility is that discontinuous (mixed order) PT remains discontinuous and the heterogeneity adds a Griffiths phase subcritically [21]. Moreover, for higher-dimensional systems (three-dimensional or in the mean-field limit), it has been shown that a discontinuous phase transition can simply remain discontinuous in the presence of quenched disorder [14, 24, 25]. However, the complementary effect, i.e., change from continuous to discontinuous PT under the quenched disorder, has yet to be observed, even in the mean-field limit.

In this paper, we will show, both analytically and by Monte Carlo simulations, that such an effect is possible, at least on a complete graph (CG), which corresponds to the mean-field approach (MFA). We will show this within the framework of a model for which so far only

* bartłomiej.nowak@pwr.edu.pl

† katarzyna.weron@pwr.edu.pl

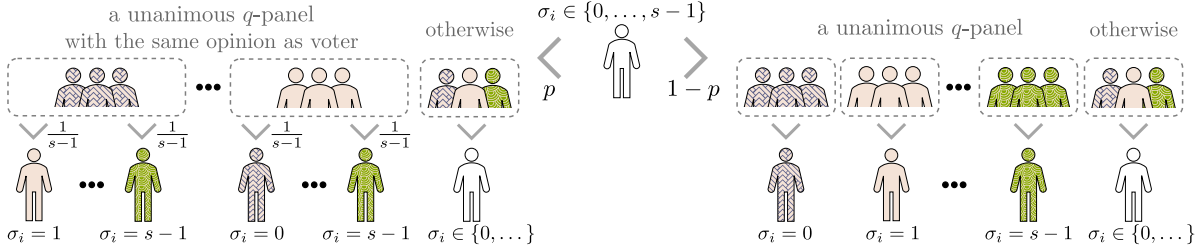


FIG. 1. Visualization of the elementary update for the multi-state q -voter model with anticonformity. Within the annealed approach, a voter can anticonform or conform to the group of influence with complementary probabilities p and $1 - p$. Within the quenched approach, a fraction p of all voters are permanently anticonformists, whereas others are always conformists.

the typical destruction (or softening) of discontinuous PT under quenched disorder has been observed, namely the q -voter model [26]. For example, it was shown that the quenched disorder rounds discontinuous PT in the multistate q -voter model with independence [25] or completely kills these transitions in the two-state version of this model [14]. Additionally, it was shown that in the two-state q -voter model with random competing interactions (conformity and anticonformity), both quenched and annealed disorder give exactly the same continuous PTs [14]. The multistate version of such a model will be the subject of this paper.

II. METHODS

The model, which we refer to as the multi-state q -voter model with anticonformity, is defined as follows. There is a system of N voters, placed in the nodes of an arbitrary graph (here we focus on CG). Each voter $i = 1, \dots, N$ can be in one of s possible states $\sigma_i = \alpha \in \{0, 1, 2, 3, \dots, s - 1\}$. As in the original q -voter model, a voter can be influenced by q neighboring agents only if they are unanimous [26]. As usually, we use a random sequential updating and a unit of time ($t \rightarrow t+1$) is defined as N elementary updates of duration Δt , i.e. $N\Delta t = 1$, which corresponds to one Monte Carlo step (MCS). An elementary update (schematically presented in Fig. 1) consists of: (1) choosing randomly voter i , (2) choosing randomly a group of q neighbors of i , (3) checking if all q neighbors are in the same state to form a group of influence, and (4) updating the state of voter i . The last step of an update depends on the considered approach, annealed or quenched.

Within the annealed approach, all agents are identical: with probability p an active voter acts as an anticonformist, and with complementary probability $1 - p$ as a conformist. Within the quenched approach, the system consists of two types of agents: each voter is set to be permanently anticonformist with probability p or conformist with complementary probability $1 - p$. If the active voter is an anticonformist and all q neighbors are in the same state as the state of an active voter, it changes its state to

any other, randomly chosen from the remaining equally probable $s - 1$ states. On the other hand, if the active voter is a conformist and all q neighbors are in the same state, the active voter copies their state.

To describe the system on the macroscopic scale, we introduce a random variable c_α describing the concentration of agents having opinion α :

$$c_\alpha = \frac{N_\alpha}{N}, \quad \text{and} \quad \sum_{\alpha=0}^{s-1} c_\alpha = 1, \quad (1)$$

where N_α is the number of voters in a given state. Because we use the random sequential updating, c_α can change only by $\pm 1/N$ with the respective transition probabilities:

$$\begin{aligned} \gamma^+(c_\alpha) &= \Pr \left\{ c_\alpha(t + \Delta t) = c_\alpha(t) + \frac{1}{N} \right\}, \\ \gamma^-(c_\alpha) &= \Pr \left\{ c_\alpha(t + \Delta t) = c_\alpha(t) - \frac{1}{N} \right\}. \end{aligned} \quad (2)$$

The specific form of γ^+, γ^- can be easily calculated within MFA for the annealed as well as the quenched approach. Detailed calculations for the transition probabilities (2), as well as other detailed calculations, to which we will refer later in this paper, can be found in the Supplementary Material (SM). Although, c_α is a random variable, we can write the evolution equation of the corresponding expected value:

$$\langle c_\alpha(t + \Delta t) \rangle = \langle c_\alpha(t) \rangle + \frac{1}{N} \gamma^+(c_\alpha) - \frac{1}{N} \gamma^-(c_\alpha). \quad (3)$$

Since $\Delta t = 1/N$ we obtain:

$$\frac{\langle c_\alpha(t + \Delta t) \rangle - \langle c_\alpha(t) \rangle}{\Delta t} = \gamma^+(c_\alpha) - \gamma^-(c_\alpha). \quad (4)$$

Under the realistic assumption that for $N \rightarrow \infty$ random variable c_α localizes to the expectation value and thus:

$$\frac{dc_\alpha}{dt} = \gamma^+(c_\alpha) - \gamma^-(c_\alpha) = F(c_\alpha), \quad (5)$$

where $F(c_\alpha)$ can be interpreted as the effective force acting on the system [27]. Because in this paper we focus

on PTs, we are not interested in the temporal evolution of the system, but only in the stationary states:

$$\frac{dc_\alpha}{dt} = 0. \quad (6)$$

Due to the equivalence of all opinions, one can claim that the only possible symmetry-breaking schemes are those with at most two distinct stationary values [25, 28, 29]. If initially several (one, two, or more) opinions are equinumerous and dominate over all the others, the system reaches an absorbing state in which these opinions still dominate and are equinumerous. At the same time, all remaining opinions become equinumerous. Based on this observation, confirmed by Monte Carlo simulations,

and the normalization condition (1) we are able to write down all solutions in terms of a single arbitrarily chosen state, denoted by c :

$$c_0 = \dots = c_{s-(\xi+1)} = c, \\ c_{s-\xi} = \dots = c_{s-1} = \frac{1 - (s - \xi)c}{\xi}, \quad (7)$$

where $\xi = 1, 2, 3, \dots, s - 1$. By $\xi = 0$ we denote the solution, where all states are equinumerous $c_0 = c_1 = \dots = c_{s-1} = 1/s$. Knowing the above, we can determine the stationary states of the annealed and the quenched version of the model.

Under the annealed approach on the complete graph, Eq. (5) takes the form (see SM):

$$\frac{dc_\alpha}{dt} = -pc_\alpha^{q+1} + p \sum_{i \neq \alpha} \left[\frac{c_i^{q+1}}{s-1} \right] + (1-p) \sum_{i \neq \alpha} [c_i c_\alpha^q - c_\alpha c_i^q]. \quad (8)$$

Combining Eq. (7) with Eqs. (6) and (8) we obtain

$$p = \frac{c^q - (s - \xi)c^{q+1} - \xi c \left(\frac{1 - (s - \xi)c}{\xi} \right)^q}{c^q - (s - \xi)c^{q+1} - \xi c \left(\frac{1 - (s - \xi)c}{\xi} \right)^q - \frac{\xi}{s-1} \left[\left(\frac{1 - (s - \xi)c}{\xi} \right)^{q+1} - c^{q+1} \right]}. \quad (9)$$

Based on the value of ξ we are able to recover s stationary solutions. Some of them are stable and some unstable. We can determine the stability, by looking at the sign of the derivative of the effective force $\frac{dF(c_\alpha)}{dc}$ (see SM for details). It turns out that only two types of stable stationary states of the system are possible: (**disordered**) concentrations of all opinions are identical $c_\alpha = 1/s$ for all α and (**ordered**) in which the symmetry between opinions is broken and one opinion dominates over the others. As seen in Fig. 2, in the annealed case this order-disorder PT is continuous for all values of the model's parameters q and s .

Under the quenched approach the system consists of two types of agents, who respond differently to group influence. Therefore, we must consider these two groups separately and write one evolution equation for the con-

centration $c_{(\mathbf{A}, \alpha)}$ of anticonformists in state α , and the second one for concentration $c_{(\mathbf{C}, \alpha)}$ of conformists in this state [14, 30]. This will ultimately allow us to obtain the total concentration of voters in state α :

$$c_\alpha = pc_{(\mathbf{A}, \alpha)} + (1-p)c_{(\mathbf{C}, \alpha)}, \quad (10)$$

and the evolution of the system is given by two equations

$$\frac{dc_{(\mathbf{A}, \alpha)}}{dt} = -c_{(\mathbf{A}, \alpha)} c_\alpha^q + \sum_{i \neq \alpha} \left[\frac{c_{(\mathbf{A}, i)} c_i^q}{s-1} \right], \\ \frac{dc_{(\mathbf{C}, \alpha)}}{dt} = \sum_{i \neq \alpha} [c_{(\mathbf{C}, i)} c_\alpha^q - c_{(\mathbf{C}, \alpha)} c_i^q]. \quad (11)$$

By performing analogous reasoning to the annealed approach, we compute the stationary states,

$$p = \frac{\left(\frac{1 - (s - \xi)c}{\xi} \right)^q c^q [cs^2 - (1 + 2c\xi)(s - \xi)] + \xi c^{2q} [c(s - \xi) - 1] + c\xi(s - \xi) \left(\frac{1 - (s - \xi)c}{\xi} \right)^{2q}}{\xi \left(\frac{1 - (s - \xi)c}{\xi} \right)^{2q} - \xi c^{2q}} \quad (12)$$

and determine their stability (see the SM for details). We again obtain a phase transition between the **disor-**

dered state, in which concentrations of all opinions are identical $c_\alpha = 1/s$ and the **ordered** state, in which one

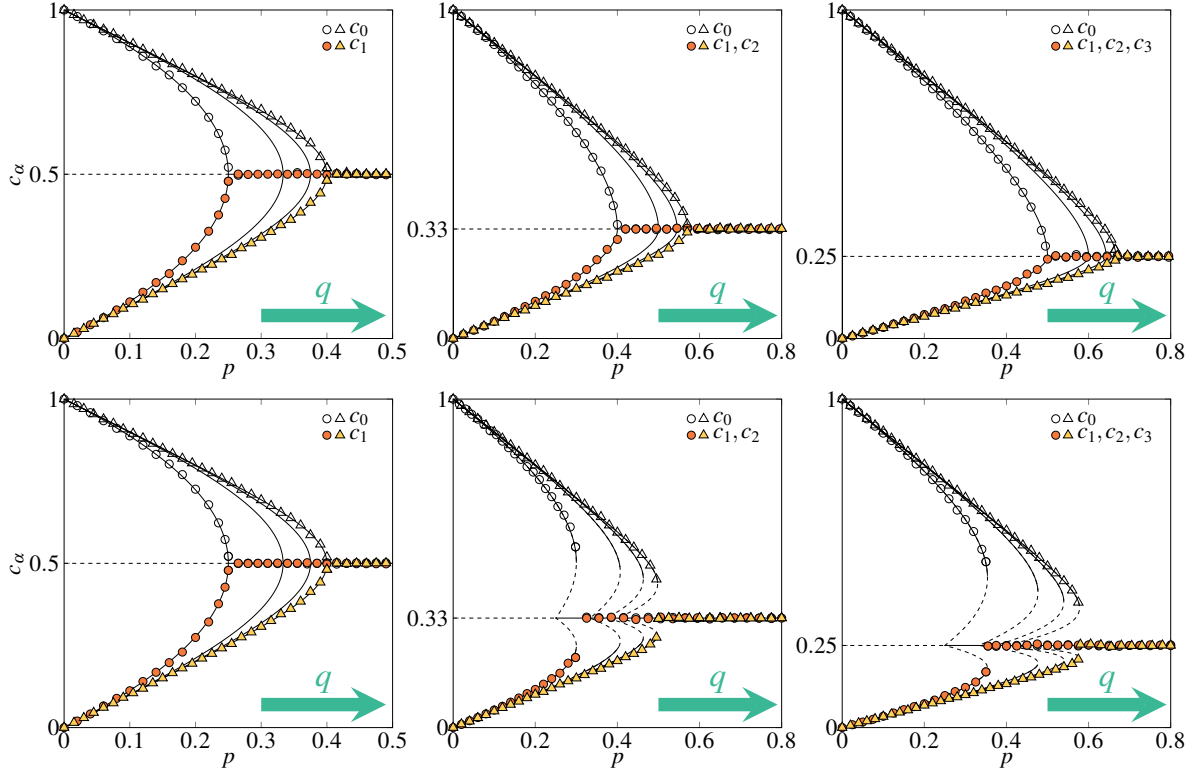


FIG. 2. Stationary concentration of agents in a given state as a function of the probability of anticonformity p within the annealed (upper panels) and quenched (bottom panels) approach for different values of the influence group size $q = \{2, 3, 4, 5\}$ (changing from left to right as indicated by arrows). The number of states $s = 2$ (left column), $s = 3$ (middle column), and $s = 4$ (right column). Lines represent analytical results: solid and dashed lines correspond to stable and unstable steady states, respectively. Symbols represent the outcome of MC simulations for $q = \{2, 5\}$ and the system size $N = 5 \times 10^5$ performed from initial condition $c_0 = 1$. The results are averaged over ten runs and collected after $t = 5 \times 10^4$ MCS.

opinion dominates. However, in contrast to the annealed case, this time for $s > 2$ this transition is discontinuous, as shown in the bottom panels of Fig. 2. For $s = 2$, the results for the annealed and quenched approach are identical, as already shown in Ref. [14].

III. DISCUSSION

For the binary q -voter model with anticonformity, that is, $s = 2$, the quenched approach gives the same result as the annealed one, and the phase transitions are continuous regardless of q , as shown in the left panels of Fig. 2. This result has already been obtained in the previous paper [14] and appears here only as a special case of the general multistate model. The new results refer to $s > 2$, for which the quenched model unexpectedly induces discontinuous phase transitions. While in the annealed version the phase transitions are still continuous, the quenched model displays discontinuous transitions already for $q > 1$ (see Figs. 2 and 3). For all values of the

model parameters, the Monte Carlo results overlap analytical ones, as shown in Fig. 2, which was expected due to the structure of the complete graph.

As seen in Fig. 3 for the fixed value of $s > 2$, the size of the hysteresis, that is, the area in which ordered phase coexists with disordered one, and thus the final state depends on the initial one, depends nonmonotonically on the size of the influence group q . Initially, it increases with q and reaches the maximum value at

$$q = \frac{s}{s-2}, \quad (13)$$

which can be calculated analytically, as shown in SM. At this point, we would like to draw attention to a fact that was already mentioned in the original paper on the q -voter model [1]. Although in the definition of the model both q and s are integer numbers, all analytical calculations make sense for any positive real values of q, s . Therefore, in Fig. 3 the phase boundaries appear as continuous lines as a function of q .

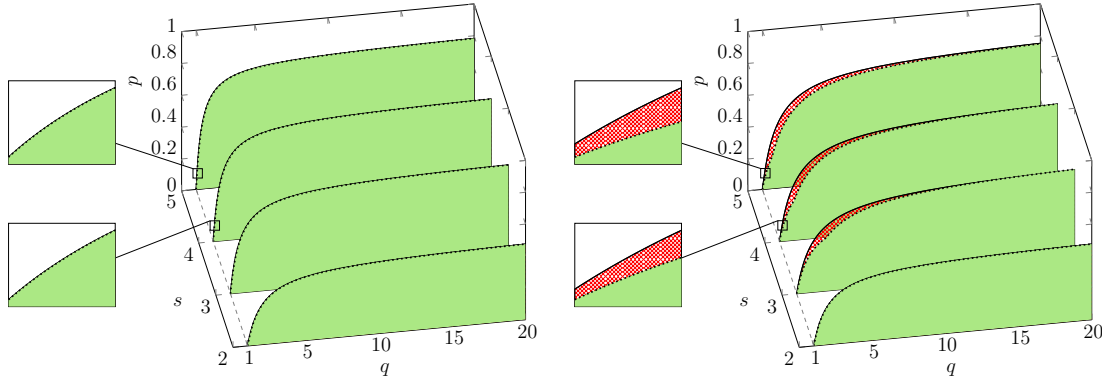


FIG. 3. Phase diagrams obtained within MFA for the multi-state q -voter model under the annealed (left panels) and the quenched (right panels) approaches. The ordered phases are marked by solid color (green). The coexistence regions are marked by a crosshatched pattern (red). The disordered phases are shown as open regions (white). Lower and upper spinodals are marked by dotted and solid lines, respectively.

IV. CONCLUSIONS

The initial inspiration for this research came from social science and was specifically related to the question of factors that influence the emergence of discontinuous phase transitions in social systems. This question with respect to models of social dynamics has been asked before in several papers [25, 31–34]. One might wonder why discontinuous phase transitions are relevant to social systems at all. In fact, they are important because it turns out that hysteresis and critical mass, which are indicators of discontinuous phase transitions, are empirically observed in real social systems [35–37]. The importance of discontinuous phase transitions was one of the reasons why, for example, the q -voter model with independence was studied more intensively than the q -voter model with anticonformity [38–43].

Within the annealed approach, the q -voter model with anticonformity displays only continuous PT, independently of the number of states s and the size of the influence source q . On the contrary, the q -voter model with independence shows discontinuous PTs under the annealed approach above the tricritical point $q^*(s)$, where $q^*(2) = 5$ [14, 27] and $q^*(s > 2) = 1$ [25]. Moreover, it was shown that for the q -voter model with independence replacing the annealed disorder by the quenched one kills discontinuous phase transitions for $s = 2$ [14] or rounds them for $s > 2$ [25]. These previous results were in agreement with the state of the art [16, 17, 19, 20, 22, 23]. On the contrary, in this paper, we have shown that the opposite phenomenon can also be observed.

We are aware that obtaining the same results independently within the two methods (analytical and Monte Carlo simulations) does not mean that we understand the observed phenomenon. Unfortunately, heuristic un-

derstanding is still lacking. Nevertheless, we have decided to present these results, hoping for the help of the readers. Admittedly, nowhere in the literature have we found a proof that the phenomenon we observe is impossible for a complete graph. On the other hand, we have not found any paper in which anyone has observed such a phenomenon. From this perspective, the model studied here should be treated as an example that shows that a quenched disorder can support discontinuous phase transitions in some cases.

We realize that a complete graph is very different from finite-dimensional systems, because in the latter case the nodes are not equivalent. Moreover, here, we consider only a bimodal disorder (conformist or anticonformist). This means that there are only two classes of sites in the complete graph, and the sites within either class are completely equivalent to each other. It would be desirable to consider the same model on top of other graphs to check what is responsible for the observed phenomena, the structure of the system, or maybe just a bimodal disorder. The consideration of the model on other structures would also allow us to analyze the behavior of the correlation length. This will help us to determine whether we are actually dealing with a binary division into continuous/discontinuous phase transitions or whether hybrid transitions, as reported for the asymmetric q -voter model on multiplex networks [41], also appear. Although many questions remain open, we believe that our finding goes far beyond social physics and will be interesting to a broad audience.

AUTHOR CONTRIBUTIONS

B.N. was responsible for all analytical calculations and Monte Carlo simulations. K.S.-W. was responsible for supervising the research and funding acquisition. Both authors wrote, reviewed, and edited the manuscript.

ACKNOWLEDGMENTS

This work was partially supported by funds from the National Science Center (NCN, Poland) through Grant No. 2019/35/B/HS6/02530.

-
- [1] C. Castellano, S. Fortunato, and V. Loreto, Statistical physics of social dynamics, *Reviews of Modern Physics* **81**, 591 (2009).
 - [2] J. Kwapień and S. Drozdz, Physical approach to complex systems, *Physics Reports* **515**, 115 (2012).
 - [3] M. Perc, J. Jordan, D. Rand, Z. Wang, S. Boccaletti, and A. Szolnoki, Statistical physics of human cooperation, *Physics Reports* **687**, 1 (2017).
 - [4] M. Jusup, P. Holme, K. Kanazawa, M. Takayasu, I. Romić, Z. Wang, S. Geček, T. Lipić, B. Podobnik, L. Wang, W. Luo, T. Klanjšček, J. Fan, S. Boccaletti, and M. Perc, Social physics, *Physics Reports* **948**, 1 (2022).
 - [5] P. Ball, The physical modelling of society: A historical perspective, *Physica A: Statistical Mechanics and its Applications* **314**, 1 (2002).
 - [6] A. Sousa, K. Malarz, and S. Galam, Reshuffling spins with short range interactions: When sociophysics produces physical results, *International Journal of Modern Physics C* **16**, 1507 (2005).
 - [7] S. Galam and A. Martins, Two-dimensional ising transition through a technique from two-state opinion-dynamics models, *Physical Review E - Statistical, Nonlinear, and Soft Matter Physics* **91** (2015).
 - [8] S. Galam and F. Jacobs, The role of inflexible minorities in the breaking of democratic opinion dynamics, *Physica A: Statistical Mechanics and its Applications* **381**, 366 (2007).
 - [9] M. Mobilia, Does a single zealot affect an infinite group of voters?, *Phys. Rev. Lett.* **91**, 028701 (2003).
 - [10] B. Derrida and D. Stauffer, Phase transitions in two-dimensional kauffman cellular automata, *EPL* **2**, 739 (1986).
 - [11] S. Galam, Contrarian deterministic effects on opinion dynamics: “the hung elections scenario”, *Physica A: Statistical Mechanics and its Applications* **333**, 453 (2004).
 - [12] R. Lucas and M. Donnellan, If the person-situation debate is really over, why does it still generate so much negative affect?, *Journal of Research in Personality - J RES PERSONAL* **43**, 146 (2009).
 - [13] K. Sznajd-Weron, J. Szwabiński, and R. Weron, Is the person-situation debate important for agent-based modeling and vice-versa?, *PLoS ONE* **9**, 10.1371/journal.pone.0112203 (2014).
 - [14] A. Jędrzejewski and K. Sznajd-Weron, Person-situation debate revisited: Phase transitions with quenched and annealed disorders, *Entropy* **19**, 415 (2017).
 - [15] T. Vojta and J. Hoyos, Criticality and quenched disorder: Harris criterion versus rare regions, *Physical Review Letters* **112**, 10.1103/PhysRevLett.112.075702 (2014).
 - [16] Y. Imry and S.-K. Ma, Random-field instability of the ordered state of continuous symmetry, *Physical Review Letters* **35**, 1399 (1975).
 - [17] M. Aizenman and J. Wehr, Rounding of first-order phase transitions in systems with quenched disorder, *Physical Review Letters* **62**, 2503 (1989).
 - [18] K. Binder, Theory of first-order phase transitions, *Reports on Progress in Physics* **50**, 783 (1987).
 - [19] T. Vojta, Rare region effects at classical, quantum and nonequilibrium phase transitions, *Journal of Physics A: Mathematical and General* **39**, R143 (2006).
 - [20] M. Muñoz, R. Juhász, C. Castellano, and G. Ódor, Griffiths phases on complex networks, *Physical Review Letters* **105**, 10.1103/PhysRevLett.105.128701 (2010).
 - [21] G. Ódor and B. De Simoni, Heterogeneous excitable systems exhibit griffiths phases below hybrid phase transitions, *Physical Review Research* **3**, 10.1103/PhysRevResearch.3.013106 (2021).
 - [22] C. Borile, A. Maritan, and M. Muñoz, The effect of quenched disorder in neutral theories, *Journal of Statistical Mechanics: Theory and Experiment* **2013**, 10.1088/1742-5468/2013/04/P04032 (2013).
 - [23] P. Villa Martín, J. Bonachela, and M. Muñoz, Quenched disorder forbids discontinuous transitions in nonequilibrium low-dimensional systems, *Physical Review E - Statistical, Nonlinear, and Soft Matter Physics* **89**, 10.1103/PhysRevE.89.012145 (2014).
 - [24] L. Fernández, A. Gordillo-Guerrero, V. Martín-Mayor, and J. Ruiz-Lorenzo, First-order transition in a three-dimensional disordered system, *Physical Review Letters* **100**, 10.1103/PhysRevLett.100.057201 (2008).
 - [25] B. Nowak, B. Stoić, and K. Sznajd-Weron, Discontinuous phase transitions in the multi-state noisy q-voter model: quenched vs. annealed disorder, *Scientific Reports* **11**, 10.1038/s41598-021-85361-9 (2021).
 - [26] C. Castellano, M. Muñoz, and R. Pastor-Satorras, Nonlinear q-voter model, *Physical Review E - Statistical, Nonlinear, and Soft Matter Physics* **80** (2009).
 - [27] P. Nyczka, K. Sznajd-Weron, and J. Cislo, Phase transitions in the q-voter model with two types of stochastic driving, *Phys. Rev. E* **86**, 011105 (2012).
 - [28] A. Mansouri and F. Taghiyareh, Phase transition in the social impact model of opinion formation in log-normal networks, *Journal of Information Systems and Telecommunication* **9**, 1 (2021), cited By 0.
 - [29] J.-C. Lin and P. L. Taylor, Symmetry-breaking schemes for the potts model on a bethe lattice, *Phys. Rev. B* **48**, 7216 (1993).
 - [30] A. Jędrzejewski and K. Sznajd-Weron, Nonlinear q-voter model from the quenched perspective, *Chaos* **30**, 10.1063/1.5134684 (2020).
 - [31] A. Vieira and N. Crokidakis, Phase transitions in the majority-vote model with two types of noises, *Physica A: Statistical Mechanics and its Applications* **450**, 30 (2016).

- [32] G. Li, H. Chen, F. Huang, and C. Shen, Discontinuous phase transition in an annealed multi-state majority-vote model, *Journal of Statistical Mechanics: Theory and Experiment* **2016**, 10.1088/1742-5468/2016/07/073403 (2016).
- [33] J. Encinas, P. Harunari, M. De Oliveira, and C. Fiore, Fundamental ingredients for discontinuous phase transitions in the inertial majority vote model, *Scientific Reports* **8**, 10.1038/s41598-018-27240-4 (2018).
- [34] I. Iacopini, G. Petri, A. Barrat, and V. Latora, Simplicial models of social contagion, *Nature Communications* **10**, 10.1038/s41467-019-10431-6 (2019).
- [35] M. Strand and O. Lizardo, The hysteresis effect: Theorizing mismatch in action, *Journal for the Theory of Social Behaviour* **47**, 164 (2017).
- [36] D. Centola, J. Becker, D. Brackbill, and A. Baronchelli, Experimental evidence for tipping points in social convention, *Science* **360**, 1116 (2018).
- [37] D. Guilbeault, A. Baronchelli, and D. Centola, Experimental evidence for scale-induced category convergence across populations, *Nature Communications* **12**, 10.1038/s41467-020-20037-y (2021).
- [38] A. Jędrzejewski, Pair approximation for the q -voter model with independence on complex networks, *Physical Review E* **95**, 10.1103/PhysRevE.95.012307 (2017).
- [39] A. Vieira, A. Peralta, R. Toral, M. Miguel, and C. Anteneodo, Pair approximation for the noisy threshold q -voter model, *Physical Review E* **101**, 10.1103/PhysRevE.101.052131 (2020).
- [40] T. Gradowski and A. Krawiecki, Pair approximation for the q -voter model with independence on multiplex networks, *Physical Review E* **102**, 10.1103/PhysRevE.102.022314 (2020).
- [41] A. Chmiel, J. Sienkiewicz, A. Fronczak, and P. Fronczak, A veritable zoology of successive phase transitions in the asymmetric q -voter model on multiplex networks, *Entropy* **22**, 10.3390/e22091018 (2020).
- [42] J. Civitarese, External fields, independence, and disorder in q -voter models, *Physical Review E* **103**, 10.1103/PhysRevE.103.012303 (2021).
- [43] R. Jankowski and A. Chmiel, Role of time scales in the coupled epidemic-opinion dynamics on multiplex networks, *Entropy* **24**, 10.3390/e24010105 (2022).

**Supplementary material for
Switching from a continuous to a discontinuous phase transition under quenched
disorder.**

Bartłomiej Nowak* and Katarzyna Sznajd-Weron†

Department of Theoretical Physics, Wrocław University of Science and Technology, 50-370 Wrocław, Poland

(Dated: July 18, 2022)

In this Supplementary Material, we will provide the details of the mathematical calculations for the q -voter model with anticonformity under two types of disorder: quenched and annealed.

I. DERIVATION OF THE MODEL

A. Annealed approach

The total concentration of voters in a state α can increase by $1/N$ only if we pick an active voter in a different state than α . Then the active voter can anticonform with probability p or conform with probability $1 - p$. In both cases, a lobby of q neighbors is chosen randomly (without repetitions) and it can change the state of an active voter only if it is unanimous. In this supplementary material we derive analytically evolution equations, as well as stationary states, for the infinitive system, $N \rightarrow \infty$, within the mean-field approach.

To present the detailed calculation, we introduce the following notation:

- $P(i)$ – the probability of choosing randomly an active (i.e., the one whose state will be updated) voter in state $i = \{0, 1, \dots, s - 1\}$.
- $P(\alpha|i)$ – the conditional probability of picking a neighbor in state α given that an active voter is in state i .

Within the above notation, the probability of choosing q neighbors in state α is equal to $P^q(\alpha|i)$. In the case of conformity, α has to be different from i to change the state of an active voter. On the other hand, in the case of anticonformity, $\alpha = i$ is needed to change the state of an active voter, and then state α must be chosen. The latter occurs with probability $1/(s - 1)$, because a voter chooses a new state randomly from $s - 1$ states.

Analogous reasoning can be carried out for the situation in which the total concentration of voters in a state α decreases. In result, the transition probabilities can be expressed explicitly as:

$$\begin{aligned} \gamma^+(c_\alpha) &= \sum_{i \neq \alpha} P(i) \left[p \frac{P^q(i|i)}{s-1} + (1-p)P^q(\alpha|i) \right] \\ \gamma^-(c_\alpha) &= \sum_{i \neq \alpha} P(\alpha) \left[p \frac{P^q(\alpha|\alpha)}{s-1} + (1-p)P^q(i|\alpha) \right] \end{aligned} \quad (1)$$

Within MFA, the events of picking an active voter in a given state i and a neighbor in a state α are independent, so all conditional probabilities $P(\alpha|i)$, $P(i|\alpha)$ are equal to $P(\alpha)$, $P(i)$ respectively. Moreover, the local concentration of agents is the state α or i is equal to the global one, which means that $P(\alpha) = c_\alpha$ and $P(i) = c_i$. Therefore, within MFA Eq. (1) boils down to:

$$\begin{aligned} \gamma^+(c_\alpha) &= \sum_{i \neq \alpha} c_i \left[p \frac{c_i^q}{s-1} + (1-p)c_\alpha^q \right] \\ \gamma^-(c_\alpha) &= \sum_{i \neq \alpha} c_\alpha \left[p \frac{c_\alpha^q}{s-1} + (1-p)c_i^q \right]. \end{aligned} \quad (2)$$

This leads to:

$$\begin{aligned} \frac{dc_\alpha}{dt} &= \gamma^+(c_\alpha) - \gamma^-(c_\alpha) \\ &= -pc_\alpha^{q+1} + p \sum_{i \neq \alpha} \left[\frac{c_i^{q+1}}{s-1} \right] + (1-p) \sum_{i \neq \alpha} [c_i c_\alpha^q - c_\alpha c_i^q]. \end{aligned} \quad (3)$$

Stationary states can be found by solving the following equation

$$\frac{dc_\alpha}{dt} = 0. \quad (4)$$

Recalling the notation

$$\begin{aligned} c_0 &= \dots = c_{s-(\xi+1)} = c, \\ c_{s-\xi} &= \dots = c_{s-1} = \frac{1 - (s - \xi)c}{\xi}, \end{aligned} \quad (5)$$

Eq. (4) takes form

$$\begin{aligned} \frac{p\xi}{s-1} \left[\left(\frac{1 - (s - \xi)c}{\xi} \right)^{q+1} - c^{q+1} \right] + (1-p)c^q \\ - (1-p) \left[(s - \xi)c^{q+1} + \xi c \left(\frac{1 - (s - \xi)c}{\xi} \right)^q \right] = 0. \end{aligned} \quad (6)$$

Solving it for p yields the stationary solution

* bartłomiej.nowak@pwr.edu.pl

† katarzyna.weron@pwr.edu.pl

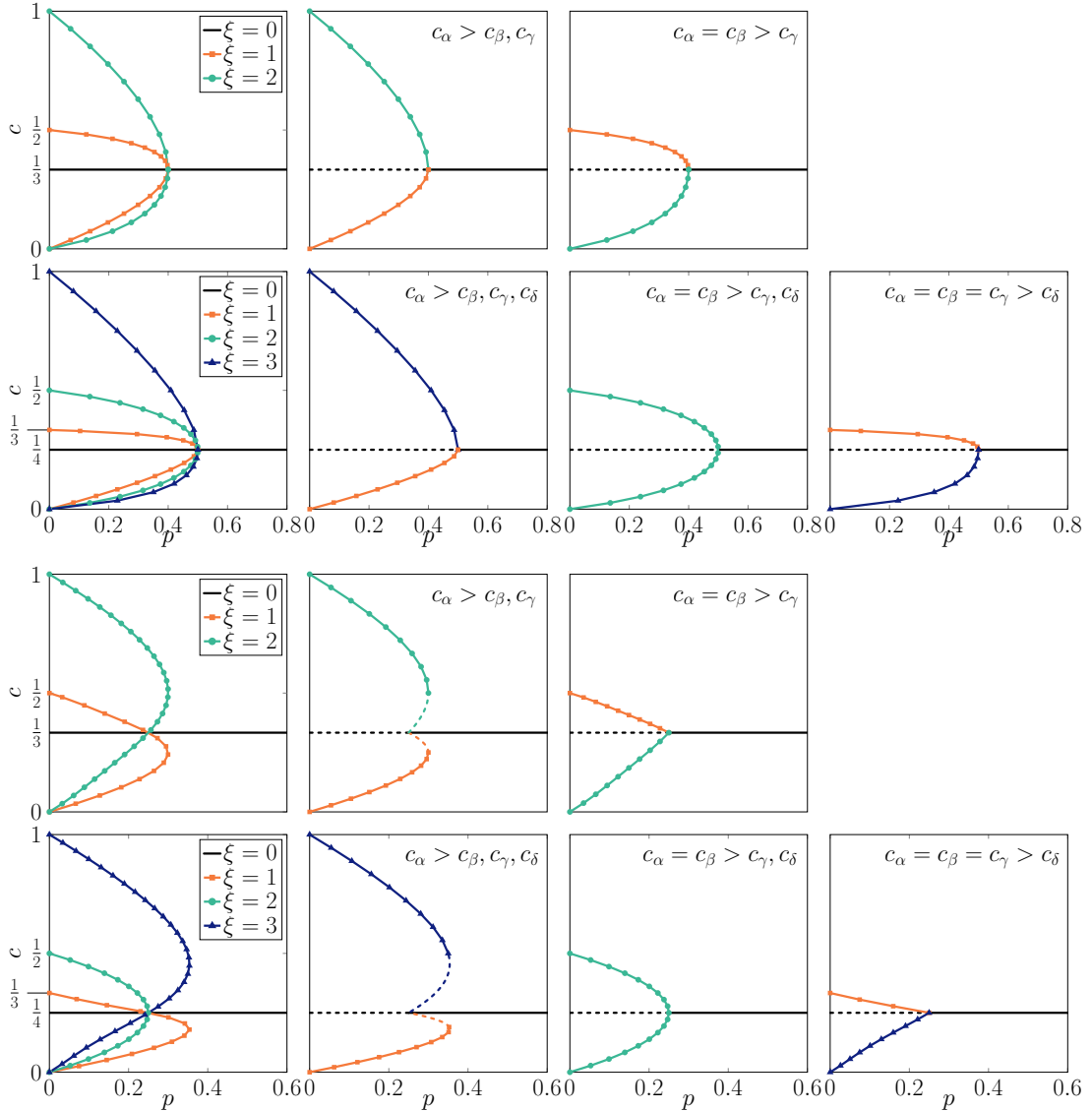


FIG. 1. Steady states for $q = 2$ within the annealed (two upper rows) as well as the quenched approach (two bottom rows) for: $s = 3$ (the shorter rows, i.e. the first and third), $s = 4$ (the longer rows, i.e. the second and fourth). Plots in the first column show all possible solutions indexed ξ without the distinction between the stable and unstable ones obtained from Eq. (7) for the annealed approach and from Eq. (19) for the quenched one. The remaining columns represent stationary states for initial conditions indicated in the top right corners of each panel, where $\alpha, \beta, \gamma, \delta \in \{0, 1, \dots, s - 1\}$. Stable solutions are marked with solid lines with symbols, and unstable with dashed lines.

$$p = \frac{c^q - (s - \xi)c^{q+1} - \xi c \left(\frac{1-(s-\xi)c}{\xi} \right)^q}{c^q - (s - \xi)c^{q+1} - \xi c \left(\frac{1-(s-\xi)c}{\xi} \right)^q - \frac{\xi}{s-1} \left[\left(\frac{1-(s-\xi)c}{\xi} \right)^{q+1} - c^{q+1} \right]}. \quad (7)$$

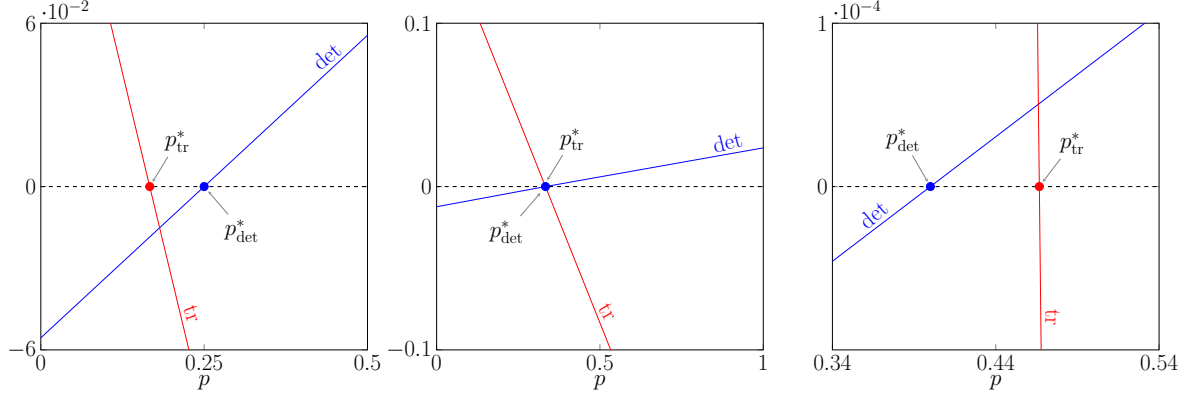


FIG. 2. Dependence between the determinant (28), trace (29) and value of the parameter p for different number of states and size of the influence group: $s = 3$ and $q = 2$ (left); $s = 3$ and $q = 3$ (middle); $s = 3$ and $q = 5$ (right). Lines indicate values of the trace (tr) and determinant (det) denoted above each line. Points describe the values of p at which trace and determinant change sign, see Eqs. (31) and (30).

From equation (7) one can reproduce all s stationary solutions, see two upper rows in Fig. 1.

B. Quenched approach

Within the quenched approach, two groups of agents exist: conformists and anticonformists. Therefore, the separate reasoning has to be provided within each group and the dynamics is given by two equations for concentration of agents in state α among anticonformists $c_{(\mathbf{A},\alpha)}$ and conformists $c_{(\mathbf{C},\alpha)}$

$$\frac{dc_{(\mathbf{A},\alpha)}}{dt} = \gamma_{\mathbf{A}}^+(c_{(\mathbf{A},\alpha)}) - \gamma_{\mathbf{A}}^-(c_{(\mathbf{A},\alpha)}) = F_{\mathbf{A}}(c_{(\mathbf{A},\alpha)}), \quad (8)$$

$$\frac{dc_{(\mathbf{C},\alpha)}}{dt} = \gamma_{\mathbf{C}}^+(c_{(\mathbf{C},\alpha)}) - \gamma_{\mathbf{C}}^-(c_{(\mathbf{C},\alpha)}) = F_{\mathbf{C}}(c_{(\mathbf{C},\alpha)}), \quad (9)$$

where $\gamma_{\mathbf{A}}^+(c_{(\mathbf{A},\alpha)})$, $\gamma_{\mathbf{A}}^-(c_{(\mathbf{A},\alpha)})$ denotes transition rates for anticonformist and $\gamma_{\mathbf{C}}^+(c_{(\mathbf{C},\alpha)})$, $\gamma_{\mathbf{C}}^-(c_{(\mathbf{C},\alpha)})$ for conformist agents. Forces acting on the system for anticonformist and conformist agents are denoted with $F_{\mathbf{A}}(c_{(\mathbf{A},\alpha)})$ and $F_{\mathbf{C}}(c_{(\mathbf{C},\alpha)})$, respectively.

The concentration of anticonformists in state α can increase by $1/N$ only if an anticonformist in state $i \neq \alpha$ is randomly chosen to be an active voter. On the other hand, the concentration of conformists in state α can increase by $1/N$ only if a conformist in state $i \neq \alpha$ is randomly chosen to be an active voter. Therefore, to derive the explicit form of transition probabilities, we keep notation from IA, and additionally we introduce:

- $P_{\mathbf{A}}(i)$ – the probability of choosing anticonformist in state $i = \{0, 1, \dots, s-1\}$ to be an active voter.
- $P_{\mathbf{C}}(i)$ – the probability of choosing conformist in state $i = \{0, 1, \dots, s-1\}$ to be an active voter.

Within such a notation, the transition probabilities can be expressed explicitly as

$$\begin{aligned} \gamma_{\mathbf{A}}^+(c_{(\mathbf{A},\alpha)}) &= \sum_{i \neq \alpha} \left[\frac{P_{\mathbf{A}}(i) P^q(i|i)}{s-1} \right], \\ \gamma_{\mathbf{A}}^-(c_{(\mathbf{A},\alpha)}) &= \sum_{i \neq \alpha} \left[\frac{P_{\mathbf{A}}(\alpha) P^q(\alpha|\alpha)}{s-1} \right], \\ \gamma_{\mathbf{C}}^+(c_{(\mathbf{C},\alpha)}) &= \sum_{i \neq \alpha} [P_{\mathbf{C}}(i) P^q(\alpha|i)], \\ \gamma_{\mathbf{C}}^-(c_{(\mathbf{C},\alpha)}) &= \sum_{i \neq \alpha} [P_{\mathbf{C}}(\alpha) P^q(i|\alpha)]. \end{aligned} \quad (10)$$

Within MFA $P(\alpha|\beta) = P(\alpha)$, $P(\alpha) = c_\alpha$, $P_{\mathbf{A}}(\alpha) = c_{(\mathbf{A},\alpha)}$ and $P_{\mathbf{C}}(\alpha) = c_{(\mathbf{C},\alpha)}$ and thus:

$$\begin{aligned} \gamma_{\mathbf{A}}^+(c_{(\mathbf{A},\alpha)}) &= \sum_{i \neq \alpha} \left[\frac{c_{(\mathbf{A},i)} c_i^q}{s-1} \right], \\ \gamma_{\mathbf{A}}^-(c_{(\mathbf{A},\alpha)}) &= \sum_{i \neq \alpha} \left[\frac{c_{(\mathbf{A},\alpha)} c_\alpha^q}{s-1} \right], \\ \gamma_{\mathbf{C}}^+(c_{(\mathbf{C},\alpha)}) &= \sum_{i \neq \alpha} [c_{(\mathbf{C},i)} c_\alpha^q], \\ \gamma_{\mathbf{C}}^-(c_{(\mathbf{C},\alpha)}) &= \sum_{i \neq \alpha} [c_{(\mathbf{C},\alpha)} c_i^q]. \end{aligned} \quad (11)$$

and in result the model can be described as follows

$$\begin{aligned} \frac{dc_{(\mathbf{A},\alpha)}}{dt} &= -c_{(\mathbf{A},\alpha)} c_\alpha^q + \sum_{i \neq \alpha} \left[\frac{c_{(\mathbf{A},i)} c_i^q}{s-1} \right], \\ \frac{dc_{(\mathbf{C},\alpha)}}{dt} &= \sum_{i \neq \alpha} [c_{(\mathbf{C},i)} c_\alpha^q - c_{(\mathbf{C},\alpha)} c_i^q] \end{aligned} \quad (12)$$

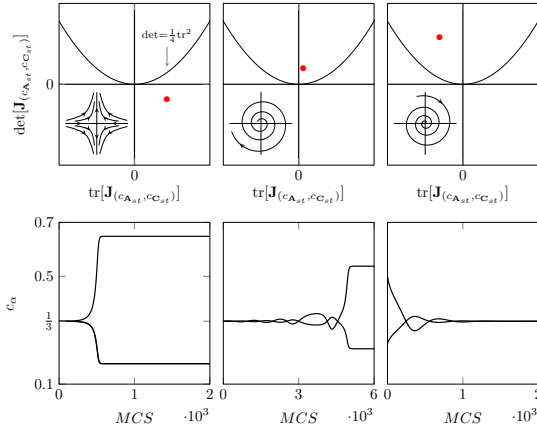


FIG. 3. The dependence between determinant and trace (Poincaré diagrams, upper panels) and sample trajectories (bottom panels) for parameters $q = 5$ and $s = 3$, and three values of p : $p = 0.35$ (left column), $p = 0.45$ (middle column), $p = 0.55$ (right column). Dots in Poincaré diagrams correspond to values of determinant and trace for the solution $(c_A, c_C) = (1/s, 1/s)$. Stability of this solution depends on p , which is shown by flow diagrams in the left corners of upper panels: negative determinant implies unstable saddle solution (left column), positive determinant and positive trace above critical parabola implies unstable spiral (middle column), positive determinant and negative trace above critical parabola implies stable spiral (right column).

and the total concentration of agents in the state α is given by

$$c_\alpha = pc_{(\mathbf{A}, \alpha)} + (1 - p)c_{(\mathbf{C}, \alpha)}. \quad (13)$$

Similarly to annealed version, we can express all stationary concentrations by a concentration of arbitrarily chosen state denoted with c using Eq. (5), whereas by c_A, c_C we express concentrations of anticonformists and conformists in this state respectively

$$\begin{aligned} c_{(\mathbf{A}, 0)} &= \dots = c_{(\mathbf{A}, s-(\xi+1))} = c_A, \\ c_{(\mathbf{A}, s-\xi)} &= \dots = c_{(\mathbf{A}, s-1)} = \frac{1 - (s - \xi)c_A}{\xi}; \end{aligned} \quad (14)$$

$$\begin{aligned} c_{(\mathbf{C}, 0)} &= \dots = c_{(\mathbf{C}, s-(\xi+1))} = c_C, \\ c_{(\mathbf{C}, s-\xi)} &= \dots = c_{(\mathbf{C}, s-1)} = \frac{1 - (s - \xi)c_C}{\xi}. \end{aligned} \quad (15)$$

$$\begin{aligned} \frac{\xi}{s-1} \left[\frac{1 - (s - \xi)c_A}{\xi} \left(\frac{1 - (s - \xi)c}{\xi} \right)^q - c_A c^q \right] &= 0 \\ \xi \left[\frac{1 - (s - \xi)c_C}{\xi} c^q - c_C \left(\frac{1 - (s - \xi)c}{\xi} \right)^q \right] &= 0 \end{aligned} \quad (16)$$

and total concentration is given by

$$c = pc_A + (1 - p)c_C. \quad (17)$$

Eqs. (16) give following stationary solutions

$$\begin{aligned} c_A &= \frac{\left(\frac{1 - (s - \xi)c}{\xi} \right)^q}{(s - \xi) \left(\frac{1 - (s - \xi)c}{\xi} \right)^q + \xi c^q} \\ c_C &= \frac{c^q}{(s - \xi)c^q + \xi \left(\frac{1 - (s - \xi)c}{\xi} \right)^q} \end{aligned} \quad (18)$$

and combining them with (17) we obtain

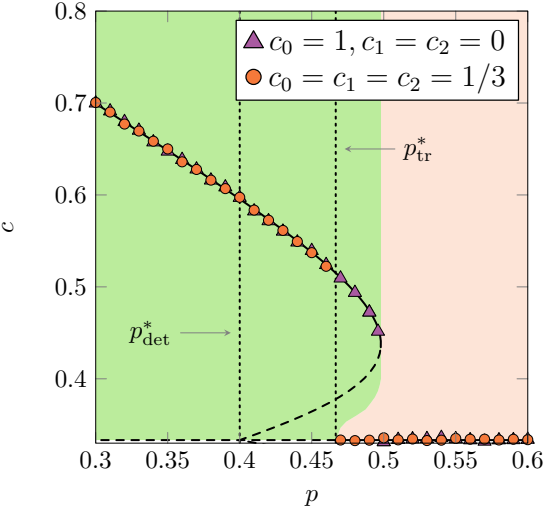


FIG. 4. The dependence between the stationary concentration c of agents in state 0 and probability of anticonformity p within the quenched approach for $q = 5$ and $s = 3$. Lines are given by Eq. (19): solid and dashed lines correspond to stable and unstable steady states, respectively. Vertical dotted lines represent critical points p_{det}^* and p_{tr}^* . Two color shaded areas correspond to two different basins of attraction obtained numerically from Eqs. (12) and (13): (left area, green color online) trajectories converge to stationary ordered state, (right area, pink color online) trajectories converge to the stationary disordered state. Symbols represent the outcome of MC simulations for the system size $N = 5 \times 10^5$ performed from two initial conditions indicated in the legend. The results are averaged over ten runs and collected after $t = 5 \times 10^4$ MCS.

$$p = \frac{\left(\frac{1-(s-\xi)c}{\xi}\right)^q c^q [cs^2 - (1+2c\xi)(s-\xi)] + \xi c^{2q} [c(s-\xi) - 1] + c\xi(s-\xi) \left(\frac{1-(s-\xi)c}{\xi}\right)^{2q}}{\xi \left(\frac{1-(s-\xi)c}{\xi}\right)^{2q} - \xi c^{2q}} \quad (19)$$

With Eq. (19) one can reproduce all s stationary solutions for the quenched q-voter model with anticonformity, see two bottom rows in Fig. 1.

II. STABILITY ANALYSIS

A. Annealed approach

Information about the stability of the system is given by the sign of the derivative

$$\begin{aligned} \frac{dF(c)}{dc} &= (1-p)qc^{q-1} - (1-p)(s-\xi)(q+1)c^q \\ &+ (1-p)cq(s-\xi) \left(\frac{1-(s-\xi)c}{\xi}\right)^{q-1} \\ &- (1-p)\xi \left(\frac{1-(s-\xi)c}{\xi}\right)^q - p \frac{(q+1)\xi}{s-1} c^q \\ &- p \frac{(q+1)}{s-1} (s-\xi) \left(\frac{1-(s-\xi)c}{\xi}\right)^q. \end{aligned} \quad (20)$$

Stability analysis allows us to calculate the lower spinodal, that is, the point at which the disordered phase $c = 1/s$ loses stability. Thus, to calculate it one should check the sign of derivative (20) at $c = 1/s$:

$$\frac{dF(c)}{dc} \Big|_{c=1/s} = \left(\frac{1}{s}\right)^q \left[(1-p)s(q-1) - ps \frac{q+1}{s-1} \right]. \quad (21)$$

For the fixed values of q and s , the derivative (21) is equal to 0 at

$$p_1^* = \frac{(s-1)(q-1)}{(s-1)(q-1) + q+1}. \quad (22)$$

The derivative given by Eq. (21) has a positive sign for $p < p_1^*$ (unstable solution) and a negative sign for $p > p_1^*$ (stable solution). Thus, p_1^* is the lower spinodal. Since there is only a continuous PT in the annealed approach, so p_1^* is simultaneously the upper spinodal.

B. Quenched approach

The stability of the system under the quenched approach is determined by the signs of the determinant and the trace of the following Jacobian matrix:

$$\mathbf{J}(c_{\mathbf{A}}, c_{\mathbf{C}}) = \begin{bmatrix} \frac{\partial F_{\mathbf{A}}}{\partial c_{\mathbf{A}}} & \frac{\partial F_{\mathbf{A}}}{\partial c_{\mathbf{C}}} \\ \frac{\partial F_{\mathbf{C}}}{\partial c_{\mathbf{A}}} & \frac{\partial F_{\mathbf{C}}}{\partial c_{\mathbf{C}}} \end{bmatrix}. \quad (23)$$

The appropriate derivatives are as follows

$$\begin{aligned} \frac{\partial F_{\mathbf{A}}}{\partial c_{\mathbf{A}}} &= \frac{qp(s-\xi)}{\xi(s-1)} \left(\frac{1-(s-\xi)c}{\xi}\right)^{q-1} ((s-\xi)c_{\mathbf{A}} - 1) \\ &- \frac{qp\xi}{s-1} c_{\mathbf{A}} c^{q-1} - \frac{s-\xi}{s-1} \left(\frac{1-(s-\xi)c}{\xi}\right)^q \\ &- \frac{\xi}{s-1} c^q, \end{aligned} \quad (24)$$

$$\begin{aligned} \frac{\partial F_{\mathbf{A}}}{\partial c_{\mathbf{C}}} &= \frac{q(1-p)(s-\xi)}{\xi(s-1)} \left(\frac{1-(s-\xi)c}{\xi}\right)^{q-1} ((s-\xi)c_{\mathbf{A}} - 1) \\ &- \frac{q(1-p)\xi}{s-1} c_{\mathbf{A}} c^{q-1}, \end{aligned} \quad (25)$$

$$\begin{aligned} \frac{\partial F_{\mathbf{C}}}{\partial c_{\mathbf{A}}} &= qpc^{q-1}(1-(s-\xi)c_{\mathbf{C}}) \\ &+ qp(s-\xi)c_{\mathbf{C}} \left(\frac{1-(s-\xi)c}{\xi}\right)^{q-1}, \end{aligned} \quad (26)$$

$$\begin{aligned} \frac{\partial F_{\mathbf{C}}}{\partial c_{\mathbf{C}}} &= q(1-p)c^{q-1}(1-(s-\xi)c_{\mathbf{C}}) \\ &+ q(1-p)(s-\xi)c_{\mathbf{C}} \left(\frac{1-(s-\xi)c}{\xi}\right)^{q-1} \\ &- (s-\xi)c^q - \xi \left(\frac{1-(s-\xi)c}{\xi}\right)^q. \end{aligned} \quad (27)$$

Similarly to the annealed approach, we are able to calculate the lower spinodal point. It will be given by the sign of the trace and the determinant of the stationary solution ($c_{\mathbf{A}} = 1/s, c_{\mathbf{C}} = 1/s$)

$$\begin{aligned} \det \left[\mathbf{J} \left(\frac{1}{s}, \frac{1}{s} \right) \right] &= \frac{\partial F_{\mathbf{A}}}{\partial c_{\mathbf{A}}} \frac{\partial F_{\mathbf{C}}}{\partial c_{\mathbf{C}}} - \frac{\partial F_{\mathbf{A}}}{\partial c_{\mathbf{C}}} \frac{\partial F_{\mathbf{C}}}{\partial c_{\mathbf{A}}} \\ &= \left(\frac{1}{s}\right)^{2q} \frac{s^2}{s-1} [q(2p-1) + 1], \end{aligned} \quad (28)$$

$$\begin{aligned} \text{tr} \left[\mathbf{J} \left(\frac{1}{s}, \frac{1}{s} \right) \right] &= \frac{\partial F_{\mathbf{A}}}{\partial c_{\mathbf{A}}} + \frac{\partial F_{\mathbf{C}}}{\partial c_{\mathbf{C}}} \\ &= \left(\frac{1}{s}\right)^{q-1} \left[q - \frac{s(qp+1)}{s-1} \right]. \end{aligned} \quad (29)$$

From Eq. (28) we can observe that the determinant is strictly increasing with p and changes the sign from negative to positive at the point

$$p_{\det}^* = \frac{q-1}{2q}. \quad (30)$$

On the other hand, the trace strictly decreases with p and changes sign from positive to negative at the point

$$p_{\text{tr}}^* = 1 - \frac{1}{s} - \frac{1}{q}. \quad (31)$$

The steady state is stable when the trace is negative while the determinant is positive, thus the solution ($c_{\mathbf{A}} = 1/s, c_{\mathbf{C}} = 1/s$) is stable when $p > p_{\text{det}}^*$ and $p > p_{\text{tr}}^*$. This relation can be divided into three cases.

1. Root for the determinant is bigger than root for the trace $p_{\text{det}}^* > p_{\text{tr}}^*$, see left panel in Fig. 2. Thus lower spinodal is given by $p_1^* = p_{\text{det}}^*$, because trace is already negative when determinant changes its sign to positive, i.e. the disordered state becomes stable. This case occurs for example if $s = 2$, because then regardless of q the condition $p_{\text{det}}^* > p_{\text{tr}}^*$ is fulfilled.
2. Roots p_{det}^* and p_{tr}^* are equal and lower spinodal is given by $p_1^* = p_{\text{det}}^* = p_{\text{tr}}^*$, see middle panel in Fig. 2. This happens when the following relation is fulfilled

$$q = \frac{s}{s-2}. \quad (32)$$

The only possible integer solutions are ($s = 3, q = 3$) and ($s = 4, q = 2$).

3. Root for the trace is bigger than root for the determinant $p_{\text{tr}}^* > p_{\text{det}}^*$, see right panel in Fig. 2. In this case, we can point out three regions:

- (a) For $p < p_{\text{det}}^*$ the determinant is negative and in the result the disordered solution is the saddle point, see left panels in Fig. 3.
- (b) For $p_{\text{det}}^* < p < p_{\text{tr}}^*$ both determinant and trace are positive, thus the disordered solution is a source and in most cases it is a spiral source (unstable spiral). This spiral source correspond to spreading oscillations which reach attractive stable solution different from $1/s$, see middle panels in Fig. 3.
- (c) For $p > p_{\text{tr}}^*$ determinant is positive while trace is negative, so the disordered state is a sink and in most cases it is a spiral sink (stable spiral). This spiral sink correspond to damped oscillations which reach stable solution equals to $1/s$, see right panels in Fig. 3. Hence, the disordered solution become stable when $p > p_{\text{tr}}^*$, see Fig. 4.